HEMODYNAMICS AND VASCULAR DEVELOPMENT IN THE CHICKEN EMBRYO

AND THE EFFECTS OF HOMOCYSTEINE AND FOLIC ACID TREATMENT

Annelien M. Oosterbaan

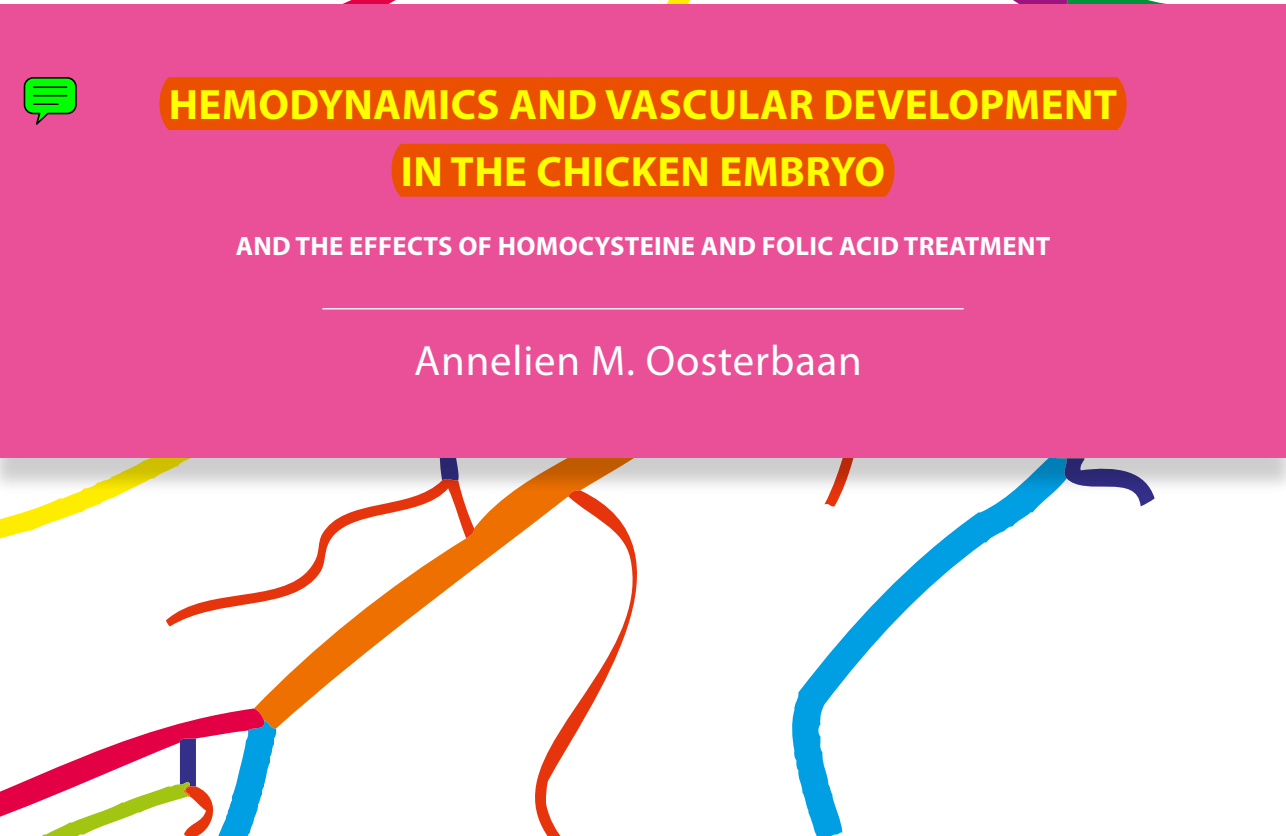

HEMODYNAMICS AND VASCULAR DEVELOPMENT IN THE CHICKEN EMBRYO

AND THE EFFECTS OF HOMOCYSTEINE AND FOLIC ACID TREATMENT

Annelien M. Oosterbaan

Hemodynamics and Vascular Development in the Chicken Embryo
and the Effects of Homocysteine and Folic Acid Treatment
Thesis, Erasmus University Rotterdam, The Netherlands

The research described in this thesis has been performed at the Department of Obstetrics and Gynecology, division of Obstetrics and Prenatal Medicine of the Erasmus MC University Medical Center, Rotterdam, The Netherlands.

The printing of this thesis has been financially supported by the Department of Obstetrics and Gynecology of the Erasmus MC University Medical Center, Rotterdam, the Erasmus University Rotterdam and the J.E. Jurriaanse Stichting.

Additional financial support was kindly provided by:

Dr. H.P. Oosterbaan

ChipSoft GOODLIFE

MSD B.V.
Bayer Schering
Sorg-Saem
Leerhuis Albert Schweitzer Ziekenhuis Dordrecht
Olympus Nederland B.V.
Astellas Pharma
Abbott B.V.
HOLOGIC Benelux B.V.
BMA B.V. (Mosos)
Medical Dynamics
Vifor Pharma
Drost Loosdrecht B.V.

Cover: A.M. Oosterbaan and JP Offset
Lay-out & Printing: JP Offset, Duiven, jp.nl

ISBN: 978-90-9026755-5

HEMODYNAMICS AND VASCULAR DEVELOPMENT IN THE CHICKEN EMBRYO

AND THE EFFECTS OF HOMOCYSTEINE AND FOLIC ACID TREATMENT

Hemodynamiek en vasculaire ontwikkeling in het kippenembryo
en het effect van homocysteïne en foliumzuur behandeling

Proefschrift

ter verkrijging van de graad van doctor
aan de Erasmus Universiteit Rotterdam
op gezag van de rector magnificus
Prof. dr. H.G. Schmidt

en volgens besluit van het College van Promoties.
De openbare verdediging zal plaatsvinden
op vrijdag 15 juni 2012 om 9.30 uur
door

Annelien Maria Oosterbaan
Geboren op 30 maart 1983 te 's-Hertogenbosch

Promotiecommissie

Promotor:
Prof. dr. E.A.P. Steegers

Copromotor:
Dr. N.T.C. Ursem

Overige leden:
Prof. dr. J. Lindemans
Prof. dr. R.E. Poelmann (LUMC)
Prof. dr. I.K.M. Reiss

Paranimfen
Karin M. Burgerhout
Evelyne M. van Uitert

When the rain is blowing in your face
And the whole world is on your case
I could offer you a warm embrace
To make you feel my love

I'd go hungry
I'd go black and blue
I'd go crawling down the avenue
No
There's nothing that I wouldn't do
To make you feel my love

(From: Adele, Make You Feel My Love)

Aan mijn ouders

CONTENTS

1

Introduction

1.1 CONGENITAL HEART DEFECTS

Congenital heart defects (CHD) are the most common birth defects in newborns, with a prevalence rate in the Netherlands of 7-8 per 1000 live births per year [1]. Prenatal screening has led to early detection of approximately one third of CHD, and consequently to increased rates of terminations of pregnancy [2].

Although, due to medical and surgical improvements, the majority of these children reach adulthood, CHD are still the most frequent cause of infant death related to birth defects [3-4]. Unfortunately, in only about 15 percent of cases a cause can be identified [5]. These CHD are caused by genetic or environmental factors [6]. The remaining cases are thought to be complex and multifactorial. Studies on the etiology of CHD are needed to increase our knowledge and reveal possible underlying mechanisms and pathways. Hopefully, this will lead to the implementation of preventative measures in the future.

1.2 EARLY HEART FUNCTION AND DEVELOPMENT

In order to distinguish abnormal from normal cardiac development, first normal cardiogenesis needs to be understood. During embryogenesis, the heart is already functioning well before its morphology is complete. The heart develops from a muscle wrapped tube into a septated four-chambered heart in only a few weeks. Human heart development has completed by the 10th week of pregnancy. Previously, it has been thought that the early embryonic heart functions like a peristaltic pump. Recently however, a suction pump-like functioning of the heart has been suggested [7-8]. Still there is no consensus on the exact functioning during these early stages of development, as the heart undergoes constant morphological changes. It is thought that different consecutive cardiac pumping mechanisms are present. Correct early heart functioning is vital, as alterations in heart function may precede the onset of structural heart defects. Therefore, studies on early hemodynamics are needed to increase our insight into the way the embryonic heart functions and to be able to achieve earlier and improved detection of abnormalities.

1.3 THE CHICKEN EMBRYO

The human embryo is not a suitable model to study early embryonic heart function. Firstly, because of limited resolution of current ultrasound techniques that do not allow detailed studying of the human embryonic heart. Secondly, the safety of early ultrasound scans, in particular Doppler ultrasonography, has not been proven [9]. Therefore it is not applicated in early first trimester. Thirdly, embryo treatment or intervention is not possible. The chicken embryo, however, has been used to study early cardiac form and function for many decades [10-12]. This model continues to be of great help in gaining insight into the physiological

and pathophysiological changes of the developing heart, since early development of avian and mammalian hearts is largely similar. Additionally, the chicken embryo is a relatively cheap animal model that is easily accessible. Also, no approval of an Animal Ethics Committee is needed in the Netherlands.

The hypothesis that in heart development form follows function has been substantiated by chicken embryo studies. The venous clip model consists of ligation of the right lateral vitelline vein with a microclip. This model can be used to alter hemodynamic parameters such as the intracardiac blood flow [13-14]. The chicken embryos displayed cardiovascular malformations, mostly outflow tract (OFT) defects like ventricular septal defects, valve anomalies and pharyngeal arch artery malformations after clipping [15]. The interaction between blood flow and the vessel wall has been shown to regulate the formation of the heart [16-17] and responds to shear stress [18]. Shear stress is the frictional force acting on the endocardial cells, lining the inner vessel wall of the heart, parallel to blood flow. Venous clipping studies have provided increasing *in vivo* evidence on the effects of shear-stress on the expression of genes implicated in heart development [19-20]. Therefore, shear stress is considered to play a substantial role in cardiovascular development and, consequently, is seen as an important epigenetic factor in embryonic cardiogenesis [15, 21].

1.4 HOMOCYSTEINE

Hyperhomocysteinemia, an elevated level of the methionine derivative homocysteine in the blood of the mother, has been implicated in the development of congenital birth defects [22-24]. Homocysteine has been reported to increase the risk of cardiovascular developmental defects [25]. Additionally, homocysteine is linked to the risk of vascular disease in later life [26]. Because of the high prevalence of hyperhomocysteinemia in both the reproductive and general population, research on underlying mechanisms is warranted.

Multiple teratogenic effects of homocysteine have been demonstrated in animal experimental studies [27]. In the chicken embryo, homocysteine exposure has been shown to induce CHD [28-31]. The CHD reported after homocysteine exposure, mostly OFT defects, are comparable to those seen in the venous clipped chicken embryo. Therefore, we hypothesized that homocysteine may induce changes of early heart function that precede the onset of morphological abnormalities. To test this hypothesis we want to study whether homocysteine affects early hemodynamics and shear stress levels in the chicken embryonic heart. Also vasculotoxic properties of homocysteine, causing endothelial cell damage and dysfunction, have been described after homocysteine exposure [32-35]. Since maternal hyperhomocysteinemia has been associated with an increased risk of cardiovascular

developmental defects in the offspring, and homocysteine has been identified as a vascular pathogen, we wanted to study the effects of homocysteine on embryonic peripheral vascular development in the chicken embryo.

1.5 THE ROLE OF FOLIC ACID

Folic acid is a water-soluble B vitamin involved in DNA and RNA synthesis and cell division [36]. Folic acid serves as a substrate in the remethylation of homocysteine into methionine, reducing blood homocysteine levels. Mefolinate is the synthetic form of 5-methyl-THF, the primary circulatory form of folic acid in the body. A deficient folate status can lead to an elevation of blood homocysteine concentration and consequently, an increased risk on homocysteine induced birth defects. Folic acid has also been described to have direct effects on embryonic growth and development. It is known to serve as a cofactor in nucleic acid synthesis and cell division [36], being involved in purine and thymidine synthesis.

The preventative effect of periconceptional folic acid use on neural tube defects in infants is well established [37-38]. This finding has led to the recommendation to mothers to use folic acid supplementation from 4 weeks before to 8 weeks after conception. The potentially protective effect of folic acid on other congenital malformations, specifically CHD, has been described in different studies [39-40]. Some chicken embryo studies support these findings [28, 41-42]. Therefore, we wanted to study whether folic acid, and also mefolinate, have beneficial effects on development and whether folic acid prevents from the effects induced by homocysteine.

1.6 METHODOLOGY

1.6.1 Chicken Embryo Treatment

Fertilized white-Leghorn (*Gallus Gallus* (L.)) chicken eggs (Drost Loosdrecht BV, Loosdrecht, The Netherlands) were incubated at a temperature of 37.5 degrees Celcius. During incubation, the chicken embryos start to develop, floating on the egg yolk, mostly on their left side (Figure 1a). The eggs were incubated with the air chamber up to allow embryo treatment at 24, 48 and 72 hours of incubation. After treatment, the eggs were placed back in the incubator, horizontally, for further development. As the embryos had reached the developmental stage needed, the eggs were taken out of the incubator and the embryo was localized. Then a window of approximately 1.5 by 1.5 cm was sawn in the egg shell to allow staging of the embryo and consequently ultrasonographic examination.

Figure 1

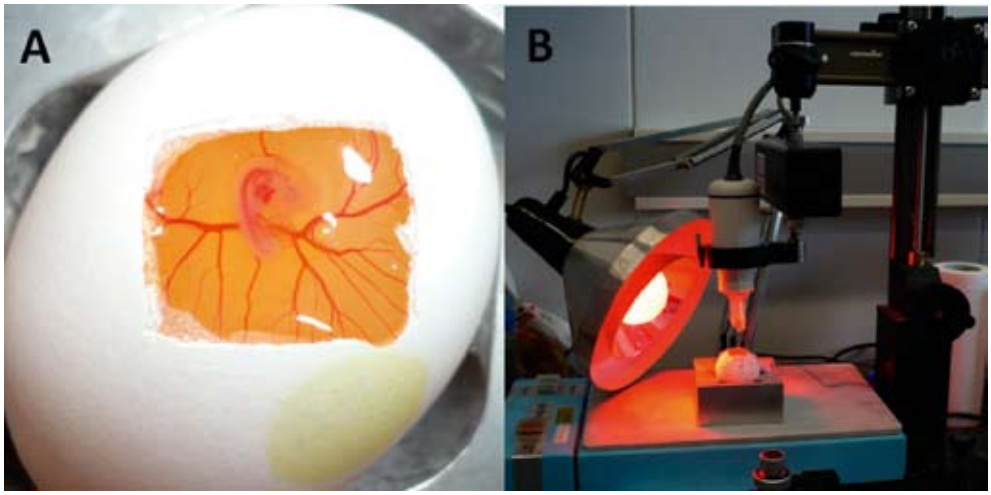

A. HH 21 chicken embryo. A window was sawn in the eggshell to visualize the embryo and to allow staging and imaging. B. Experimental set-up for ultrasound biomicroscopy. A heat lamp and a heated plate was used to maintain embryo temperature at 37.5 degrees Celcius. The embryo was scanned with the transducer mounted in an XYZ micromanipulation system.

1.6.2 Ultrasound Biomicroscopy

Ultrasonographic techniques are under constant development. One of the most recent developments is high frequency high resolution *in vivo* micro-imaging, called ultrasound biomicroscopy. We have used the Vevo 770 system (Visualsonics, Inc., Toronto, Canada) equipped with a 55-MHz transducer (RMV 708), exhibiting an axial and lateral resolution of approximately 30 and 75 µm, respectively [43-44]. The high resolution of the system allows detailed B-mode imaging of the small chicken embryonic heart (Figure 1b). The Power Doppler mode was used to visualize the blood flow in the cross sections through the heart, and after identifying these flows, the sample volume was placed in the centre of the bloodstream and Pulsed-Wave Doppler mode was used to collect flow velocity waveforms. With Doppler ultrasonography the direction, intensity and velocity of blood flow can be measured. The ultrasound probe serves both as an emitter and a receiver of waves, and sends out a signal that is reflected by the blood cells. The moving blood cells cause a change in frequency of the emitted sound. This is called the Doppler shift or Doppler effect.

1.6.3 Microscopic Particle Image Velocimetry

In collaboration with the Delft Technical University we have implemented an advanced technique called Microscopic Particle Image Velocimetry (μPIV). μPIV was first described in the late 1990s [45] and has been under constant development since. It can be used to obtain flow velocity vector measurements in a cross section of flow. We have implemented μPIV to obtain blood flow velocity fields and to determine shear stress rates in the OFT of chicken embryonic hearts. The velocity of a fluid is measured by imaging fluorescent seed particles that are suspended in the fluid. We injected polyethylene glycol (PEG)-coated polystyrene fluorescent tracer particles (Microparticles GmbH, Berlin, Germany) into the right vitelline artery of the chicken embryo. Placed under an epifluorescent microscope (Leica MZ 16 FA), the tracer particles were illuminated with a dual-cavity Nd:YLF laser (Pegasus, New Wave). Imaging of the particles was done with a CCD camera (Image Intense QE, Lavision) at a frame rate of 9.9 Hz. Each light pulse was captured in a separate image frame. Then the acquired images were divided in small subsections, so called interrogation areas (IA). The IA were cross-correlated into consecutive images. The displacement vector was calculated from the correlation peak. The velocity field then follows from dividing the displacement field by the delay time between the images. Detailed description of the procedure of *in vivo* μPIV was given by Vennemann et al. [46] and Poelma et al [47].

1.6.4 Computational Quantification of the Vascular Bed

Since a program that performs standardized and detailed analysis of the vascular bed was lacking, we have developed a program named Vascalc 1.0. Vascalc 1.0, designed in LabVIEW (National Instruments, Austin, Texas, USA), allows loading of TIFF images of the chicken extra-embryonic vascular bed, obtained with the use of a light microscope (Leica KL 1500 LCD, Leica Microsystems, Germany). A circular region of interest was extracted from the image and binarized to separate vascular from nonvascular areas. Subsequently, a different color value was assigned to each pixel, equal to the shortest distance to the vessel border. This method, called the Danielsson function, displays vessel diameter in layers of different colours per pixel of vessel width. Finally, the image was skeletonized to obtain vessel length. The vessels were divided in subgroups G1-G9, according to their diameter, G9 contained the vessels of smallest diameter. Output measures contained the ratio of vascular/non vascular areas in mm^2 and in percentage, overall vessel area (mm^2), overall vessel length (mm), vessel diameter (mm) per subgroup and vessel length (mm) per subgroup.

1.6.5 Real Time Polymerase Chain Reaction

Real time polymerase chain reaction (PCR) was developed because of the need to quantitate differences in messenger RNA (mRNA) expression, that could not be obtained with conventional PCR. Even though Northern blotting as well as ribonuclease protection assays (RPA) are the gold standards, they cannot be used in case of small amounts of tissue like the chicken extra-embryonic vascular bed, since they require more amounts of RNA. Therefore, real time PCR was performed in our study. In order to measure mRNA, it is converted into complementary DNA (cDNA) using reverse transcriptase, which is then amplified by PCR. We studied the expression of the protein vascular endothelial growth factor A (VEGF-A) and of its receptor, the vascular endothelial growth factor receptor (VEGF-R). VEGF signaling is known to be crucial for the regulation and promotion of developmental vasculogenesis as well as angiogenesis [48-50].

1.7 AIMS OF THE THESIS

1. To test the use of high frequency ultrasound biomicroscopy in studying early embryonic chicken heart function.
2. To test our hypothesis regarding the influence of hemodynamics on cardiac morphology: homocysteine exposure was related to changes in hemodynamic parameters and shear stress, since previous studies have shown that both homocysteine exposure as well as altered hemodynamics have been implicated in the development of cardiovascular malformations.
3. To study the effects of homocysteine on embryonic peripheral vascular development.
4. To test the possible protective effects of folic acid and mefolinate on homocysteine induced effects during cardiogenesis.

1.8 CHAPTER OUTLINE

Chapter 2 provides Doppler flow velocity profiles of the chicken embryonic heart at developmental stages that coincide with 5-8 weeks of human pregnancy, obtained with high frequency ultrasound biomicroscopy. We were the first to collect these waveforms during these early stages of cardiac development, before morphology has completed, and they provide significant information on normal early embryonic hemodynamics. We have shown that location as well as stage specific flow velocity waveforms are present.

Chapter 3 is a review of studies on the teratogenicity of homocysteine in animal experimental studies and elaborated on the possible underlying mechanisms. These mechanisms affect growth and differentiation processes as well as implantation, embryogenesis and placentation.

In **chapter 4** we show the effects of homocysteine exposure on hemodynamic parameters of early embryonic chicken heart function. Homocysteine in general causes inhibiting effects like, among others, a reduction of heart rate. This chapter also shows the effects of homocysteine on shear stress rates at the site of the OFT. The results support our hypothesis that homocysteine exposure causes early functional changes that may precede the development of CHD.

In **chapter 5** the effects of folic acid and mefolinate, as well as combined treatment of folic acid together with homocysteine, on early embryonic heart function and embryo survival are studied. We conclude that folic acid and mefolinate equally stimulate embryo survival and that folic acid in combination with homocysteine does not improve survival rates. This combined treatment did show a protective effect of folic acid since the specific effects previously subscribed to homocysteine were not present in these embryos. This could be one of the mechanisms through which human periconceptional FA use prevents CHD in the offspring.

In **chapter 6** the effects of homocysteine on early extra-embryonic vascular development are explored. We conclude that homocysteine exposure impairs vascularization, demonstrated by altered composition of the vascular bed as well as a reduction in the expression of VEGF-A and its receptor. These homocysteine induced effects may be involved in the development of cardiovascular developmental defects, as well as early placentation problems.

In the General Discussion, **chapter 7**, the findings and implications of this thesis are discussed and ideas for future research are provided.

REFERENCES

1. van Beynum, I.M., et al., *Protective effect of periconceptional folic acid supplements on the risk of congenital heart defects: a registry-based case-control study in the northern Netherlands.* Eur Heart J, 2009. 31(4): p. 464-71.
2. van der Bom, T., et al., *The changing epidemiology of congenital heart disease.* Nat Rev Cardiol, 2011. **8**(1): p. 50-60.
3. Tennant, P.W., et al., *20-year survival of children born with congenital anomalies: a population-based study.* Lancet, 2010. **375**(9715): p. 649-56.
4. Botto, L.D. and A. Correa, *Decreasing the burden of congenital heart anomalies: an epidemiologic evaluation of risk factors and survival.* Prog Pediatr Cardiol, 2003. **18**: p. 111-121.
5. Nora, J.J., *Causes of congenital heart diseases: old and new modes, mechanisms, and models.* Am Heart J, 1993. **125**(5 Pt 1): p. 1409-19.
6. Kuciene, R. and V. Dulskiene, *Selected environmental risk factors and congenital heart defects.* Medicina (Kaunas), 2008. **44**(11): p. 827-32.
7. Forouhar, A.S., et al., *The embryonic vertebrate heart tube is a dynamic suction pump.* Science, 2006. **312**(5774): p. 751-3.
8. Butcher, J.T., et al., *Transitions in early embryonic atrioventricular valvular function correspond with changes in cushion biomechanics that are predictable by tissue composition.* Circ Res, 2007. **100**(10): p. 1503-11.
9. Abramowicz, J.S., *Fetal Doppler: how to keep it safe?* Clin Obstet Gynecol, 2010. **53**(4): p. 842-50.
10. Hu, N. and E.B. Clark, *Hemodynamics of the stage 12 to stage 29 chick embryo.* Circ Res, 1989. **65**: p. 1665-1670.
11. Clark, E.B. and N. Hu, *Developmental hemodynamic changes in the chick embryo from stage 18 to 27.* Circ Res, 1982. **51**: p. 810-815.
12. Nakazawa, M., et al., *Effect of atrial natriuretic peptide on hemodynamics of the stage 21 chick embryo.* Pediatric Research, 1990. **27**(6): p. 557-560.
13. Hogers, B., et al., *Unilateral vitelline vein ligation alters intracardiac blood flow patterns and morphogenesis in the chick embryo.* Circ Res, 1997. **80**(4): p. 473-481.
14. Broekhuizen, M.L., et al., *Altered hemodynamics in chick embryos after extraembryonic venous obstruction.* Ultrasound Obstet Gynecol, 1999. **13**(6): p. 437-45.
15. Hogers, B., et al., *Extraembryonic venous obstructions lead to cardiovascular malformations and can be embryolethal.* Cardiovasc Res, 1999. **41**(1): p. 87-99.
16. Nerem, R.M., et al., *Hemodynamics and vascular endothelial biology.* J Cardiovasc Pharmacol, 1993. **21**(Suppl 1): p. S6-10.
17. Hierck, B.P., et al., *Fluid shear stress and inner curvature remodeling of the embryonic heart. Choosing the right lane!* ScientificWorldJournal, 2008. **8**: p. 212-22.
18. Takahashi, M., et al., *Mechanotransduction in endothelial cells: temporal signaling events in response to shear stress.* J Vasc Res, 1997. **34**(3): p. 212-9.
19. Groenendijk, B.C., et al., *The role of shear stress on ET-1, KLF2, and NOS-3 expression in the developing cardiovascular system of chicken embryos in a venous ligation model.* Physiology (Bethesda), 2007. **22**: p. 380-9.
20. Groenendijk, B.C.W., et al., *Development-related changes in the expression of shear stress responsive genes KLF-2, ET-1, and NOS-3 in the developing cardiovascular system of chicken embryos.* Dev Dyn, 2004. **230**(1): p. 57-68.
21. Hove, J.R., et al., *Intracardiac fluid forces are an essential epigenetic factor for embryonic cardiogenesis.* Nature, 2003. **421**(6919): p. 172-177.
22. Steegers-Theunissen, R.P., et al., *Neural-tube defects and derangement of homocysteine metabolism.* N Engl J Med, 1991. **324**(3): p. 199-200.

23. Steegers-Theunissen, R.P., et al., *Maternal hyperhomocysteinemia: a risk factor for neural-tube defects?* Metabolism, 1994. **43**(12): p. 1475-80.
24. Mills, J.L., et al., *Homocysteine metabolism in pregnancies complicated by neural-tube defects.* Lancet, 1995. **345**(8943): p. 149-51.
25. Verkleij-Hagoort, A., et al., *Hyperhomocysteinemia and MTHFR polymorphisms in association with orofacial clefts and congenital heart defects: a meta-analysis.* Am J Med Genet A, 2007. **143A**(9): p. 952-60.
26. McCully, K.S., *Homocysteine, vitamins, and vascular disease prevention.* Am J Clin Nutr, 2007. **86**(5): p. 1563S-8S.
27. van Mil, N.H., A.M. Oosterbaan, and R.P. Steegers-Theunissen, *Teratogenicity and underlying mechanisms of homocysteine in animal models: A review.* Reprod Toxicol, 2010.
28. Rosenquist, T.H., S.A. Ratashak, and J. Selhub, *Homocysteine induces congenital defects of the heart and neural tube: effect of folic acid.* Proc Natl Acad Sci U S A, 1996. **93**(26): p. 15227-32.
29. Boot, M.J., et al., *Cardiac outflow tract malformations in chick embryos exposed to homocysteine.* Cardiovasc Res, 2004. **64**(2): p. 365-73.
30. Han, M., et al., *Folate rescues lithium-, homocysteine- and Wnt3A-induced vertebrate cardiac anomalies.* Dis Model Mech, 2009. **2**(9-10): p. 467-78.
31. Lee, H. and J.J. Redmond, *Alleviation of inhibitory action of 5-bromode-oxyuridine by methionine in early chick embryos.* Experientia, 1975. **31**(3): p. 353-4.
32. Harker, L.A., et al., *Homocystine-induced arteriosclerosis. The role of endothelial cell injury and platelet response in its genesis.* J Clin Invest, 1976. **58**(3): p. 731-41.
33. Wall, R.T., et al., *Homocysteine-induced endothelial cell injury in vitro: a model for the study of vascular injury.* Thromb Res, 1980. **18**(1-2): p. 113-21.
34. Lee, S.J., et al., *Nitric oxide inhibition of homocysteine-induced human endothelial cell apoptosis by down-regulation of p53-dependent Noxa expression through the formation of S-nitrosohomocysteine.* J Biol Chem, 2005. **280**(7): p. 5781-8.
35. Boot, M.J., et al., *Homocysteine induces endothelial cell detachment and vessel wall thickening during chick embryonic development.* Circ Res, 2004. **94**(4): p. 542-9.
36. Smith, A.D., Y.I. Kim, and H. Refsum, *Is folic acid good for everyone?* Am J Clin Nutr, 2008. **87**(3): p. 517-33.
37. *Prevention of neural tube defects: results of the Medical Research Council Vitamin Study. MRC Vitamin Study Research Group.* Lancet, 1991. **338**(8760): p. 131-7.
38. Czeizel, A.E. and I. Dudas, *Prevention of the first occurrence of neural-tube defects by periconceptional vitamin supplementation.* N Engl J Med, 1992. **327**(26): p. 1832-5.
39. Botto, L.D., et al., *Periconceptional multivitamin use and the occurrence of conotruncal heart defects: results from a population-based, case-control study.* Pediatrics, 1996. **98**(5): p. 911-7.
40. van Beynum, I.M., et al., *Protective effect of periconceptional folic acid supplements on the risk of congenital heart defects: a registry-based case-control study in the northern Netherlands.* Eur Heart J, 2010. **31**(4): p. 464-71.
41. Boot, M.J., et al., *Folic acid and homocysteine affect neural crest and neuroepithelial cell outgrowth and differentiation in vitro.* Dev Dyn, 2003. **227**(2): p. 301-8.
42. Kobus, K., E.M. Nazari, and Y.M. Muller, *Effects of folic acid and homocysteine on spinal cord morphology of the chicken embryo.* Histochem Cell Biol, 2009.
43. McQuinn, T.C., et al., *High-frequency ultrasonographic imaging of avian cardiovascular development.* Dev Dyn, 2007. **236**(12): p. 3503-3513.
44. Zhou, Y.Q., et al., *Applications for multifrequency ultrasound biomicroscopy in mice from implantation to adulthood.* Physiol Genomics, 2002. **10**(2): p. 113-26.

45. Santiago, J.G., et al., *A particle image velocimetry system for microfluidics.* Exp Fluids, 1998. **25**: p. 316-319.
46. Vennemann, P., et al., *In vivo micro particle image velocimetry measurements of blood-plasma in the embryonic avian heart.* J Biomech, 2006. **39**(7): p. 1191-1200.
47. Poelma, C., et al., *Measurements of the wall shear stress distribution in the outflow tract of an embryonic chicken heart.* J R Soc Interface, 2010. **7**(42): p. 91-103.
48. Ferrara, N. and T. Davis-Smyth, *The biology of vascular endothelial growth factor.* Endocr Rev, 1997. **18**(1): p. 4-25.
49. Ferrara, N., H.P. Gerber, and J. LeCouter, *The biology of VEGF and its receptors.* Nat Med, 2003. **9**(6): p. 669-76.
50. Neufeld, G., et al., *Vascular endothelial growth factor (VEGF) and its receptors.* FASEB J, 1999. **13**(1): p. 9-22.

2

Doppler flow velocity waveforms in the embryonic chicken heart at developmental stages corresponding to 5-8 weeks of human gestation

A.M. Oosterbaan, N.T.C. Ursem, P.C. Struijk, J.G. Bosch, A.F.W. van der Steen, E.A.P. Steegers

Ultrasound in Obstetrics and Gynecology 2009; 33: 638–644

ABSTRACT

Introduction The objective of this study was to obtain Doppler velocity waveforms from the early embryonic chicken heart by means of ultrasound biomicroscopy and to compare these waveforms at different stages of embryonic development.

Methods We collected cardiac waveforms using high frequency Doppler ultrasound with a 55-MHz transducer at Hamburger-Hamilton (HH) stages 18, 21 and 23, which are comparable to humans at 5 to 8 weeks of gestation. Waveforms were obtained at the inflow tract, the primitive left ventricle, the primitive right ventricle, and at the outflow tract in 10 different embryos per stage. By exploring the temporal relationship between the waveforms, using a secondary Doppler device, cardiac cycle events were outlined.

Results Our results demonstrate that stage- and location-dependent intracardiac blood flow velocity waveforms can be obtained in the chicken embryo. The blood flow profiles assessed at the four locations in the embryonic heart demonstrated an increase in peak velocity with advancing developmental stage. In the primitive ventricle the 'passive' (P) filling peak decreased whereas the 'active' (A) filling peak increased, resulting in a decrease in P to A ratio with advancing developmental stage. M-mode recordings demonstrated that the fractional closure time of the atrioventricular cushions increased from 20% at stage HH 18 to 60% at stage HH 23.

Conclusions High frequency ultrasound biomicroscopy can be used to define flow velocity waveforms in the embryonic chicken heart. This may contribute to an understanding of Doppler signals derived from valveless embryonic human hearts at 5-8 weeks of gestation, prior to septation.

INTRODUCTION

The human embryonic heart is functioning before structural cardiac morphogenesis is complete. During early embryonic development the heart transforms from a muscle wrapped tube into a septated four-chambered heart at the end of the first trimester. Previously it has been thought that the early embryonic heart functions as a peristaltic pump, but recent studies in the zebrafish and chicken, have shown that the embryonic heart tube acts like a suction pump [1-2]. The chicken embryo is a widely accepted and appropriate model to study cardiac morphology and function during embryogenesis, as early development of avian and mammalian hearts is largely similar. This model has been used for many decades and continues to be of great help to gain insight in the physiological and pathophysiological changes of the developing heart [3-4].

Several studies have demonstrated that abnormal blood flow patterns lead to structural heart defects [5-7]. Permanent obstruction of the right lateral vitelline vein with a microclip causes alterations in intracardiac flow patterns and blood flow velocities [7], and eventually results in specific cardiovascular malformations[8]. This suggests that during embryogenesis early heart function regulates cardiac morphology. The study of blood flow velocities can be used to asses information on cardiac function[9-10]. Knowledge of the flow velocity waveforms in the embryonic heart might discriminate normal from disturbed development.

With advances in ultrasound technology, cardiac Doppler blood velocity waveforms can be recorded as early as in the first trimester of pregnancy. In humans, duplex Doppler ultrasound must exhibit satisfactory sensitivity at large penetration depths. This requirement dictates the use of relatively low center frequencies, limiting the axial resolution of human ultrasound systems. Therefore, the possibilities for studying blood flow velocitiy in the fetal heart during the early first trimester of pregnancy are limited. We hypothesize that specific blood flow velocity waveforms are already present at different anatomic locations within the heart in the early stages of cardiac development, and that these waveforms change during development. Knowledge of flow velocity waveforms obtained from an animal model such as the embryonic chicken might be helpful for the interpretation of first-trimester cardiac flow velocity waveforms in humans.

Ultrasound biomicroscopy has improved resolution over standard echocardiographic equipment. High frequency ultrasound technology has limited penetration depth, but it can perform excellently in experimental animal models such as the mouse[11] and chicken[12] embryo.

The objectives of this observational study were firstly to obtain velocity waveforms derived from the inflow tract, primitive left and right ventricle, and the outflow tract in chicken

embryos, secondly to explore the temporal relationship between these waveforms using simultaneously obtained Doppler recordings of the entire heart to facilitate synchronization, and thirdly to compare these waveforms at different stages of embryonic development.

MATERIALS AND METHODS

Fertilized White Leghorn (*Gallus gallus* (L.)) chicken eggs were incubated blunt-end up at 37.5 ºC. The eggs were taken out of the incubator and held under a bright light to localize the embryo, then a window of approximately 1.5 by 1.5 cm was sawn out of the eggshell. The eggshell and the outer membrane were removed to visualize the embryo. The embryo was staged by microscopic examination according to Hamburger and Hamilton (HH) (1951) [13]. Embryos that were dysmorphic or that showed visible bleeding were excluded. Embryos of stage HH 18 (3 d), HH 21 (3.5 d) and HH 23 (4 d) were studied *in ovo*, with a total of 10 embryos per stage. During these stages the embryo is floating on its left side on the egg yolk. Embryo temperature was maintained at 37 ºC with the help of a heated plate and a heat lamp. A Vevo 770 high frequency duplex Doppler ultrasound system (Visualsonics, Inc., Toronto, Canada) equipped with a 55-MHz transducer (RMV 708) was used, exhibiting an axial and lateral B-mode resolution of approximately 30 and 75 µm, respectively [12, 14]. Scanning was performed with the transducer mounted in an XYZ micromanipulation system. The window in the eggshell was covered with a piece of thin polyethylene film, and warmed ultrasonic gel was used as a standoff to allow vertical probe adjustment to image the embryonic heart at the focal depth of 4.5 mm. The sample gate of the transducer was set at 0.15 mm and the scanning depth varied between 4.2 and 5.2 mm. The transducer was aligned in the direction from the apex to the outflow tract (Figure 1a). Line 1 in Figure 1a represents the probe position from which the first cross-section of the heart was obtained. The ventricle and the outflow tract signals were recorded in this cross section (Figure 1a). Two dimensional ultrasound and power Doppler images of this cross section are presented in Figures 1b and c. The outer distance between the primitive left and right ventricles at maximum filling was determined as a measure of epicardial diameter. In order to record the inflow tract signal, the whole egg was moved in a dorsal direction to obtain the cross-section as shown by line 2 in Figure 1a. This movement was achieved by micromanipulation. B-mode and power Doppler images of this cross section are presented in Figures 1d and e. The variation in the angle of insonation between embryos is limited since the embryo is always floating on its left side. B-mode ultrasound was used to ensure accurate probe positioning. Power Doppler mode was used to visualize the blood flow in each of the cross sections through the heart, and, after identifying the flows in each case, the Doppler sample volume was placed in the centre of the bloodstream to obtain

flow velocity waveforms recordings (Figure 2). As the flow direction could not be assessed accurately, the Doppler angle correction was arbitrarily set to zero. Therefore, the Doppler velocities should be interpreted as relative velocities, and are more precisely the vectorial velocity in the direction of the ultrasound beam.

Figure 1

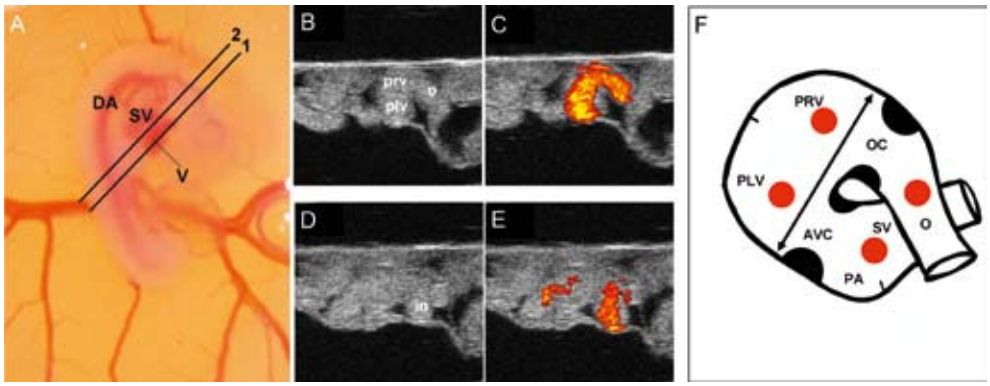

A: Hamburger-Hamilton stage 23 chicken embryo, right-side-up. DA, dorsal aorta; SV, sinus venosus; V, ventricle. Line 1 represents cross section 1, with measurement points of the primitive left ventricle (PLV), primitive right ventricle (PRV) and outflow tract (O) and line 2 represents cross section 2, with measurement point of the inflow tract (in). From a transducer position between lines 1 and 2, M-mode recordings were obtained to investigate the opening and closing of the atrioventricular and/or outflow cushions.
B-E: B-mode and power Doppler images of the embryonic heart measured with a 55-MHz transducer at line 1, representing the PLV, PRV and outflow tract (b,c) and at line 2, representing the inflow tract (d,e).
F: Schematic representation of the anatomy of the embryonic heart, with the inflow tract, consisting of the sinus venosus (SV) flowing into the primitive atrium (PA). The atrioventricular cushions (AVC) are between the primitive atrium and the PLV. The outflow cushions (OC) are situated between the PRV and the outflow tract (O). The four filled red circles represent the measurement points. The arrow indicates the epicardial diameter measured as the outer distance of the PLV and PRV during maximal expansion.

We focused on the signals of the inflow tract, the ventricles and the outflow tract. Signals at these four cardiac sites were recorded in each embryo (Figure 1f). Pulsed Doppler recordings were assessed at two different locations in the ventricle, as illustrated schematically by the red circles in figure 1f. The first location corresponds to the primitive left ventricle (PLV), and the second location corresponds to the primitive right ventricle (PRV) [15]. The term "forward" is used when blood is moving in the main direction from inflow tract to outflow tract. The positive and negative signs are used to indicate whether the blood is moving

towards or away from the ultrasound transducer. When considering the main blood stream it can be noted from Figure 1f that blood at the inflow tract is moving away (negative) from the ultrasound transducer, the blood in the primitive ventricles is moving towards (positive) the transducer, and the blood in the outflow tract is again moving away from the transducer.

By slight repositioning of the transducer, we also collected M-mode recordings of the ultrasound beam crossing the atrioventricular cushions, and the outflow tract cushions in stage HH18 embryos, to examine the opening and closure of the cushions. In the M-mode recording, closure of the cushions can be recognized as parallel lines, while opening of the cushions is presented by a decorrelated speckle patterns as a result of blood streaming.

Measurements were performed in 10 different embryos per stage. We analyzed the flow patterns by determining the peak velocity (cm/s) and the velocity time integral (mm) of the blood flow velocity waveform. The ratio of the areas under the velocity/time curve of the first 'passive' (P) component and of the second 'active' (A) component of ventricular filling - the P : A ratio – was determined.

To determine the temporal relationship between the four flow patterns, we used a secondary Doppler device (model 545C-4; Iowa Doppler Products, Iowa City, IA, USA), with a 20-MHz transducer that was positioned next to the Vevo transducer. Its ultrasound beam was aimed at the heart with a sample volume that obtained Doppler signals from all regions of the heart. This signal was displayed on the screen of the Vevo ultrasound machine, via its external signal input. The Doppler ultrasound recordings at the four locations in the heart and the M-mode recordings were obtained successively, but the secondary Doppler signal was obtained simultaneously in each case so that the five sequential recordings could later be synchronized.

Statistical Analysis

The data are presented as mean (SD), and for statistical comparison of the three study groups an one-way analysis of variance (ANOVA) was performed. If the result was significant pair-wise comparisons with a Bonferroni correction were used; $P < 0.05$ was considered statistically significant.

RESULTS

The epicardial diameter - measured as distance between the outer edges of the primitive left and right ventricles at maximum filling (Figure 1f) - showed an increase from stage HH 18 to stage HH 23. The mean heart rate at the different stages ranged from 170 to 189 bpm, with a statistically significant increase from HH 21 to HH 23 (Table 1). Typical examples of the

recorded Doppler velocity and M-mode profiles together with the external Doppler signal used for synchronization are shown in Figure 2. As can be noted from the M-mode signal at the bottom of Figure 2, at HH stage 18 both the AV and outflow cushions can be visualized. However at later stages, owing to structural development of the heart, the AV and outflow cushions cannot be visualized in the same plane. In Figure 2 the AV cushions are shown at HH stage 21 and 23.

Table 1 Epicardial diameter, heart rate and closure time of the inflow and outflow cushions in Hamburger-Hamilton (HH) stages 18, 21 and 23 chicken embryos

Parameter	*HH 18 (n=10)*	*HH 21 (n=10)*	*HH 23 (n=10)*
Epicardial diameter (mm)	1.31 (0.09)	1.49 (0.08) *	1.78 (0.12) †‡
Heart rate (bpm)	178 (27)	170 (25)	189 (13) †
Closure time AV cushions (%)	20.7 (6.8)	36.7 (17.6)	58.0 (25.7) †‡
Closure time outflow cushions (%)	18.8 (10.7)	---	---

Data are presented as mean and standard deviation. * Stage HH 18 was statistically significantly different from Stage HH 21 ($P<0.05$). † Stage HH 21 was statistically significantly different from Stage HH 23 ($P<0.05$). ‡ Stage HH 18 was statistically significantly different from stage HH 23 ($P<0.05$).

Stage Dependent Differences

Figure 3 shows schematic flow velocity waveforms from the inflow to the outflow tract of the heart during one cardiac cycle. The individual values of peak velocity of the blood flow velocity waveforms depicted in Figure 3 are summarized in Table 2. In Figure 3, areas I to III indicate the different ventricular phases during one cardiac cycle; I: "passive" (P) filling, II: "active" (A) filling, III: ejection phase. Our data show that blood flows into the ventricles in two phases. This mode of action is comparable to the biphasic flow pattern seen in the mature heart. However, in the embryonic heart prior to septation (before stage HH 25) the primitive ventricle is not activated through the His-Purkinje system and we therefore cannot use the terminology of "true" passive and active filling phases during this stage of development [16]. The fractional closure time of the AV cushions increased from 20% at stage HH 18 to 60% at HH 23 (Figure 3).

Figure 2

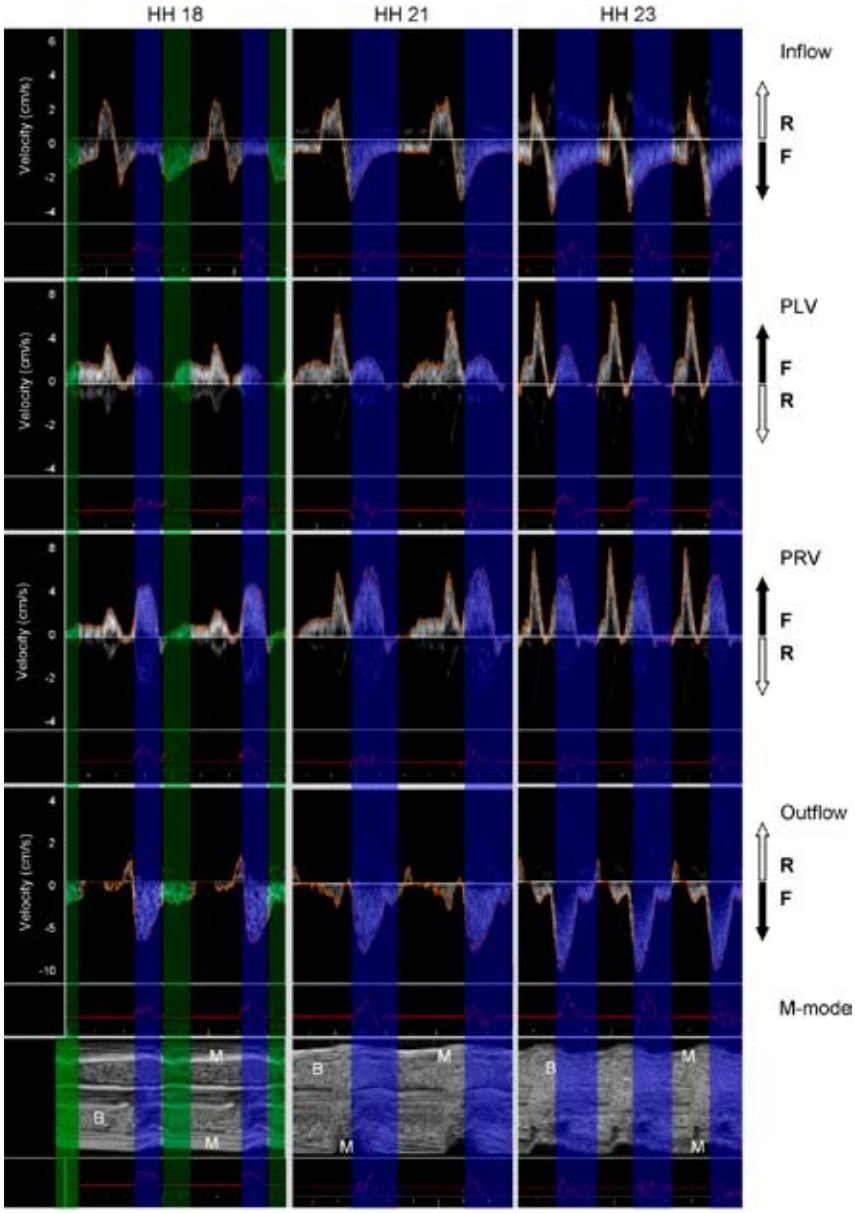

Cardiac Doppler blood flow velocity waveforms in chicken embryos of Hamburger-Hamilton stages 18, 21 and 23 at 4 different locations in the heart. The external Doppler signal used for synchronization is indicated in red. Bottom panels show M-mode recordings through the atrioventricular cushions. The outflow cushions can also be seen in the HH 18 embryos. The shaded blue bars indicate closure time of the atrioventricular cushions and the shaded green bars indicate the closure time of the outflow cushions. B, blood; F, forward direction of flow; M, myocardium; PLV and PRV, primitive left and right ventricles; R, reversed direction of flow.

Figure 3

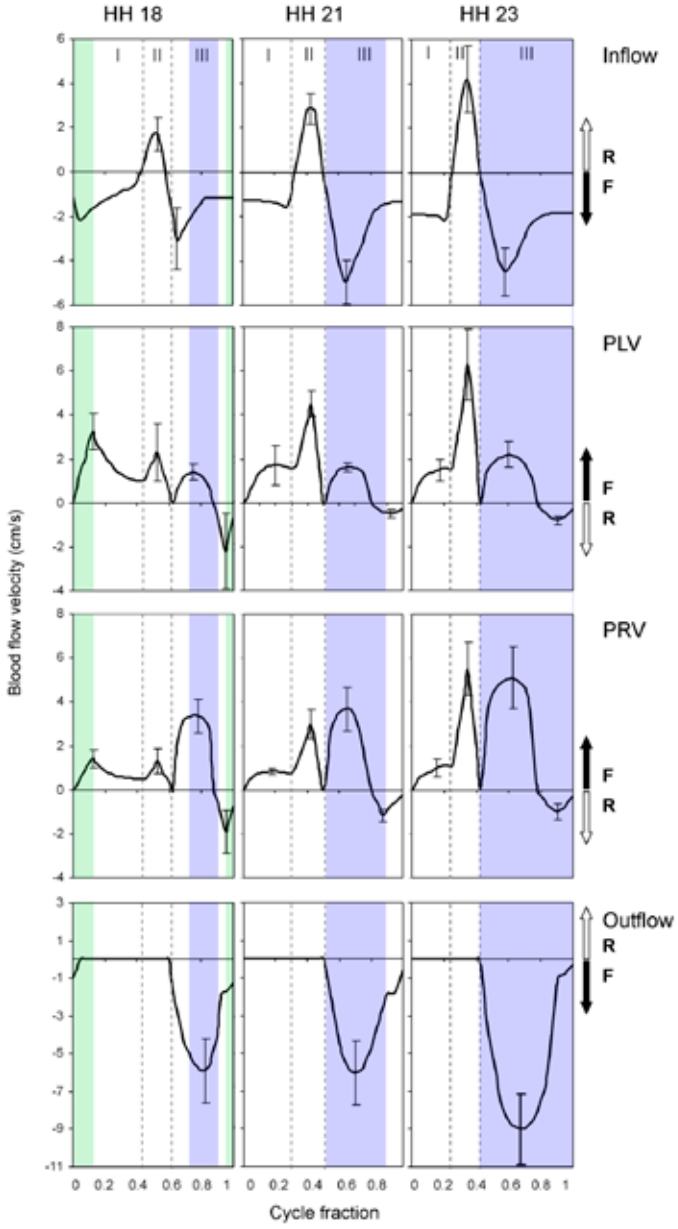

Representative blood flow velocity waveforms at Hamburger-Hamilton stages 18, 21 and 23 at the four different locations in the heart, with peak data presented as mean ± SD, generated from 10 Doppler recordings per location per stage. Areas I to III indicate the different ventricular phases during one cardiac cycle: I, 'passive' filling; II, 'active' filling; III, ejection phase. F represents forward and R represents reversed direction of flow. The shaded blue bars indicate closure time of the atrioventricular cushions and the shaded green bars indicate the closure time of the outflow cushions.

Table 2

Peak velocities measured in inflow tract, primitive left (PLV) and right (PRV) ventricles and outflow tract of the heart in Hamburger-Hamilton stage 18, 21 and 23 chicken embryos.

			Peak Velocity (cm/s)		
Location	*Direction*	*Phase*	*HH 18 (n=10)*	*HH 21 (n=10)*	*HH 23 (n=10)*
Inflow tract	Reversed	II	1.7 (0.8)	2.9 (0.7) *	4.2 (1.5) †‡
	Forward	III	-3.1 (1.4)	-5.0 (1.6) *	-4.5 (1.1) ‡
PLV	Forward	I	3.2 (0.8)	1.7 (0.9) *	1.5 (0.5) ‡
	Forward	II	2.3 (1.3)	4.5 (0.6) *	6.3 (2.1) †‡
	Forward	III	1.4 (0.4)	1.6 (0.2)	2.2 (0.6) †‡
	Reversed	III	-2.2 (2.2)	-0.4 (0.3) *	-0.8 (0.2) †‡
P : A ratio			1.90 (1.18)	0.38 (0.15) *	0.26 (0.14) †
Ej : A ratio			0.78 (0.45)	0.36 (0.06) *	0.35 (0.06) †
PRV	Forward	I	1.4 (0.4)	0.8 (0.2) *	1.1 (0.4) †
	Forward	II	1.2 (0.6)	2.9 (0.7) *	5.5 (1.2) †‡
	Forward	III	3.4 (0.8)	3.7 (1.1)	5.1 (1.4) †‡
	Reversed	III	-2.0 (1.0)	-1.2 (0.3) *	-1.0 (0.4) ‡
P : A ratio			1.39 (0.87)	0.28 (0.10) *	0.20 (0.08) †
Ej : A ratio			3.24 (1.36)	1.32 (0.52) *	0.95 (0.28) †
Outflow tract	Forward	III	-5.9 (1.7)	-6.1 (1.8)	-8.9 (2.0) †‡

Data are presented as mean and standard deviation. * Stage HH 18 is significantly different from Stage HH 21 ($P<0.05$). † Stage HH 21 was significantly different from Stage HH 23 ($P<0.05$). ‡ Stage HH 18 was significantly different from Stage HH 23 ($P<0.05$). Ej : A ratio, ratio of ejection peak velocity and peak 'active' filling velocity; P : A ratio, ratio of peak 'passive' filling velocity and peak 'active' filling velocity.

Inflow Tract

The inflow tract flow velocity waveforms showed a reversed (positive) and a forward (negative) peak during phases II and III, respectively, of the cardiac cycle, and these peaks were seen consistently through HH stages 18 to 23.

Primitiv Left and Right Ventricles

The relative blood flow velocity during filling (phases I and II) and the first part of the ejection phase (III) of the ventricles was similar in the primitive left and right ventricles (Figure 3). At stage HH 18, the peak velocity in both the PRV and the PLV in phase I is larger than the peak velocity seen in phase II. At stages HH 21 and 23 the peak in phase I subsequently decreased and the peak in phase II increased. As a consequence the ratio between passive and active ventricular filling is bigger than 1 at HH 18 and smaller than 1 at stages HH 21 and 23. The same pattern was seen for the velocity area (Figure 4). The maximum velocity of the forward (positive) outflow component (phase III) in both PRV and PLV increased with advancing developmental stage. The peak velocity in the PRV during phase III (ejection phase) exceeded the peak velocity in phase II (active filling phase) only at stages HH 18 and 21 (Table 2). Moreover, these angle-independent parameters demonstrate significant shape changes during early development. The reversed (negative) peak seen at the end of phase III is most probably the result of reflection of the closed outflow cushions. The reversed peak in some cases approaches zero as shown in the example waveforms of Figure 2, but was seen in all cases. The reversed flow peak showed a large variation in magnitude between cases, resulting in a considerable standard deviation of the mean (Table 2).

Outflow Tract

The outflow tract waveform revealed a consistent forward peak at the beginning of phase I that was only present at stage HH 18. Phase III demonstrated a dominant forward (negative) outflow peak that significantly increased during development.

DISCUSSION

Our study describes detailed Doppler flow velocity waveforms in the chicken embryo at various specific locations in the developing heart. During phase I of the cardiac cycle forward flow is seen in the inflow tract resulting in 'passive' ventricular filling. At the first part of phase I forward flow was observed in the outflow tract, which diminished to zero during the second part of phase I. Remarkably the forward flow coincided with the closure of the outflow cushions, as can be seen from the M-mode recordings. Due to the distance between the measurement point and cushions in the outflow tract, what we probably see is conotruncal blood that is propelled forward during closure time of the outflow cushions.

In all stages, forward flow was seen in both ventricles as the 'active' filling component, and reversed flow was simultaneously seen in the inflow tract (Figures 2 and 3). It seems that during atrial contraction, a bidirectional wave is generated and blood flows both forward from

the primitive atrium into the ventricle and backward from the primitive atrium into the sinus venosus. This reversed flow has been described in the zebrafish [17] and was also previously seen in the early chicken embryo [18]. As demonstrated in the zebrafish the looping heart is a relatively inefficient pump with significant reversed flow. Transition to an efficient pump with unidirectional flow emerges only as the cushions transform into leaflets [17]. However, in the chicken embryo this cushion transformation takes place after stage HH 28 [19]. In the outflow tract no distinct pattern was recognized. Note that during phase II both the AV and outflow cushions are open.

Figure 4

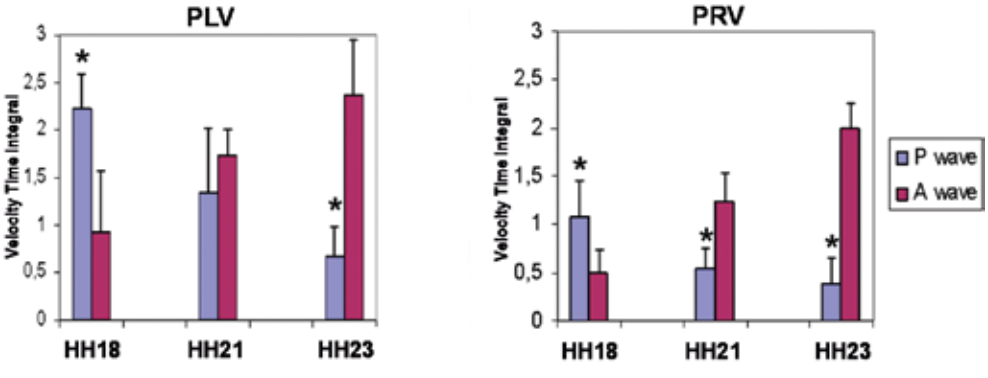

'Passive' to 'active' filling characteristics of the primitive left ventricle (a) and the primitive right ventricle (b) at Hamburger-Hamilton stages 18, 21 and 23. Data are presented as mean ± SD.
* Significant differences between the passive filling wave and the active filling component (p<0.01).

During phase III forward flow was observed at all four locations of the heart. As the AV cushions were closed, the forward flow observed in the inflow tract must represent atrial filling. The small negative peak observed at the second part of phase III coincided with the transition from the closure of the AV cushions to the closure of the outflow cushions. Strikingly, at stage HH 18 the AV cushions were found to be open during most (805) of the cardiac cycle. A similar finding has been observed in stage HH 17 chicken embryos by Butcher et al [2]. At stage HH 18 we were able to obtain an M-mode recording that simultaneously displayed the opening and closing of the AV and outflow cushions. From these recordings we could conclude that the length of the closure time of both sets of cushions was similar. The AV cushions closure succeeded the closure of the outflow cushions without overlap. As

a consequence, for 60% of the cardiac cycle, during the second part of passive filling and active filling, both sets of cushions are open. As previously reported by others, it is unlikely that at this stage of development the pump mechanism of the heart can be explained by peristaltic movements alone [1-2, 17]. In the Zebrafish, Forouhar et al elegantly demonstrated that negative pressure is present in a part of the cardiac cycle that sucks rather than pressed blood through the primitive ventricle of the valveless heart [1]. A recent study in the chicken embryo supported this theory [2]. The complex temporal relationship between blood flow and ventricular volume found by these authors might explain the velocity waveforms at stage HH 18 observed in this study.

The decrease in P : A ratio with advancing developmental stage, which has been previously reported by others[5, 20], indicates that from stage HH 21 active myocardial contraction, and not suction, dominates ventricular filling. Active filling dominance can partly be explained by the morphological change of the AV canal. According to Butcher et al, the AV canal becomes restrictive to blood flow crossing the AV junction, as the junction remodels during development.[2] This might explain why active myocardial contraction of the atrium is needed to accomplish ventricular filling.

Butcher et al investigated Doppler waveforms of blood velocity at the site of the atrioventricular cushions[2], reporting a biphasic signal at stages HH 17 and HH 21, which became monophasic at HH 25. Our Doppler profiles show different blood flow velocity waveforms because of the difference in measurement locations. Butcher et al collected their waveforms in the AV-canal, while we obtained recordings from either side of the AV canal. We were able to reproduce their signals, and in the AV canal only blood flow reflecting ventricular filling was detected. Behind the AV cushions, at the location of the primitive left ventricle, the outflow component is seen as the third forward peak in the velocity waveform. The ventricular filling components observed in our study compare well with the AV Doppler velocity profiles previously published by others [2, 20].

First trimester human fetal cardiac function has been studied with transvaginal Doppler ultrasonography by Mäkikallio et al [21]. We measured the inflow and outflow tract signal in the same direction because of the angle by which we approached the ventricle and the fact that early in development the heart is composed of a looped tube. Owing to limited resolution and relatively large sample volume, the signals measured by Mäkikallio et al are a mixture of inflow, ventricular and outflow velocity waveforms, as illustrated by their simultaneously presented forward and reversed velocity components [21]. The interpretation of in and outflow signals of human derived Doppler velocities based on the direction of flow is not valid during early developmental stages, when the heart can be considered as a muscular tube. The non-holosystolic atrioventricular valve regurgitation at 7 weeks of human

pregnancy, as suggested by Mäkikallio et al [21] might be doubted since at that time cardiac cushions are not yet transformed into valves.

In conclusion, high frequency ultrasonographic biomicroscopy can be used to help define flow velocity waveforms in the chicken embryonic heart, which may contribute to our understanding of Doppler signals derived from valveless embryonic human hearts at 5 to 8 weeks of gestation, prior to septation. This might eventually result in the development of clinical diagnostic tests to be applied during early human pregnancy. In future studies we will focus on inducing cardiac malformations using an intervention model, such as venous clipping, to gain further insight into the etiology of congenital heart defects, which may result in a higher detection rate of congenital structural heart defects.

REFERENCES

1. Forouhar, A.S., et al., *The embryonic vertebrate heart tube is a dynamic suction pump.* Science, 2006. **312**(5774): p. 751-3.
2. Butcher, J.T., et al., *Transitions in early embryonic atrioventricular valvular function correspond with changes in cushion biomechanics that are predictable by tissue composition.* Circ Res, 2007. **100**(10): p. 1503-11.
3. Clark, E.B. and N. Hu, *Developmental hemodynamic changes in the chick embryo from stage 18 to 27.* Circ Res, 1982. **51**(6): p. 810-5.
4. Nakazawa, M., et al., *Developmental hemodynamic changes in rat embryos at 11 to 15 days of gestation: normal data of blood pressure and the effect of caffeine compared to data from chick embryo.* Pediatr Res, 1988. **23**(2): p. 200-5.
5. Ursem, N.T., et al., *Ventricular diastolic filling characteristics in stage-24 chick embryos after extra-embryonic venous obstruction.* J Exp Biol, 2004. **207**(Pt 9): p. 1487-90.
6. Hogers, B., et al., *Unilateral vitelline vein ligation alters intracardiac blood flow patterns and morphogenesis in the chick embryo.* Circ Res, 1997. **80**(4): p. 473-81.
7. Stekelenburg-de Vos, S., et al., *Systolic and diastolic ventricular function assessed by pressure-volume loops in the stage 21 venous clipped chick embryo.* Pediatr Res, 2005. **57**(1): p. 16-21.
8. Hogers, B., et al., *Extraembryonic venous obstructions lead to cardiovascular malformations and can be embryolethal.* Cardiovasc Res, 1999. **41**(1): p. 87-99.
9. Hu, N. and E.B. Clark, *Hemodynamics of the stage 12 to stage 29 chick embryo.* Circ Res, 1989. **65**(6): p. 1665-70.
10. Broekhuizen, M.L., et al., *Hemodynamic parameters of stage 20 to stage 35 chick embryo.* Pediatr Res, 1993. **34**(1): p. 44-6.
11. Phoon, C.K., *Imaging tools for the developmental biologist: ultrasound biomicroscopy of mouse embryonic development.* Pediatr Res, 2006. **60**(1): p. 14-21.
12. McQuinn, T.C., et al., *High-frequency ultrasonographic imaging of avian cardiovascular development.* Dev Dyn, 2007. **236**(12): p. 3503-3513.
13. Hamburger, V. and H.L. Hamilton, *A series of normal stages in the development of the chick embryo.* J Morphol, 1951. **88**(4): p. 49-92.
14. Zhou, Y.Q., et al., *Applications for multifrequency ultrasound biomicroscopy in mice from implantation to adulthood.* Physiol Genomics, 2002. **10**(2): p. 113-26.
15. Gittenberger-de Groot, A.C., et al., *Basics of cardiac development for the understanding of congenital heart malformations.* Pediatr Res, 2005. **57**(2): p. 169-76.
16. Rothenberg, F., et al., *Emerging patterns of cardiac conduction in the chick embryo: waveform analysis with photodiode array-based optical imaging.* Dev Dyn, 2005. **233**(2): p. 456-65.
17. Liebling, M., et al., *Rapid three-dimensional imaging and analysis of the beating embryonic heart reveals functional changes during development.* Dev Dyn, 2006. **235**(11): p. 2940-8.
18. Hu, N. and B.B. Keller, *Relationship of simultaneous atrial and ventricular pressures in stage 16-27 chick embryos.* Am J Physiol, 1995. **269**(4 Pt 2): p. H1359-62.
19. Sissman, N.J., *Developmental landmarks in cardiac morphogenesis: comparative chronology.* Am J Cardiol, 1970. **25**(2): p. 141-8.
20. Hu, N., et al., *Diastolic filling characteristics in the stage 12 to 27 chick embryo ventricle.* Pediatr Res, 1991. **29**(4 Pt 1): p. 334-7.
21. Makikallio, K., P. Jouppila, and J. Rasanen, *Human fetal cardiac function during the first trimester of pregnancy.* Heart, 2005. **91**(3): p. 334-8.

3

Teratogenicity and underlying mechanisms of homocysteine in animal models: a review

N.H. van Mil, A.M. Oosterbaan, R.P.M. Steegers-Theunissen

Reproductive Toxicology 2010 Dec; 30(4):520-31

ABSTRACT

Introduction Hyperhomocysteinemia in humans is a risk factor for adverse pregnancy outcome, especially congenital malformations. This review summarizes the studies directed on the teratogenicity of homocysteine carried out in animal studies, and elaborates on the underlying mechanisms.

Methods Literature was searched in Pubmed (NCBI) through January 2010 and selected manually. Keywords comprised homocysteine, congenital abnormalities and animals.

Results Increased frequencies of a wide range of congenital malformations are reported especially in the chicken embryo after exposure to homocysteine (Hcy) in various dosages and forms. Reduced embryonic growth and abnormalities of the vascularization of the yolk sac are described in mouse studies. A study in rats revealed a reduced development of blastocysts. The congenital malformations observed in the chicken embryo model share the mutual involvement of Hcy sensitive neural crest cells. Derangements in the behavior of these cells by interactions between Hcy and pathways involved in vascularization, growth, metabolism, signaling, and DNA synthesis and methylation may explain the wide range of effects on embryonic organs, the yolk sac and placental tissues.

Conclusions The associations between human hyperhomocysteinemia and congenital malformations are substantiated by chicken and rodent studies. Moreover, derangements of several pathways induced by Hcy are demonstrated with adverse effects on both reproduction and long term health. Because of the high prevalence of hyperhomocysteinemia in both the reproductive and general population, research on underlying epigenetic mechanisms is warranted.

INTRODUCTION

Congenital malformations are the most important cause of perinatal morbidity and mortality and affect over 8 million children worldwide each year [1]. More than 80% of congenital malformations have a complex etiology, in which interactions between subtle structural genetic, i.e., single nucleotide polymorphisms (SNP) and environmental exposures such as periconception malnutrition and unhealthy lifestyles are implicated.

Three decades ago the pediatrician Professor Smithells was the first to suggest that a maternal folate shortage plays a part in the development of neural tube defects (NTD). His group showed that a low maternal folate status in the first trimester of pregnancy, which coincides with the period of neural tube closure, i.e., 21-28 days after conception, was associated with an increased risk of NTD offspring [2]. In a nonrandomised trial they also showed that periconception multivitamin use, including 360 µg of folic acid per day, reduced the recurrence risk of NTD by 86% [3]. These findings stimulated both human and animal studies on associations between folate and other complex congenital malformations and on the clarification of underlying mechanisms, e.g. the homocysteine (Hcy) pathway (figure 1) [4-6]. Moreover, worldwide this has resulted in the recommendation of a daily intake of 400 µg of folic acid in the periconception period by governments and international organizations, such as the World Health Organization and the Food and Drug Administration from 1991 onwards. Additionally, this has led to the stimulation of folic acid use through local and national campaigns, and to the launch of food fortification programs in several countries. These programs have already shown to significantly reduce birth prevalence rates of NTD [7-8].

The most recent meta-analysis of systematically reviewed human intervention studies revealed that, dependent on study design, i.e., case control (cc) or cohort studies and randomised controlled trials (c-rct), folic acid-containing multivitamins protect against NTD (cc 33% and c-rct 48%), cardiovascular defects (cc 22% and rct 39%), limb defects (cc 52% and rct 43%), orofacial clefts (cc 24% - 37%), urinary tract anomalies (cc 52%) and congenital hydrocephalus (cc 63%) [9].

In the early nineties Steegers-Theunissen et al. were the first to suggest that plasma Hcy is a more sensitive marker of the folate status than serum or plasma folate. This hypothesis was based on case-control studies in mothers with and without NTD offspring showing that a fasting Hcy concentration above approximately 14 µmol/L was associated with a 2 to 3 fold enhanced risk of NTD offspring [10]. This finding has been substantiated by studies of others [11-12]. The question remained, however, whether Hcy should be considered a sensitive biomarker of a compromised folate, vitamin B12, and vitamin B6 status, or a direct teratogen [5].

Figure 1

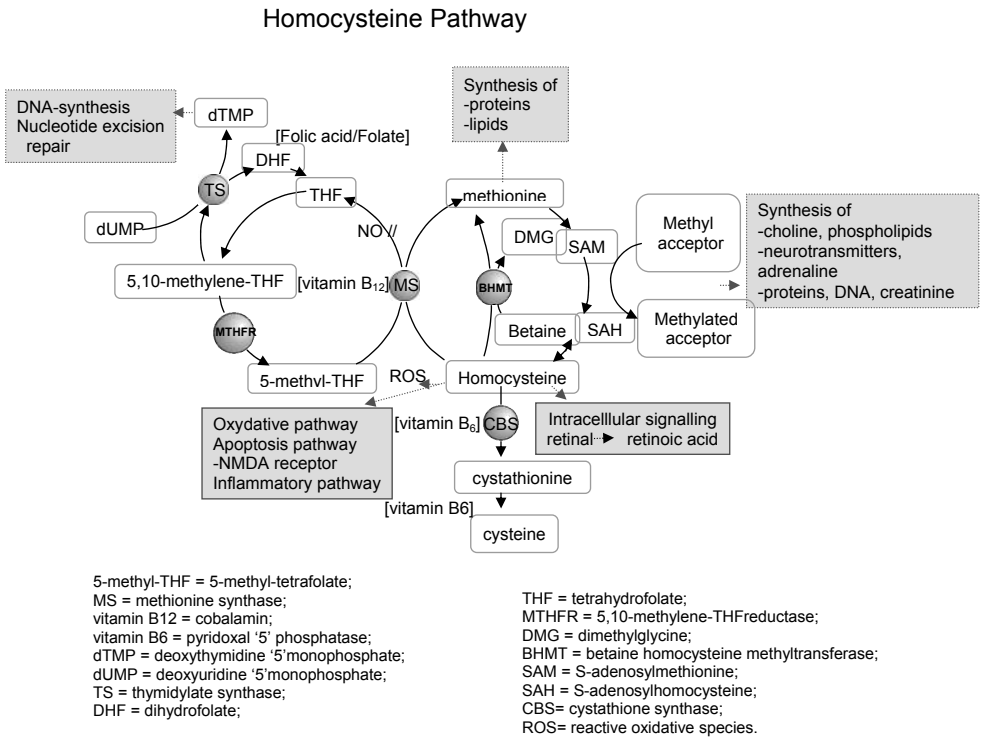

The homocysteine pathway, modified with permission of Mrs J. Boxmeer of the department of Obstetrics and Gynecology, Erasmus MC, University Medical Center, Rotterdam, The Netherlands.

Experimental animal studies were performed to explore the direct effects of Hcy after exogenous Hcy application and showed varying effects [13-18]. The effects were different between species and models used and appeared to be dependent on the period of Hcy exposure and the chemical structure of Hcy used. The focus of this review is to describe the congenital malformations reported in chicken, mouse and rat studies after exogenous Hcy application in animal models without a known genetic contribution (mutation, knock out) and to elaborate on the suggested associations and underlying mechanisms.

MATERIALS AND METHODS

Literature was searched in PUBMED (NCBI) through January 2010 that contained the keywords "homocysteine", "congenital abnormalities" and "animals". This was followed by the manual screening of the abstracts. In this review we only included original articles in which the teratogenicity of exogenous Hcy treatment in the chicken, mouse and rat were studied. Studies on genetic animal models of hyperhomocysteinemia were not in the scope of this review. This resulted in 22 articles, of which 16 studies were described in the chicken, 5 in the mouse and 2 in the rat. One study contained both mouse and rat experiments [14], and another study contained both chicken and mouse experiments [19]. The articles were sorted per species and summarized in the tables 1 and 2.

Homocysteine Pathway

The Hcy pathway is presented in figure 1. Folate as 5-methyltetrahydrofolate serves as a substrate in the remethylation of Hcy into methionine. A deficient folate intake induces a mild to moderate hyperhomocysteinemia. Elevated Hcy concentrations enhance the synthesis of Hcy thiolactone [20]. Thiolactone is a reactive metabolite to proteins which may explain some of the observed pathological features [21]. In most cases hyperhomocysteinemia and folate deficiency can be treated by folic acid use or by an increased intake of folate-rich foods [22]. Besides folate, numerous of other determinants are implicated in Hcy homeostasis varying from other vitamins, e.g. vitamin B12, vitamin B1 and vitamin B6, unhealthy lifestyles, e.g., high caffeine intake and smoking, medication use, renal and liver function, endocrine and physiological processes, to SNPs in folate related genes, e.g. MTHFR 677 C>T [23]. Although maternal hyperhomocysteinemia is significantly associated with NTD, orofacial clefts and congenital heart disease, current knowledge strongly suggests that Hcy is an epiphenomenon [12, 24-26].

Animal Studies

In table 1 an overview is given of the studies on the embryotoxic effects of Hcy in the chicken embryo. Three studies reported embryonic death (0-85%) [13, 27-28] and NTD was observed in five studies, with prevalence ranging from 11-100% [13, 29-32]. Orofacial clefts were described in one study (5.8% prevalence) [30], cardiovascular disease in three studies (28-83%) [19, 31, 33], somite deformities were reported in one study (92%) [31], brain abnormalities in two studies (86%) [31, 34] and ocular malformations in one study with a range of 9.5-100% [35].

Table 1 Overview of the studies on the embryotoxic effects of Hcy in the chick

Chick	Treatment	Period and place of Hcy application	Time of assessment	Outcome assessment	Morphological congenital malformations	Suggested underlying mechanism
Afman et al., 2003 [36]	- *In ovo* study - White Leghorn - 50 µL 0.1M L-Hcy-T - *In vitro* study - White Leghorn - 80 µL 30 mM L-Hcy-T, 10 or 30 mM L-Hcy	*In ovo*: - Period: HH2-10 - Place: inner shell membrane - 3 doses at HH2, 7 and 10 *In vitro*: - Period: HH8/9 - Place: droplet on embryo in bowl - Single dose	*In ovo:* HH21-22, HH23-24, HH25 *In vitro*: HH8/9 + 6 hr	*In ovo*: - Morphological examination *In vitro*: - Stereo microscope with video camera to count the number of somites	*In ovo* study: - NTD and somites comparable - More other malformations (29%, blisters, caudal regression, blood spots, abnormal vein development) - More degenerated embryos (36%) *In vitro* study: - Dose dependent widening ANP during 3-4 hr most pronounced in embryos with 4 somites - Reduced somite gain	- Hcy may react by homocysteinylation of protein lysine residues leading to protein damage. - Hcy induces alteration of neural crest cells of the eyes.
Andaloro et al., 1998 [28]	- *In ovo* study - Chicken embryos - 5 µmol DL-Hcy-T	- Period: HH1-13 - Place: droplet on inner shell membrane - 3 doses at HH1, 6 and 13	HH21-22	- Morphological examination	- 27.7% NTD - 46.8% mortality	- NMDA receptor antagonists like Hcy are teratogens, most probably by blocking the NMDA or a closely related receptor.
Boot et al., 2003 [56]	- *In vitro* study - White Leghorn - 30 or 300 µM Hcy	- Period: HH9-10 - Place: culture medium - Single dose	HH9/10+24-48hr	- Immunohistochemistry: HNK-1 –antibody (meural crest and differentiated nerves) and HHF35-antibody (muscle-specific actin - TUNEL technique (apoptosis) - Morphological examination	- ↑ neural crest cell outgrowth and migration from NT - inhibition of neural crest cell differentation	- Hcy increases neuroepithelial to neural crest cell transformation, resulting in shortage of neuroepithelial cells in NT, causing NTDs - Hcy affects neural crest cell differentiaton, leading to orofacial and conotruncal defects

Abbreviations: ANP: anterior neuropore; CS: injection in circulatory system; FA: fatty acids; HH: Hamburger and Hamilton stage; Hcy: homocysteine; LC: long chain; L-Hcy-T: L-homocysteine thiolactone; NCAM: neural cell adhesion molecule; NTD: neural tube defects; NT: injection in neural tube; PUFAs: polyunsaturated fatty acids; SC: short chain; VEGF: vascular endothelial cell growth factor

Boot et al., 2004a [33]	- *In vitro* study - White Leghorn - 30 µmol/l L-Hcy-T (NT), 30 or 300 µmol/l L-Hcy-T (CS)	- Period: HH9-10/14 - Place: NT (HH9-10), CS (HH14) - Single dose	HH30-40	- Immunohistochemistry: HHF35 (muscle specific actins), JB3 (antifibrillin-2), anti-fibronectin - Endothelin-1 in situ - Artery vessel wall analysis	NT: - HH30-31:detachment of endothelial cell from smooth muscle cell layer, ↓ fibrillin-2 and ↓ fibronectin expression in pharyngeal arteries - No effects on endothelin-1 expression, HHF35 and MF20 - HH40: ↓ lumen diameter brachiocephalic arteries, ↑ intima and media thickness, ↑ number of actin layers CS: None of the abnormal observations	- Hcy affects neural crest-derived pharyngeal arch arteries, leading to endothelial cell detachment.
Boot et al., 2004b [78]	- *In vitro* study - White Leghorn - NT: 30 µmol/l L-Hcy-T - CS: 30 or 300 µmol/l L-Hcy-T	- Period: HH9-10/14 - Place: NT (HH9-10), CS (HH14) - Single dose	HH18-35	- Immunohistochemistry: HHF35 (muscle specific actins), JB3 (antifibrillin-2), MF20 (antimyosin heavy chain) - Pax-3 in situ hybridization (neural crest cell expression) - TUNEL technique (apoptosis) - 3-D reconstructions	NT: - HH18: No difference in neural crest cell migration and Pax-3 expression, ↓ subendothelial fibrillin-2 expression and ↓ number mesenchymal cells in cardiac jelly of outflow tract - HH31: ↓ actin positive myocardial cells, 60% ↓ apoptosis outflow tract - HH35: 83% ↑ subarterial VSD, 25% ↑ non-myocardialized outflow tract cushion tissue, CS: None of the abnormal observations	- Hcy stimulates NMDA receptor resulting in increased ER, oxidative stress and subsequent apoptosis and neurotoxicity via membrane peroxidation (reduction of PUFA's). - Hcy increases SAH that reduces N-methyltransferases and thus the methylation of phosphatidylethanol-amine into phosphatidylcholine.
Brouns et al., 2005 [17]	- *In vitro* study - White Leghorn - 10 or 30 mM L-Hcy-T	- Period: HH6-8 - Place: droplet on inner shell membrane and closure site - Single dose	HH6-8	- Quantitative time-lapse video microscopy	- Flattening of head fold and neural tube - Closure delay at the initial closure site and at the anterior and posterior neuropores - Halting of cell movement	- Possible interference of Hcy with actin microfilaments because Hcy induces same effect as cytochalasin-D.
Epeldegui et al., 2002 [29]	- *In ovo* study - White Leghorn - 20 µmol L-Hcy-T	- Period: HH3-10 - Place: droplet on inner shell membrane - Single dose	HH18-23	- Morphological examination - 3-D reconstructions	- 39% open spina bifida - 26% more than 1 tube forming the spinal cord - 26% disorganized spinal cord - 75% ↓ cervical 3 dorsal root ganglia cells	- Hcy may antagonize the NMDA receptor thereby inducing NTD and other neural crest related defects.
Han et al, 2009 [19]	- *In vitro* study - White Leghorn - 30, 50, 75, 100 µM L-Hcy-T	- Period: HH 3-7 - Place: culture medium - Single dose		- Morphological examination - In situ hybridization for Hex and Islet-1	HH 3+/4-5 -78% cardiac abnormalities HH6-7 - normal development	- Hcy modulates WnT-β-catenin pathway during gastrulation.

The variations in frequencies of these malformations can partly be explained by differences in experimental set-up. Although similar chicken strains were used, variations in the chickens' diets, possibly influencing the yolk sac composition, and variations in developmental rates may have led to outcome differences[36]. The time of first treatment varied from HH1 to HH9 and the frequency of Hcy exposure varied from one to three times between these studies. There were also differences in study design, *in vitro* or *in ovo*, and the absence of tissue and intestinal barriers *in vitro* may result in a higher Hcy exposure than in the *in ovo* experiments. Additionally, the manner of Hcy application, i.e., injection into the neural tube, the circulatory system or the amniotic sac, or the *in ovo* administration of Hcy through droplets on the inner shell membrane, and the *in vitro* addition of Hcy to the medium, is also of influence. *In ovo* administration of Hcy leads to less precise timing and concentration of exposure.

Table 2 summarizes the studies on the embryotoxic effects of Hcy in the mouse and the rat. Ten different mouse strains were studied, and only one *in vitro* study in the CD-1 strain and one *in vivo* study in the C57 strain showed significantly more embryonic abnormalities after Hcy exposure [16, 19]. No increase in NTD frequency was reported in both the *in vivo* [37] and the *in vitro* [18] rodent studies. Morphological features of derangements in early neural tissues were observed in two *in vitro* rodent studies [14, 16]. Reduced embryonic growth and abnormalities of the yolk sac vascularization and diameter were reported in two *in vitro* mouse studies [16, 18]. One non invasive *in vivo* ultrasound study showed 66% valve regurgitation after Hcy exposure caused by cardiac valve defects [19]. Hcy also decreased placental weight, crown-rump length and body weight. One *in vitro* mouse study revealed a 4-fold reduction of embryos developing into blastocysts [14]. *In vitro* mice studies, Hcy showed to have a dose dependent effect, and high Hcy concentrations added to the medium caused blisters, growth retardation and abnormalities in somite development [16]. The observed dose-dependent lethality, growth retardation and frequency of congenital malformations is supported by the toxic effects of very high Hcy concentrations and the beneficial effects of low Hcy exposure, resulting in a reduction of dysmorphological features in the rat *in vitro* compared to control embryos [15]. Van Aerts et al. state that this beneficial effect may be explained by the conversion of L-homocysteine to L-methionine, probably a limiting amino acid in embryonic development. Due to this conversion THF is also liberated and available for its essential functions, such as purine and thymidine synthesis.

The variability of the results in rodent studies are comparable to chicken studies, and can partly be explained by differences in the moment and duration of Hcy exposure, the finally achieved Hcy level, the maternal diet, the period between exposure and

morphological outcome assessment, the method of outcome assessment and the rodent strain studied. The study by Han et al. emphasizes the critical importance of the application of Hcy at the right moment during development to induce a defect. The heart defects described in this study were only seen if exposure was very early at embryonic day 6.75. If treated earlier lethality of the embryos occurred, and if treated 24 hours later no defects were seen [19]. Also the importance of the method of outcome assessment was shown by this study. With the use of non invasive ultrasound examination changes in cardiac function were demonstrated after Hcy exposure in a mouse strain without a genetic predisposition for NTD, as no cardiac defects were reported in all other nonmutant mouse studies after morphological examination. Han et al. only analyzed malformations of the heart, while others mainly focussed on the presence of NTD, thereby missing on other malformations.

The failure of Hcy to induce effects in the experimental rodent model may also be related to the importance of the yolk sac. *In vitro*, the yolk sac provides a large surface for respiratory and nutritional exchange between embryo and substrate. This might explain why the pre-organogenesis staged rodents, where the yolk sac is not well developed, have proved very difficult to grow *in vitro* [38-39]. Probably, when a whole-embryo culture system is used, Hcy is not taken up by the yolk sac [18], which may explain the lack of Hcy effects. The variability of sera used in rodent studies can also explain differences in study outcome. Van Aerts et al. primarily or entirely used human serum for their rodent studies [14-15]. Heterologous serum like human serum used in rodent studies contains embryotrophic activity. In contrast, the use of rodent serum demonstrates immunologic reactivity. Both sera can cause toxic effects and are therefore not the ideal culture media to observe teratogenicity of exogenous Hcy treatment [38-40].

Effects of Hcy were stereospecific, where D-Hcy failed to cause effects, L-Hcy showed to cause an effect in the *in vitro* rodent studies and L-Hcy-thiolactone caused detrimental effects in *in vivo* and *in vitro* chicken models [13-14, 29]. In chickens but not in rodents, malformalities like NTD were induced by Hcy. The chicken and *in vitro* rodent embryo models have the advantage of a technically easier manner of drug application compared to *in vivo* rodent studies. Additionally, chicken and rodent embryo *in vitro* studies both have the advantage of the absence of maternal influences, such as the clearance of Hcy by the placenta [38]. Also in chicken embryos, resorption of non viable litter during early embryogenesis does not occur. A limitation in the rodent studies may have been the hindering effect or metabolizing capacity of the amniotic membranes after Hcy application. But even when eliminating these effects by injecting Hcy into the amniotic sac, mouse embryos failed to show malformations [18-19, 37].

Table 2 Overview of the studies on the embryotoxic effects of Hcy in rodents

Chick	Treatment	Period and place of Hcy application	Time of assessment	Outcome assessment	Morphological congenital malformations	Suggested underlying mechanism
Afman et al., 2003 [36]	- *In ovo* study - White Leghorn - 50 µL 0.1M L-Hcy-T - *In vitro* study - White Leghorn - 80 µL 30 mM L-Hcy-T, 10 or 30 mM L-Hcy	*In ovo*: - Period: HH2-10 - Place: inner shell membrane - 3 doses at HH2, 7 and 10 *In vitro*: - Period: HH8/9 - Place: droplet on embryo in bowl - Single dose	*In ovo:* HH21-22, HH23-24, HH25 *In vitro*: HH8/9 + 6 hr	*In ovo*: - Morphological examination *In vitro*: - Stereo microscope with video camera to count the number of somites	*In ovo* study: - NTD and somites comparable - More other malformations (29%, blisters, caudal regression, blood spots, abnormal vein development) - More degenerated embryos (36%) *In vitro* study: - Dose dependent widening ANP during 3-4 hr most pronounced in embryos with 4 somites - Reduced somite gain	- Hcy may react by homocysteinylation of protein lysine residues leading to protein damage. - Hcy induces alteration of neural crest cells of the eyes.
Andaloro et al., 1998 [28]	- *In ovo* study - Chicken embryos - 5 µmol DL-Hcy-T	- Period: HH1-13 - Place: droplet on inner shell membrane - 3 doses at HH1, 6 and 13	HH21-22	- Morphological examination	- 27.7% NTD - 46.8% mortality	- NMDA receptor antagonists like Hcy are teratogens, most probably by blocking the NMDA or a closely related receptor.
Boot et al., 2003 [56]	- *In vitro* study - White Leghorn - 30 or 300 µM Hcy	- Period: HH9-10 - Place: culture medium - Single dose	HH9/10+24-48hr	- Immunohistochemistry: HNK-1 –antibody (meural crest and differentiated nerves) and HHF35-antibody (muscle-specific actin - TUNEL technique (apoptosis) - Morphological examination	- ↑ neural crest cell outgrowth and migration from NT - inhibition of neural crest cell differentation	- Hcy increases neuroepithelial to neural crest cell transformation, resulting in shortage of neuroepithelial cells in NT, causing NTDs - Hcy affects neural crest cell differentiaton, leading to orofacial and conotruncal defects

Abbreviations: AUC: area under curve; L-Hcy-T: L-homocysteine thiolactone; D, L-Hcy L-Hcy; E: gestational day; SAM: S-adenosyl-methionine; SAH: S-adenosyl-homocysteine

Boot et al., 2004a [33]	- *In vitro* study - White Leghorn - 30 µmol/l L-Hcy-T (NT), 30 or 300 µmol/l L-Hcy-T (CS)	- Period: HH9-10/14 - Place: NT (HH9-10), CS (HH14) - Single dose	HH30-40	- Immunohistochemistry: HHF35 (muscle specific actins), JB3 (antifibrillin-2), anti-fibronectin - Endothelin-1 in situ - Artery vessel wall analysis	NT: - HH30-31:detachment of endothelial cell from smooth muscle cell layer, ↓ fibrillin-2 and ↓ fibronectin expression in pharyngeal arteries - No effects on endothelin-1 expression, HHF35 and MF20 - HH40: ↓ lumen diameter brachiocephalic arteries, ↑ intima and media thickness, ↑ number of actin layers CS: None of the abnormal observations	- Hcy affects neural crest-derived pharyngeal arch arteries, leading to endothelial cell detachment.
Boot et al., 2004b [78]	- *In vitro* study - White Leghorn - NT: 30 µmol/l L-Hcy-T - CS: 30 or 300 µmol/l L-Hcy-T	- Period: HH9-10/14 - Place: NT (HH9-10), CS (HH14) - Single dose	HH18-35	- Immunohistochemistry: HHF35 (muscle specific actins), JB3 (antifibrillin-2), MF20 (antimyosin heavy chain) - Pax-3 in situ hybridization (neural crest cell expression) - TUNEL technique (apoptosis) - 3-D reconstructions	NT: - HH18: No difference in neural crest cell migration and Pax-3 expression, ↓ subendothelial fibrillin-2 expression and ↓ number mesenchymal cells in cardiac jelly of outflow tract - HH31: ↓ actin positive myocardial cells, 60% ↓ apoptosis outflow tract - HH35: 83% ↑ subarterial VSD, 25% ↑ non-myocardialized outflow tract cushion tissue, CS: None of the abnormal observations	- Hcy stimulates NMDA receptor resulting in increased ER, oxidative stress and subsequent apoptosis and neurotoxicity via membrane peroxidation (reduction of PUFA's). - Hcy increases SAH that reduces N-methyltransferases and thus the methylation of phosphatidylethanol-amine into phosphatidylcholine.
Brouns et al., 2005 [17]	- *In vitro* study - White Leghorn - 10 or 30 mM L-Hcy-T	- Period: HH6-8 - Place: droplet on inner shell membrane and closure site - Single dose	HH6-8	- Quantitative time-lapse video microscopy	- Flattening of head fold and neural tube - Closure delay at the initial closure site and at the anterior and posterior neuropores - Halting of cell movement	- Possible interference of Hcy with actin microfilaments because Hcy induces same effect as cytochalasin-D.
Epeldegui et al., 2002 [29]	- *In ovo* study - White Leghorn - 20 µmol L-Hcy-T	- Period: HH3-10 - Place: droplet on inner shell membrane - Single dose	HH18-23	- Morphological examination - 3-D reconstructions	- 39% open spina bifida - 26% more than 1 tube forming the spinal cord - 26% disorganized spinal cord - 75% ↓ cervical 3 dorsal root ganglia cells	- Hcy may antagonize the NMDA receptor thereby inducing NTD and other neural crest related defects.
Han et al, 2009 [19]	- *In vitro* study - White Leghorn - 30, 50, 75, 100 µM L-Hcy-T	- Period: HH 3-7 - Place: culture medium - Single dose		- Morphological examination - In situ hybridization for Hex and Islet-1	HH 3+/4-5 -78% cardiac abnormalities HH6-7 - normal development	- Hcy modulates WnT-β-catenin pathway during gastrulation.

Table 2 Overview of the studies on the embryotoxic effects of Hcy in rodents

Kobus et al., 2009 [32]	- *In ovo* study - White Leghorn - 25 µmol DJ-Hcy	- Period: HH 9 - Place: injection into yolk sac - Single dose	HH23	- TUNEL technique (apoptosis) - Immunohistochemistry : NCAM-antibody	- 100% NTD - ↓ thickness mantle and marginal layers of the spinal cord - ↓ NCAM expression in spinal cord and mesenchymal tissue	- Hcy causes disruption of spinal cord layers morphology by reducing NCAM expression
Latacha et al., 2005 [27]	- *In vitro* study - Pathogen-free chicken embryos - 25, 50, 75, 100 mM L-Hcy-T	- Period: HH8, 12 - Place: droplet on inner shell membrane - 2 doses at HH8, 12	HH20	- Morphological examination - Stereo microscope with video camera to count the number of vascular branches in vitelline artery - mRNA expression analyse with VEGF and beta-actin primers - Immunocytocchemistry VEGF protein with antibodies	- 50-100 mM L-Hcy-T: - 68%, 50%, 34% ↓ embryonic survival -dose depended ↓ vascular density - ↓ mRNA and protein expression VEGF	- Hcy may impair extra-embryonic vascularization by reducing VEGF expression
Lee et al., 1975 [31]	- *In vitro* study - White Leghorn - 0.3 mM Hcy	- Period: HH 1 - Place: on subculture medium - Single dose added after pre-treatment with BrdU	HH5-6	- Morphological examination	After pretreatment with BrdU: - 92% somite deformities - 86% brain abnormalities - 78% NTD - 28% congenital heart disease	- Hcy may be unable to directly participate in transmethylation.
Maestro de las Casas et al., 2003 [35]	- *In ovo* study - White Leghorn - 8 µl or 20µmol L-Hcy-T	- Period: HH3-8/10 - Place: inner shell membrane - Single dose	HH17-20	- Morphological examination - Immunohistochemistry anti-fibrillin-1 antibody	HH 17–20 (3): - 100% microphthalmia, -40% lens dislocation, - 40% retina deformities HH 17–20 (8–10): - 42.8% microphthalmia, - 9.5% lens dislocation, - 23.8% retina deformities - All optic cup malformations (bilateral microphthalmia) had NTD - No differences in fibrillin-1 expression	- Hcy may act specifically on the neural tube and dorsal root ganglia (tissue specificity).

Miller et al., 2003 [34]	- *In ovo* study - White Leghorn - 100, 200 or 300 µmol/kg D-, L-Hcy	- Period: HH1-12 - Place: injection in air sac - 3 doses at HH1, 6 and 12	HH37	- Morphological examination - Mass measurements of brain and embryo	- ↓ brain phosphatidylcholine levels - ↑ brain phosphatidylethanolamine - ↓ LC unsaturated membrane FA - ↑ SC saturated membrane FA - ↑ 2.6 to 3.3 fold caspase-3 activity (apoptosis) - ↓ embryo mass - ↓ embryonic survival	- Hcy may change the methylation of DNA, RNA or proteins like actin caused by high S-AdenosylHcy or Hcy.
Rosenquist et al., 1996 [13]	- *In ovo* study - Chicken embryos - 0.5-20 µmol D, L-Hcy or equivalent dose L-Hcy-T - 5 µmol L-Hcy-T	- Period: HH1-12 - Place: droplet on inner shell membrane - 3 doses at HH1, 6 and 12 - Period HH12, 20, 24 - Place: droplet on inner shell membrane - 3 doses at HH6, 12 and 20	HH14 HH35	- Morphological examination - Immunofluorescence for smooth muscle alpha-actin	- 5-15 µmol D,LHcy 18%-75% NTD - ↑10 µmol D,L Hcy 85%-27% survival - 20 µmol D,L Hcy 100% lethality - 11% NTD - 79% ventral closure defects - 23% ventricular septum defects	- Hcy at low concentrations may act as a growth factor in particular on smooth muscle cells and at high concentrations it is cytotoxic due to changes in gene expression.
Rosenquist et al., 1999 [30]	- *In vitro* study - Pathogen-free chicken embryos - 5 µmol L-Hcy-T	- Period: HH1-13 - Place: droplet on inner shell membrane - 3 doses at HH1, 6 and 12-13	HH20-21	- Morphological examination	- 36.7% multiple defects - 34.8% spinal closure defects - 16.1% cranial closure defects - 6.4% torsion defects - 5.8% orofacial defects	- Hcy may act as an antagonist of the NMDA receptor or a related receptor, which may regulate key processes in neural tube closure and neural crest cell migration, plausibly by apoptosis or programmed cell death.
Tierney et al., 2004 [57]	- *In ovo* study - White Leghorn - 10 µmol D,L-Hcy	- Period: HH6-7 - Place: droplet on inner shell membrane - Single dose	HH10-11	- Immunohistochemistry : anti-BrdU and donkey anti-mouse fluorescein isothiocyanate	- ↑ number of neural tube cells - ↓ neural crest cell number - total sum of cells equal as controls - ↓ labeling index of newly formed neural crest cells. - ↓ neural crest dispersal - ↓ distance neural crest cells migrated from the NT	- Hcy either blocks cell cycle progression of neural crest progenitors needed for epithelial–mesenchymal transition, or delays the entry of newly formed neural crest cells into the S-phase needed for cell division

As embryogenesis takes place in a very narrow time window, the exact timing and duration of Hcy exposure is of main importance for the induction of different congenital malformations. NTD develop as a consequence of failure in the closure of the neural tube or developing tail bud during embryogenesis. Formation of the cranial neural tube is called primary neurulation, and the formation of the caudal neural tube through cavitation of the tail bud is called secondary neurulation. Both in the human and the chicken embryo an overlap zone has been described in which mechanisms of both primary and secondary neurulation simultaneously take place [40]. It has been shown in the chicken embryo that Hcy affects both the primary and secondary neurulation processes [29]. An overlap zone has not been discovered in rodents, which may be an explanation for the absence of Hcy induced NTD in rodent embryos.

Also differences in genetic background of the rodent strains may have influenced the results. As known in humans, a family history of NTD-affected pregnancies is one of the strongest risk factors for these birth defects. Risk of NTD is elevated with 3–8% in siblings of affected individuals and NTD are more common among certain ethnic groups [41]. NTD is not simply a condition of folate deficiency: maternal folate levels in most human NTD-affected pregnancies are in the 'normal' range [42]. Low folate status may increase susceptibility, but is not necessarily the direct cause of NTD. This is substantiated in mouse studies, as dietary folate deficiency caused significant embryonic growth retardation, but did not lead to the development of NTD [43-46]. It is plausible that especially the combination of genetic and environmental risk factors is responsible for the level of susceptibility to NTD. This is in line with the idea that the sensitivity to Hcy in rodent studies is affected by the genetic background of the strain studied [16]. Folate deficiency, however, does not induce NTD in mice without a genetic predisposition [43, 45-47]. However, as genetic risk factors in the wild-type curly tail (ct) mouse are normally insufficient to cause NTD, in combination with a folate-deficient diet leading to hyperhomocysteinemia, NTD occur [47].

Mouse mutant studies have shown that the rodent remains a suitable model to study NTD in relation to metabolites of the Hcy pathway. Mutant strains have proven to be useful to explore the mechanism by which folate prevents NTD. Rescue of the genetically originated NTD phenotype by folic acid administration has been demonstrated in the splotch mutant, both in cultured embryos and after maternal folic acid administration *in vivo* [48-49]. Also the restoration of cardiac function by folic acid due to teratogenic effects of Hcy have been shown in the C57 mouse [19]. Folate-responsiveness was also observed in the crooked tail mutant mouse (Cd) using a series of folic acid doses *in vivo* within a range comparable to those recommended for prevention of NTD in humans. Exencephaly in these Cd homozygotes showed a dose-dependent response to maternal folic acid administration,

leading to a 59% reduction of exencephaly, which is comparable to the reduction of NTD after folic acid use in humans [50]. In the mouse mutant strain lacking a functional folate-binding protein gene (Folr1) and mice showed increased Hcy levels and low folate levels, folic acid partially rescued the neural- and neural crest related defects induced by Hcy [51]. However, in humans, around 30% of NTD appear unresponsive to folic acid supplementation as do a large number of mouse genetic mutants that exhibit NTD [52]. For example, the mouse mutant strain homozygous for the ct mutation develops spina bifida and shows many similarities to the corresponding human NTD. Ct mice have higher plasma Hcy levels than controls, and it was shown that inositol supplementation did prevent spinal NTD, in contrast to folic acid [53]. This latter finding has led to inositol supplementation in some human pregnancy at high risk of NTD [54] and coincides with the situation that some families do and others do not benefit from folic acid supplementation. The complex mechanism and pathways underlying the development of NTD, including interactions of genetic and environmental factors as well as metabolic status, still need further investigation.

Mechanisms and Pathways

We conclude from the chicken and rodent studies that Hcy can induce a wide spectrum of congenital malformations varying from NTD, orofacial clefts, congenital heart disease, ocular to brain abnormalities, as well as growth restriction. One possible explanation is that all of the affected organ systems share the mutual involvement of neural crest cells [40]. As shown recently, Hcy affects the neural crest by modulating the Wnt-β-catenin pathway, repressing the Wnt-β-catenin-modulated genes Hex and Isl1 in the cardiogenic regions [19]. Canonical Wnt signaling plays an essential role in cardiac development, neural development, and neural crest induction. The rescue by folic acid of the defects induced by Hcy in this study suggests that folic acid is able to interfere with Wnt signaling. This is supported by the study of Boot et al. showing in an *in vitro* chicken embryo study that Hcy increases neural crest cell outgrowth and migration from the neural tube and inhibits neural crest cell differentiation into nerve and smooth muscle cells [33, 55]. Increased Hcy levels lead to an increase in neuroepithelial to neural crest cell transformation resulting in a shortage of neuroepithelial cells that lead to the development of NTD. The *in vivo* study by Tierney et al., however, showed that elevated Hcy increases the number of neural tube cells but decreases the number of neural crest cells [56]. They suggested that Hcy exposure reduced the number of neural crest cells either by a delay or inhibition of epithelial to mesenchymal transition of neural crest progenitor cells, or a delay in the entry of newly formed neural crest cells into the S-phase needed for cell division. They also showed that the migration of neural

crest cells was delayed or inhibited, resulting in a reduced migration distance. However, differences between these studies may be due to the timing of outcome assessment as well as the way neural crest cells were identified. We can conclude that induction of developmental malformations by Hcy can be caused by directly influencing neural crest cell proliferation or migration.

NCAM, NMDA and Folate Binding Proteins

The neural cell adhesion molecule (NCAM) is necessary for neural tube closure, as it is expressed in the neuroepithelium during neural folding [57]. Recently, Kobus et al. have found a reduced NCAM expression in both the spinal cord and mesenchymal tissue of chicken embryos after Hcy application [32]. All embryos showed failure of neural tube closure and reduced NCAM expression after Hcy administration. NCAM expression appears to play a permissive role in developmental processes of the nervous system, allowing structural remodeling by decreasing cell adhesion mediated by NCAM and thereby facilitating the guidance and targeting of axons, synaptogenesis and migration of neuronal and glial precursors [58-59]

Another interesting protein is the N-methyl-D-aspartate (NMDA) receptor expressed in neural tissue during the early stages of chicken embryo development [28, 60]. The NMDA receptor is a principal regulator of neuronal cell migration, cell-to-cell adhesion, intracellular calcium flux and apoptosis and behaves as a growth factor during neuronal development [28, 61]. Elevated Hcy acts as an NMDA receptor antagonist, thereby inducing endoplasmic (ER) stress and subsequent apoptosis, endothelial dysfunction, and neurotoxicity [34]. Inhibition of the NMDA receptor induces neural crest related congenital malformations [30, 60]. Furthermore, Hcy interacts with other NMDA receptor antagonists and as such promotes abnormal development [62]. The NMDA receptor comprises of 2 or three subunits, and the NR-1 subunit is obligatory for receptor functionality. It has been shown that Hcy binds to the glycine site of the NR-1 subunit [63]. Neither the time of expression nor the protein of the NR-1 subunit of the NMDA receptor was detected in mouse embryos [64], which may explain failure of Hcy to induce congenital malformations like NTD via the NMDA receptor in the experimental rodent models.

Folate binding proteins are highly expressed in precursors of neural crest cells and neuroepithelial cells. These receptors are necessary for the transfer of folate into the cells. A folate shortage increases the intracellular Hcy concentration with teratogenetic effects. Therefore, it is very likely that derangements in the structure and function of folate receptors affect the teratogenicity of Hcy [65], as shown in the Folr1 mouse lacking a functional folate-binding protein gene [51]. Hcy levels in these mice were increased and neural crest

related defects were reported. This also emphasizes that deficiencies of cofactors of the Hcy pathway cause hyperhomocysteinemia, but they may cause primary teratogenic effects as well.

Oxidative Pathway

Derangements in the oxidative pathway result in oxidative stress and more specifically ER stress. ER stress leads to an upregulation of apoptose- inducing proteins such as c-Jun N-terminal kinases. Most evidence is available on the induction of oxidative and ER stress by Hcy via the following three mechanisms. Firstly, the highly reactive thiol group of Hcy can undergo auto-oxidation, thereby generating increased production of reactive oxygen species (ROS). Excessive ROS production, not being counteracted by antioxidant enzymes and substrates, induces oxidative and ER stress [66]. Secondly, hyperhomocysteinemia decreases the transcription, translation and catalytic activity of antioxidant enzymes, such as glutathione peroxidase (GPx) and superoxide dismutase (SOD). This leads to an accumulation of oxidative products of Hcy like hydrogen peroxide (H_2O_2). Hcy may cause endothelial dysfunction by impairing endothelial cell's ability to detoxify H_2O_2 with subsequent reduction of bioactive Nitric Oxide (NO) [67-68]. Thirdly, high Hcy concentrations inhibit nitric-oxide synthase (NOS), resulting in a reduced bioavailability of nitric oxide and consequently in hyperoxia [66, 68-69]. The reduction of NO leads to the generation of asymmetric dimethylarginine (ADMA) that promotes the uncoupling of NOS resulting in an increased production of superoxide and other reactive oxygen species (ROS) [70]. The comprehensive pathway analysis by Sharma et al. (2006) also showed that hyperhomocysteinemia leads to the expression of several genes of the oxidative pathway, such as inducible NOS, NOS2 and SOD [71]. Neural crest cells contain lower endogenous levels of ROS, SOD and catalase and therefore might be particularly susceptible to the harmful effects of ROS [72]. High levels of ROS may block the closure of the neural tube by inhibition of the methionine synthase reaction via accumulation of vitamin B12 (figure 1) [73-74]. In case of high NO, methionine synthase activity can be rescued by folic acid or vitamin B12. As Hcy leads to a reduced bioavailability of NO resulting in increased production of ROS, Hcy may in this way inhibit neural tube closure.

Vascular Pathway

The observed abnormalities in angiogenesis after elevated Hcy exposure that lead to changes in embryogenesis, placentation, growth restriction and death are of interest [33]. Normal development of the extra-embryonic vasculature is critical for maintaining pregnancy. Latacha and Rosenquist showed decreased angiogenesis in extra-embryonic

vasculature after Hcy administration in the chicken embryo [27]. Hcy reduced mRNA and protein expression of vascular endothelial growth factor (VEGF), which is essential for normal vascular development. Oxidative and ER stress significantly affected vascularization processes during yolk sac development and embryogenesis *in vitro* [18, 75-76]. The Hcy induced reduction of NO induces vasoconstriction and as such leads to derangements in the vascularization of the embryonic organs, placenta and yolk sac. It is clear that the excessive production of ROS also directly damages endothelial cells and subsequent vascularization, with congenital malformations and death as direct consequences. This is in line with the reported abnormalities of the vessel walls in neural crest derived pharyngeal arteries [77] and vein development [36] in the chicken, and of the yolk sac circulation in the mouse [16].

Apoptosis and Inflammatory Pathways

Dose dependent elevation of Hcy exposure influences apoptosis and inflammation, thereby deranging intracellular signaling processes [78]. Intravitreal injections of Hcy in adult mice induced apoptosis in the retina [79] and in the adult brain. Moreover, Hcy has been suggested to induce apoptosis and neurotoxicity through stimulation of the NMDA receptors, resulting in increased levels of ROS and cytoplasmic Ca^{2+} [34]. In the 8.5 to 9 days old chicken embryo, Hcy induced abnormal differentiation behaviour of neural crest cells, leading to reduced extracellular matrix protein expression and reduced apoptosis in the cardiac outflow tract [33, 77]. Neural crest cells are supposed to undergo apoptosis and provide signals required for myocardialization, but after Hcy exposure they failed. This was explained by a direct or indirect toxic effect of Hcy on neural crest cells. Therefore, we conclude that Hcy influences the apoptosis pathway, either by inducing apoptosis through the derangement of intracellular signaling processes or reducing apoptosis at the level of cardiac neural crest cells by changing these cells behavior at the level of the outflow tract.

The retinoic and c-Myc pathway are important in signalling and are both affected by Hcy. Studies in mice showed that retinoic acid plays an important role in eye, craniofacial region, skeleton and heart development [80-83]. Hyperhomocysteinemia induced congenital malformations by inhibition of the oxidation of retinal to retinoic acid, the active vitamin A derivative, which may be an explanation of the teratogenicity of vitamin A [63] c-Myc is a proto-oncogene and important in apoptosis due to its stimulation of the release of cytochrome C to the cytosol, thereby triggering the pathways of CD95 and p53. Because c-Myc is responsible for a wide variety of apoptotic insults, such as DNA damage, hypoxia and nutrient deprivation, its inhibition by Hcy may not only lead to cancer, but also to derangements in embryogenesis, placentation and yolk sac development [84].

It has been suggested that Hcy stimulates chronic low-grade inflammation, thus promoting increased oxidative stress by the production of free radicals. The effects of elevated Hcy on the inflammation pathway is suggested to be due to the influence on neutrophils and endothelial cells, making them more adhesive [85]. The Hcy induced expression of the proinflammatory chemokines monocyte chemoattractant factor (MCP) -1 and interleukin (IL) -8 in human aortic endothelial cells was suggested to play a role in the pathogenesis of vascular disease through leukocyte recruitment [86]. Since inflammation increases the synthesis of NO [87], it further supports the fact that circulating Hcy is a marker related to inflammation and modulates embryonic development by affecting the oxidative pathway as described above.

The aforementioned evidence and suggestions emphasize the teratogenicity of Hcy through derangements in apoptosis and the inflammatory pathway.

Protein, Lipid and DNA Synthesis

Proteins are essential for growth and therefore the Hcy induced reduction of protein synthesis is in line with the observed increased frequency of growth retardation in the chicken and mouse embryo [16, 36] and the reduced embryonic mass in chicken [34].

A mechanism resulting in a reduced functionality of proteins is the increased homocysteinylation of amino acid residues such as lysine by Hcy, which may alter the physicochemical properties and biological activity of proteins [20, 35, 88].

Lysine oxidase, an important enzyme responsible for the posttranslational modification and essential for the biogenesis of connective tissue matrices, is irreversibly inactivated by Hcy [89-91]. Inhibition of methionine synthase activity by folate or vitamine B-12 shortage increases metabolic conversion of Hcy to Hcy thiolactone. The thiol groups of this reactive thioester incorporate in intra- and extracellular proteins. This change in physicochemical properties results in protein damage, manifested as a loss or reduction of its function [20]. The divergence of neural walls/folds, flattening and halting of cell movements, is suggested to be due to homocysteinylation of the extracellular matrix proteins fibrillin-2, fibronectin and actin [17, 33, 77, 88]. The detection of methylated proteins remains a challenge and has been established only in a handful of individual proteins due to its relatively low abundance and heterogeneous nature.

The interference of Hcy with lipid metabolism is illustrated by the study of Miller et al. (2003), which showed that hyperhomocysteinemia resulted in the inhibition of the conversion of phosphatidylethanolamine to phosphatidylcholine, contributing to cell death by increasing membrane fluidity [34]. Exposure to Hcy also decreased levels of long-chain unsaturated membrane fatty acids in the brain of the chicken embryo, associated with

necrosis and apoptosis [34, 92]. The reduction of the extracellular matrix proteins fibrillin-2 and fibronectin, VEGF expression, NCAM and the decreased phosphatidylcholine content of the brain membranes suggest that Hcy may impair embryonic development by reducing protein expression [27, 33-34, 36].

The Hcy induced reduction of DNA synthesis is supported by the observation that an increase of ROS reduces thymidine synthesis via inhibition of methionine synthase activity (figure 1). The reduced thymidine synthesis can also lead to a replacement of thymidine by uridine. Reduction of the nucleotide excision repair capacity and increased DNA damage have been reported after Hcy exposure of neural crest derived neurons [93].

Protein, Lipid and Chromatin Methylation

Hyperhomocysteinemia results in elevated S-adenosylhomocysteine (SAH), being an important inhibitor of S-adenosylmethionine-(SAM)-dependent methyltransferases, which can lead to DNA hypomethylation and associated alterations in expression of many genes, disrupted protein synthesis and repair.

The reduction of SAM and increase of SAH levels by hyperhomocysteinemia, both markers of a reduced supply of methyl groups, leads to global hypomethylation [94] . However, global DNA methylation was not affected in *splotch* mice put on a folate deficient diet [43]. Data from studies in the rat suggested that the methylation of the extracellular matrix proteins actin and tubulin is required for proper neural tube closure [95]. This is in line with the reduced methylation index of actin and myosin fibril residues in neural tube proteins of methionine-deficient rat embryos observed by Coelho and Klein [96]. Because of the similarity in effects on cranial neurulation of Hcy and the polymerization inhibiting factor for actin, cytochalasin-D, Brouns et al. suggested interference of Hcy with actin filaments [17].

Chromatin methylation involves the methylation of cytosine at the carbon-5 position in CpG dinucleotides, i.e., DNA methylation, and the methylation of histone tails as posttranslational modification. These two processes work together to affect the chromatin packaging of DNA, which in turn determines which gene(s) can be transcribed [97]. In mammals, DNA-methylation is the best-understood epigenetic signal and explains stabile gene-expression, such as imprinting, X-chromosome inactivation, and labile reversible gene-expression profiles. Several studies have demonstrated that hyperhomocysteinemia results in elevated SAH and decreased DNA methylation [94, 98-100]. Studies on the effects of Hcy on histone methylation, however, are lacking. The Hcy induced decrease of DNA methylation may have consequences for the programming and expression of genes involved in embryogenesis. A nice example is the study of Matsuda and Yasutomi (1992) showing hypomethylation of DNA in embryos with NTD. In other experiments with

the Agouti^{vy} mouse it was shown that a prenatal methyl deficiency resulted in a reduced methylation of the agouti gene across tissues, which was associated with increased gene-expression resulting in a yellow coat [101]. The gene expression modulation induced by Hcy through altered methylation leads to several pathological conditions, including congenital malformations. This is supported by the review of Sharma et al. (2006) showing that Hcy effects gene expressions, including that of methyltransferases [71].
The derangements of several pathways induced by Hcy have adverse effects on both reproduction and long term health. Because of the high prevalence of hyperhomocysteinemia in both the reproductive and general population, research on underlying epigenetic mechanisms is warranted.

Conclusion
Chicken embryo studies confirm the associations observed in humans between hyperhomocysteinemia and complex congenital malformations. Although the high Hcy concentrations used are toxic in human, the uptake of Hcy in chicken embryos is rather low, and concentrations achieved are comparable to the mild to moderate hyperhomocysteinemia in mothers of NTD offspring [18, 37]. Underlying mechanisms involved in the teratogenicity of hyperhomocysteinemia encompass the interference with the oxidative, apoptosis and inflammation pathways, the inhibition of protein and lipid synthesis and interference with methylation and DNA synthesis. These mechanisms affect progresses such as growth, differentiation, implantation, embryogenesis and placentation. Because folate and folic acid reduce elevated Hcy levels, its protective effects on complex congenital malformations can be explained by a reduction of the accompanying elevated SAH levels and subsequent restoration of oxidative stress, protein- and lipid synthesis and methylation, DNA synthesis and chromatin methylation. Because chromatin methylation is one of the epigenetic mechanisms important for imprinting and subsequent cellular differentiation and multiplication implicated in embryogenesis and growth, the importance of an optimal maternal periconception balance of folate and Hcy for health, reproduction and disease in early and later life is emphasized.

REFERENCES

1. *The March of Dimes Foundation*, in *The Hidden Toll of Dying and Disabled Children*. 2006.
2. Smithells, R.W., S. Sheppard, and C.J. Schorah, *Vitamin deficiencies and neural tube defects.* Arch Dis Child, 1976. **51**(12): p. 944-50.
3. Smithells, R.W., et al., *Further experience of vitamin supplementation for prevention of neural tube defect recurrences.* Lancet, 1983. **1**(8332): p. 1027-31.
4. Seller, M.J. and M. Adinolfi, *The curly-tail mouse: an experimental model for human neural tube defects.* Life Sci, 1981. **29**(16): p. 1607-15.
5. Steegers-Theunissen, R.P., R.W. Smithells, and T.K. Eskes, *Update of new risk factors and prevention of neural-tube defects.* Obstet Gynecol Surv, 1993. **48**(5): p. 287-93.
6. Greene, N.D. and A.J. Copp, *Mouse models of neural tube defects: investigating preventive mechanisms.* Am J Med Genet C Semin Med Genet, 2005. **135C**(1): p. 31-41.
7. De Wals, P., et al., *Reduction in neural-tube defects after folic acid fortification in Canada.* N Engl J Med, 2007. **357**(2): p. 135-42.
8. Sayed, A.R., et al., *Decline in the prevalence of neural tube defects following folic acid fortification and its cost-benefit in South Africa.* Birth Defects Res A Clin Mol Teratol, 2008. **82**(4): p. 211-6.
9. Goh, Y.I., et al., *Prenatal multivitamin supplementation and rates of congenital anomalies: a meta-analysis.* J Obstet Gynaecol Can, 2006. **28**(8): p. 680-9.
10. Steegers-Theunissen, R.P., et al., *Neural-tube defects and derangement of homocysteine metabolism.* N Engl J Med, 1991. **324**(3): p. 199-200.
11. Kirke, P.N., J.L. Mills, and J.M. Scott, *Homocysteine metabolism in pregnancies complicated by neural tube defects.* Nutrition, 1997. **13**(11-12): p. 994-5.
12. Mills, J.L., et al., *Homocysteine metabolism in pregnancies complicated by neural-tube defects.* Lancet, 1995. **345**(8943): p. 149-51.
13. Rosenquist, T.H., S.A. Ratashak, and J. Selhub, *Homocysteine induces congenital defects of the heart and neural tube: effect of folic acid.* Proc Natl Acad Sci U S A, 1996. **93**(26): p. 15227-32.
14. VanAerts, L.A., et al., *Stereospecific in vitro embryotoxicity of l-Homocysteine in pre- and post-implantation rodent embryos.* Toxicol vitro, 1993. **7**(6): p. 743-749.
15. VanAerts, L.A., et al., *Prevention of neural tube defects by and toxicity of L-homocysteine in cultured postimplantation rat embryos.* Teratology, 1994. **50**(5): p. 348-60.
16. Greene, N.D., L.E. Dunlevy, and A.J. Copp, *Homocysteine is embryotoxic but does not cause neural tube defects in mouse embryos.* Anat Embryol (Berl), 2003. **206**(3): p. 185-91.
17. Brouns, M.R., et al., *Morphogenetic movements during cranial neural tube closure in the chick embryo and the effect of homocysteine.* Anat Embryol (Berl), 2005. **210**(2): p. 81-90.
18. Hansen, D.K., et al., *Lack of embryotoxicity of homocysteine thiolactone in mouse embryos in vitro.* Reprod Toxicol, 2001. **15**(3): p. 239-44.
19. Han, M., et al., *Folate rescues lithium-, homocysteine- and Wnt3A-induced vertebrate cardiac anomalies.* Dis Model Mech, 2009. **2**(9-10): p. 467-78.
20. Jakubowski, H., *Homocysteine thiolactone: metabolic origin and protein homocysteinylation in humans.* J Nutr, 2000. **130**(2S Suppl): p. 377S-381S.
21. Jakubowski, H., *Metabolism of homocysteine thiolactone in human cell cultures. Possible mechanism for pathological consequences of elevated homocysteine levels.* J Biol Chem, 1997. **272**(3): p. 1935-42.
22. McNulty, H. and J.M. Scott, *Intake and status of folate and related B-vitamins: considerations and challenges in achieving optimal status.* Br J Nutr, 2008. **99 Suppl 3**: p. S48-54.
23. Refsum, H., et al., *The Hordaland Homocysteine Study: a community-based study of homocysteine, its determinants, and associations with disease.* J Nutr, 2006. **136**(6 Suppl): p. 1731S-1740S.
24. Steegers-Theunissen, R.P., et al., *Maternal hyperhomocysteinemia: a risk factor for neural-tube defects?* Metabolism, 1994. **43**(12): p. 1475-80.

25. Wong, W.Y., et al., *Nonsyndromic orofacial clefts: association with maternal hyperhomocysteinemia.* Teratology, 1999. **60**(5): p. 253-7.
26. Verkleij-Hagoort, A., et al., *Hyperhomocysteinemia and MTHFR polymorphisms in association with orofacial clefts and congenital heart defects: a meta-analysis.* Am J Med Genet A, 2007. **143A**(9): p. 952-60.
27. Latacha, K.S. and T.H. Rosenquist, *Homocysteine inhibits extra-embryonic vascular development in the avian embryo.* Dev Dyn, 2005. **234**(2): p. 323-31.
28. Andaloro, V.J., D.T. Monaghan, and T.H. Rosenquist, *Dextromethorphan and other N-methyl-D-aspartate receptor antagonists are teratogenic in the avian embryo model.* Pediatr Res, 1998. **43**(1): p. 1-7.
29. Epeldegui, M., et al., *Homocysteine modifies development of neurulation and dorsal root ganglia in chick embryos.* Teratology, 2002. **65**(4): p. 171-9.
30. Rosenquist, T.H., A.M. Schneider, and D.T. Monogham, *N-methyl-D-aspartate receptor agonists modulate homocysteine-induced developmental abnormalities.* Faseb J, 1999. **13**(12): p. 1523-31.
31. Lee, H. and J.J. Redmond, *Alleviation of inhibitory action of 5-bromode-oxyuridine by methionine in early chick embryos.* Experientia, 1975. **31**(3): p. 353-4.
32. Kobus, K., E.M. Nazari, and Y.M. Muller, *Effects of folic acid and homocysteine on spinal cord morphology of the chicken embryo.* Histochem Cell Biol, 2009.
33. Boot, M.J., et al., *Homocysteine induces endothelial cell detachment and vessel wall thickening during chick embryonic development.* Circ Res, 2004. **94**(4): p. 542-9.
34. Miller, R.R., et al., *Homocysteine-induced changes in brain membrane composition correlate with increased brain caspase-3 activities and reduced chick embryo viability.* Comp Biochem Physiol B Biochem Mol Biol, 2003. **136**(3): p. 521-32.
35. Maestro de las Casas, C., et al., *High exogenous homocysteine modifies eye development in early chick embryos.* Birth Defects Res A Clin Mol Teratol, 2003. **67**(1): p. 35-40.
36. Afman, L.A., et al., *Homocysteine interference in neurulation: a chick embryo model.* Birth Defects Res A Clin Mol Teratol, 2003. **67**(6): p. 421-8.
37. Bennett, G.D., et al., *Failure of homocysteine to induce neural tube defects in a mouse model.* Birth Defects Res B Dev Reprod Toxicol, 2006. **77**(2): p. 89-94.
38. Neubert, D., et al., *Results of in vivo and in vitro studies for assessing prenatal toxicity.* Environ Health Perspect, 1986. **70**: p. 89-103.
39. New, D.A.T., *Whole-embryo culture and the study of mammalian embryos during organogenesis.* Biol Rev Camb Philos Soc, 1978. **53**(1): p. 81-122.
40. Schoenwolf, G.C. and J.L. Smith, *Mechanisms of neurulation: traditional viewpoint and recent advances.* Development, 1990. **109**(2): p. 243-70.
41. Mitchell, L.E., et al., *Spina bifida.* Lancet, 2004. **364**(9448): p. 1885-95.
42. Scott, J.M., *Folate and vitamin B12.* Proc Nutr Soc, 1999. **58**(2): p. 441-8.
43. Li, D., et al., *Impact of methylenetetrahydrofolate reductase deficiency and low dietary folate on the development of neural tube defects in splotch mice.* Birth Defects Res A Clin Mol Teratol, 2006. **76**(1): p. 55-9.
44. Greene, N.D., V. Massa, and A.J. Copp, *Understanding the causes and prevention of neural tube defects: Insights from the splotch mouse model.* Birth Defects Res A Clin Mol Teratol, 2009. **85**(4): p. 322-30.
45. Heid, M.K., et al., *Folate deficiency alone does not produce neural tube defects in mice.* J Nutr, 1992. **122**(4): p. 888-94.
46. Burgoon, J.M., et al., *Investigation of the effects of folate deficiency on embryonic development through the establishment of a folate deficient mouse model.* Teratology, 2002. **65**(5): p. 219-27.
47. Burren, K.A., et al., *The genetic background of the curly tail strain confers susceptibility to folate-deficiency-induced exencephaly.* Birth Defects Res A Clin Mol Teratol. **88**(2): p. 76-83.

48. Fleming, A. and A.J. Copp, *Embryonic folate metabolism and mouse neural tube defects.* Science, 1998. **280**(5372): p. 2107-9.
49. Wlodarczyk, B.J., et al., *Spontaneous neural tube defects in splotch mice supplemented with selected micronutrients.* Toxicol Appl Pharmacol, 2006. **213**(1): p. 55-63.
50. Carter, M., et al., *Crooked tail (Cd) models human folate-responsive neural tube defects.* Hum Mol Genet, 1999. **8**(12): p. 2199-204.
51. Zhu, H., et al., *Cardiovascular abnormalities in Folr1 knockout mice and folate rescue.* Birth Defects Res A Clin Mol Teratol, 2007. **79**(4): p. 257-68.
52. Copp, A.J. and N.D. Greene, *Neural tube defects: prevention by folic acid and other vitamins.* Indian J Pediatr, 2000. **67**(12): p. 915-21.
53. Greene, N.D. and A.J. Copp, *Inositol prevents folate-resistant neural tube defects in the mouse.* Nat Med, 1997. **3**(1): p. 60-6.
54. Cavalli, P. and A.J. Copp, *Inositol and folate resistant neural tube defects.* J Med Genet, 2002. **39**(2): p. E5.
55. Boot, M.J., et al., *Folic acid and homocysteine affect neural crest and neuroepithelial cell outgrowth and differentiation in vitro.* Dev Dyn, 2003. **227**(2): p. 301-8.
56. Tierney, B.J., et al., *Homocysteine inhibits cardiac neural crest cell formation and morphogenesis in vivo.* Dev Dyn, 2004. **229**(1): p. 63-73.
57. Nakagawa, S. and M. Takeichi, *Neural crest cell-cell adhesion controlled by sequential and subpopulation-specific expression of novel cadherins.* Development, 1995. **121**(5): p. 1321-32.
58. Rutishauser, U., *Polysialic acid and the regulation of cell interactions.* Curr Opin Cell Biol, 1996. **8**(5): p. 679-84.
59. Minana, R., et al., *Alcohol exposure alters the expression pattern of neural cell adhesion molecules during brain development.* J Neurochem, 2000. **75**(3): p. 954-64.
60. Rosenquist TH, M.D., Gadson PF, Dalton ML, Witt G, Brown JC, *Homocysteine and the NMDA receptor: are they keys to conotruncal abnormalities?* Cardiovascular Development, ed. R.T. R.Runyan. 1999.
61. Michaelis, M., et al., *Inflammatory mediators sensitize acutely axotomized nerve fibers to mechanical stimulation in the rat.* J Neurosci, 1998. **18**(18): p. 7581-7.
62. Rosenquist, T.H. and R.H. Finnell, *Genes, folate and homocysteine in embryonic development.* Proc Nutr Soc, 2001. **60**(1): p. 53-61.
63. Lipton, S.A., et al., *Neurotoxicity associated with dual actions of homocysteine at the N-methyl-D-aspartate receptor.* Proc Natl Acad Sci U S A, 1997. **94**(11): p. 5923-8.
64. Bennett, G.D., et al., *The expression of the NR1-subunit of the NMDA receptor during mouse and early chicken development.* Reprod Toxicol, 2006. **22**(3): p. 536-41.
65. Antony, A., et al., *Translational upregulation of folate receptors is mediated by homocysteine via RNA-heterogeneous nuclear ribonucleoprotein E1 interactions.* J Clin Invest, 2004. **113**(2): p. 285-301.
66. Tyagi, N., et al., *Mechanisms of homocysteine-induced oxidative stress.* Am J Physiol Heart Circ Physiol, 2005. **289**(6): p. H2649-56.
67. Handy, D.E., Y. Zhang, and J. Loscalzo, *Homocysteine down-regulates cellular glutathione peroxidase (GPx1) by decreasing translation.* J Biol Chem, 2005. **280**(16): p. 15518-25.
68. Upchurch, G.R., Jr., et al., *Homocyst(e)ine decreases bioavailable nitric oxide by a mechanism involving glutathione peroxidase.* J Biol Chem, 1997. **272**(27): p. 17012-7.
69. Tawakol, A., et al., *Hyperhomocyst(e)inemia is associated with impaired endothelium-dependent vasodilation in humans.* Circulation, 1997. **95**(5): p. 1119-21.
70. Boger, R.H., et al., *Asymmetric dimethylarginine (ADMA): a novel risk factor for endothelial dysfunction: its role in hypercholesterolemia.* Circulation, 1998. **98**(18): p. 1842-7.

71. Sharma, P., et al., *Mining literature for a comprehensive pathway analysis: a case study for retrieval of homocysteine related genes for genetic and epigenetic studies.* Lipids Health Dis, 2006. **5**: p. 1.
72. Davis, W.L., et al., *Generation of radical oxygen species by neural crest cells treated in vitro with isotretinoin and 4-oxo-isotretinoin.* J Craniofac Genet Dev Biol, 1990. **10**(3): p. 295-310.
73. Nachmany, A., et al., *Neural tube closure depends on nitric oxide synthase activity.* J Neurochem, 2006. **96**(1): p. 247-53.
74. Weil, M., et al., *Folic acid rescues nitric oxide-induced neural tube closure defects.* Cell Death Differ, 2004. **11**(3): p. 361-3.
75. Steegers-Theunissen, R.P. and E.A. Steegers, *Nutrient-gene interactions in early pregnancy: a vascular hypothesis.* Eur J Obstet Gynecol Reprod Biol, 2003. **106**(2): p. 115-7.
76. Bellamy, M.F. and I.F. McDowell, *Putative mechanisms for vascular damage by homocysteine.* J Inherit Metab Dis, 1997. **20**(2): p. 307-15.
77. Boot, M.J., et al., *Cardiac outflow tract malformations in chick embryos exposed to homocysteine.* Cardiovasc Res, 2004. **64**(2): p. 365-73.
78. McCully, K.S., *Chemical pathology of homocysteine. IV. Excitotoxicity, oxidative stress, endothelial dysfunction, and inflammation.* Ann Clin Lab Sci, 2009. **39**(3): p. 219-32.
79. Moore, P., et al., *Apoptotic cell death in the mouse retinal ganglion cell layer is induced in vivo by the excitatory amino acid homocysteine.* Exp Eye Res, 2001. **73**(1): p. 45-57.
80. Kastner, P., et al., *Genetic analysis of RXR alpha developmental function: convergence of RXR and RAR signaling pathways in heart and eye morphogenesis.* Cell, 1994. **78**(6): p. 987-1003.
81. Gruber, P.J., et al., *RXR alpha deficiency confers genetic susceptibility for aortic sac, conotruncal, atrioventricular cushion, and ventricular muscle defects in mice.* J Clin Invest, 1996. **98**(6): p. 1332-43.
82. Mendelsohn, C., et al., *Function of the retinoic acid receptors (RARs) during development (II). Multiple abnormalities at various stages of organogenesis in RAR double mutants.* Development, 1994. **120**(10): p. 2749-71.
83. Lohnes, D., et al., *Function of the retinoic acid receptors (RARs) during development (I). Craniofacial and skeletal abnormalities in RAR double mutants.* Development, 1994. **120**(10): p. 2723-48.
84. Hurlin, P.J., *N-Myc functions in transcription and development.* Birth Defects Res C Embryo Today, 2005. **75**(4): p. 340-52.
85. Dudman, N.P., et al., *Homocysteine enhances neutrophil-endothelial interactions in both cultured human cells and rats In vivo.* Circ Res, 1999. **84**(4): p. 409-16.
86. Poddar, R., et al., *Homocysteine induces expression and secretion of monocyte chemoattractant protein-1 and interleukin-8 in human aortic endothelial cells: implications for vascular disease.* Circulation, 2001. **103**(22): p. 2717-23.
87. Mariotto, S., et al., *Cross-talk between NO and arachidonic acid in inflammation.* Curr Med Chem, 2007. **14**(18): p. 1940-4.
88. Jakubowski, H., *Protein homocysteinylation: possible mechanism underlying pathological consequences of elevated homocysteine levels.* Faseb J, 1999. **13**(15): p. 2277-83.
89. Liu, G., K. Nellaiappan, and H.M. Kagan, *Irreversible inhibition of lysyl oxidase by homocysteine thiolactone and its selenium and oxygen analogues. Implications for homocystinuria.* J Biol Chem, 1997. **272**(51): p. 32370-7.
90. Raposo, B., et al., *High levels of homocysteine inhibit lysyl oxidase (LOX) and downregulate LOX expression in vascular endothelial cells.* Atherosclerosis, 2004. **177**(1): p. 1-8.
91. Coral, K., et al., *Homocysteine levels in the vitreous of proliferative diabetic retinopathy and rhegmatogenous retinal detachment: its modulating role on lysyl oxidase.* Invest Ophthalmol Vis Sci, 2009. **50**(8): p. 3607-12.
92. Chen, Q., M. Galleano, and A.I. Cederbaum, *Cytotoxicity and apoptosis produced by arachidonic acid in Hep G2 cells overexpressing human cytochrome P4502E1.* J Biol Chem, 1997. **272**(23): p. 14532-41.

93. Kruman, II, et al., *Folic acid deficiency and homocysteine impair DNA repair in hippocampal neurons and sensitize them to amyloid toxicity in experimental models of Alzheimer's disease.* J Neurosci, 2002. **22**(5): p. 1752-62.
94. Castro, R., et al., *Increased homocysteine and S-adenosylhomocysteine concentrations and DNA hypomethylation in vascular disease.* Clin Chem, 2003. **49**(8): p. 1292-6.
95. Moephuli, S.R., et al., *Effects of methionine on the cytoplasmic distribution of actin and tubulin during neural tube closure in rat embryos.* Proc Natl Acad Sci U S A, 1997. **94**(2): p. 543-8.
96. Coelho, C.N. and N.W. Klein, *Methionine and neural tube closure in cultured rat embryos: morphological and biochemical analyses.* Teratology, 1990. **42**(4): p. 437-51.
97. Kiefer, J.C., *Epigenetics in development.* Dev Dyn, 2007. **236**(4): p. 1144-56.
98. Yi, P., et al., *Increase in plasma homocysteine associated with parallel increases in plasma S-adenosylhomocysteine and lymphocyte DNA hypomethylation.* J Biol Chem, 2000. **275**(38): p. 29318-23.
99. James, S.J., et al., *Elevation in S-adenosylhomocysteine and DNA hypomethylation: potential epigenetic mechanism for homocysteine-related pathology.* J Nutr, 2002. **132**(8 Suppl): p. 2361S-2366S.
100. Ingrosso, D., et al., *Folate treatment and unbalanced methylation and changes of allelic expression induced by hyperhomocysteinaemia in patients with uraemia.* Lancet, 2003. **361**(9370): p. 1693-9.
101. Cooney, C.A., A.A. Dave, and G.L. Wolff, *Maternal methyl supplements in mice affect epigenetic variation and DNA methylation of offspring.* J Nutr, 2002. **132**(8 Suppl): p. 2393S-2400S.

4

Effects of Homocysteine on Cardiac Hemodynamics and Shear Stress

4.1

Homocysteine affects hemodynamic parameters of early embryonic chicken heart function.

A.M. Oosterbaan, E Bon, R.P.M. Steegers-Theunissen, A.F.W. van der Steen, N.T.C. Ursem

The Anatomical Record: Advances in Integrative Anatomy and Evolutionary Biology Accepted for Publication March 2012

ABSTRACT

Introduction Maternal hyperhomocysteinemia has been associated with an increased risk of newborns with a congenital heart defect. This has been substantiated in the chicken embryo, as congenital heart defects have been induced after homocysteine treatment. Comparable heart defects are observed in venous clipping studies, a model of altered embryonic blood flow. Because of this overlap in heart defects, our aim was to test the hypothesis that homocysteine would cause alterations in embryonic heart function that precede the structural malformations previously described.

Methods Doppler flow velocity waveforms were recorded in both primitive ventricles and the outflow tract of the embryonic heart of homocysteine treated and control chicken embryos at embryonic day 3.5. Homocysteine treatment consisted of 50 µL 0.05 M L-homocysteine thiolactone at 24, 48 and 72 hours. Homocysteine treated embryos displayed significantly lower mean heart rates of 134 (s.d. 22) bpm, compared to 150 (14) bpm in control embryos.

Results Homocysteine treatment caused an inhibiting effect on hemodynamic parameters, and altered heart function was presented by a shift in the proportions of the different wave times in percentage of total cycle time.

Conclusions Homocysteine induces changes in hemodynamic parameters of early embryonic chicken heart function. These changes may precede morphological changes and contribute to the development of CHD defects through alterations in shear stress and shear stress related genes, as seen before in venous clipping studies.

INTRODUCTION

Congenital heart defects (CHD) are among the most common congenital malformations in newborns [1]. Epidemiological studies have shown that the periconceptional use of folic acid reduces the risk of CHD in the offspring [2] and reduces the birth prevalence rate with approximately 20% [3-4]. Low folate decreases the remethylation of homocysteine into methionine, resulting in a mild to moderate hyperhomocysteinemia [5]. A meta-analysis has shown that maternal hyperhomocysteinemia is associated with an approximately three-fold increased risk of newborns with a congenital outflow tract defect [6]. This association, as well as the association of homocysteine exposure and a wide range of other congenital malformations among which neural tube defects, have been substantiated in animal experimental models [7]. In the chicken embryo ventricular septal defects and conotruncal heart defects have been reported [8-9]. The malformations observed in the chicken embryo share the mutual involvement of neural crest cells. Cardiac neural crest cells are important in heart and pharyngeal arch artery development. A previous chicken embryo study has demonstrated that homocysteine treatment results in failure of the cardiac neural crest cells to undergo apoptosis with subsequent decreased myocardialization of the outflow tract (OFT), subarterial ventricular septal defects and increased volume of the OFT cushions at Hamburger and Hamilton (HH) [10] stage 35 (9 days incubation; ED 9) [8].

Above described defects, seen in the chicken embryo after homocysteine treatment, are comparable to those observed in chicken embryo studies in which the extra embryonic blood flow has been altered by venous clipping. The venous clip model consists of ligation of the right lateral vitelline vein with a microclip, and is used to alter hemodynamic parameters such as the intracardiac blood flow in the chicken embryo [11]. The short-term functional effects of venous clipping are acute reductions of all hemodynamic parameters, which are observed for up to five hours after clipping [12]. Moreover, at stage HH 24 (ED 4), venous clipping leads to altered heart function presented by changes in the 'active' and 'passive' filling component of the ventricle [13]. Eventually, these chicken embryos display OFT defects, in particular ventricular septal defects, valve anomalies and pharyngeal arch artery malformations [14], comparable defects as seen after homocysteine treatment [8].

Thus far morphological effects of homocysteine have been reported when the heart is already septated and the valves are functional. Possible hemodynamic alterations induced by homocysteine affecting heart development of the chicken embryo, however, are unknown. Interestingly, the embryonic heart is functioning well before cardiogenesis is complete. Therefore, it is conceivable that early functional changes may influence cardiac morphogenesis. Because of the overlap in CHD seen after elevated homocysteine exposure in human and in chicken embryos, and in CHD reported in the venous clipping model, we

hypothesized that homocysteine may cause alterations in early embryonic heart function, preceding structural malformations. Consequently, we are most interested in the effects of homocysteine on the hemodynamic parameters heart rate, peak velocity, velocity integrated over time and wave times, as a reflection of early embryonic chicken heart function.

To assess early heart function in animal experimental models, ultrasound biomicroscopy can be applied [15]. This high frequency ultrasound technique has already provided more insight into the early heart function of chicken embryos [16-17]. Previously, we have shown that it is possible to acquire specific Doppler flow velocity waveforms at different anatomic locations in the embryonic chicken heart and that these velocity waveforms are specific for different embryonic stages of development. Blood flow profiles were collected at HH stages 18, 21 and 23, comparable to humans at 5 to 8 weeks of gestation [18]. The aim of this study was to investigate whether L-homocysteine thiolactone hydrochloride, administered in concentrations comparable to the mild to moderate hyperhomocysteinemia associated with CHD in human, induces hemodynamic alterations in the ventricle and OFT of the embryonic chicken heart at HH 21 (ED 3.5).

MATERIALS AND METHODS

Application of Homocysteine

Fertilized White Leghorn chicken eggs (*Gallus gallus* (L.)) (Drost Loosdrecht BV, Loosdrecht, Netherlands) were incubated blunt-end up at 37.5°C. A hole of 2 mm was made in the outer shell membrane at the site of the air space at 24 hours of incubation. At 24, 48 and 72 hours of incubation, a homocysteine solution or a sham solution was applied through the hole, on the inner shell membrane, using a micropipette. The homocysteine treated group (n=36) received 50 µL 0.05 M of the more stable metabolite of homocysteine, L-homocysteine thiolactione hydrochloride (Sigma-Aldrich, Steinheim, Germany) in Locke's solution (0.94% NaCl, 0.045% KCl, 0.033% $CaCl_2$ w/v in Milli-Q) per application. Thus per application the embryos received 2.5 µmol homocysteine. The sham (control) group (n=37) received 50 µL Locke's solution only. After each application the hole was sealed with Scotch tape and the incubation was continued. Thirty minutes after the last application the eggs were placed horizontally in the incubator for further development until ED 3.5. This mode of application of L-homocysteine thiolactone hydrochloride has been described previously and resulted in structural CHD, in particular ventricular septal defects [9].

Ultrasound Biomicroscopy

At day 3.5 the eggs were taken out of the incubator, the embryo was localized and a window of approximately 1 by 1 cm was made in the egg shell to allow ultrasound imaging. The embryo was staged by microscopic examination according to Hamburger and Hamilton [10] and HH 21 embryos were included. Embryos that showed visible bleeding were excluded, as well as embryos floating on their right side. In total 13 out of 36 homocysteine treated embryos and 13 out of 37 control embryos were suitable for further analysis. The window in the eggshell was covered by a thin piece of polyethylene foil on which warmed ultrasonic gel was deposited. Embryo temperature was measured with a thermometer inside the egg and maintained at 37°C ± 1°C with the help of a heated egg holder on a heated plate and a heat lamp.

Ultrasound biomicroscopy measurements were performed with a high frequency ultrasound system: the Vevo 770 (VisualSonics Inc., Toronto, Ontario, Canada) equipped with a 55-MHz transducer (RMV 708) exhibiting an axial and lateral resolution of approximately 30 and 75 µm, respectively [16, 19]. The embryonic heart was imaged at a focal depth of 4.5 mm. The pulsed Doppler sample volume varied between 0.15 and 0.17 mm and the scanning depth ranged between 4.15 and 5.15 mm. The measurements were performed and described in detail previously by our research group [18]. From each embryo velocity signals were recorded at three cardiac sites, in the primitive left ventricle (PLV), the primitive right ventricle (PRV) and the OFT (Fig. 1a). To acquire signals from these sites the transducer was outlined along the cross section from the apex to the OFT (Fig. 1b). Because chicken embryos are generally floating on their left side, these embryos were included to increase group homogeneity and limit the variation in the angle of insonation. To ensure accurate probe positioning B-mode ultrasound was used (Fig. 1c). Power Doppler mode was used to visualize the blood flow in the cross section through the heart (Fig. 1d). After identifying these flows, the Doppler sample volume was placed in the centre of the blood stream to obtain flow velocity waveform recordings. From the obtained velocity waveforms we determined the heart rate (bpm; beats per minute), peak velocities (cm/s), velocities integrated over time (VTI; cm) and wave times (ms) (Fig. 2a). The Doppler angle was arbitrarily set to zero as flow direction could not be assessed accurately. Therefore, the Doppler velocities should be interpreted as relative velocities, which more precisely are the vectorial velocities in the direction of the ultrasound beam. From the cardiac cycle the 'Passive' (P) wave, phase I, and the 'Active' (A) wave, phase II of ventricular filling, and the ejection wave, phase III of the cardiac cycle, were determined (Fig. 2a). Wave times were additionally calculated in percentages of total cycle time to find proportional changes of the three phases of the cardiac cycle between homocysteine and control embryos. For each embryo we analyzed three consecutive cardiac cycles. Embryo temperature was monitored and collected simultaneously with the Doppler data.

Figure 1

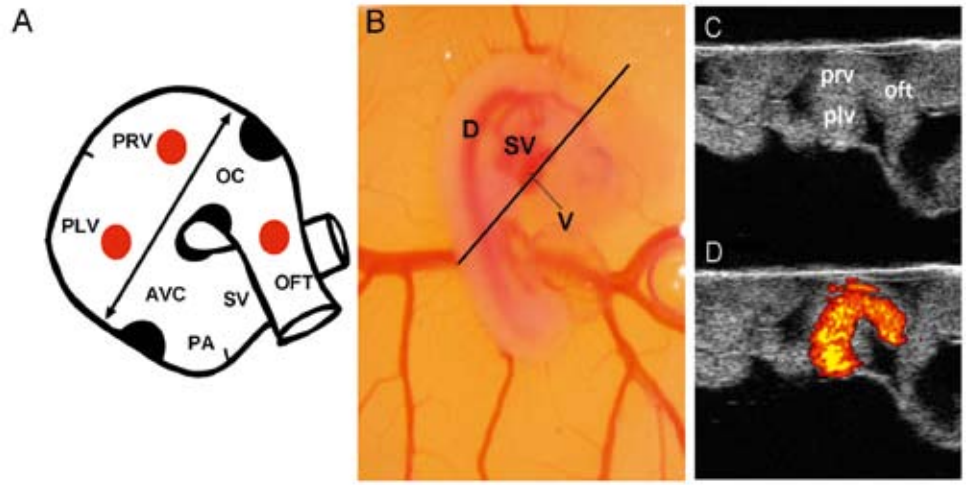

A: A schematic presentation of the anatomy of the embryonic chicken heart, with the inflow tract, consisting of the sinus venosus (SV) flowing into the primitive atrium (PA). Between the primitive atrium and the primitive left ventricle (PLV), the atrioventricular cushions are situated (AVC). Between the primitive right ventricle (PRV) and the outflow tract (OFT) the outflow cushions (OC) are situated. The three dots represent the measurement points.
B: Stage HH 21 chicken embryo, right side up. D: dorsal aorta; SV: sinus venosus; V: ventricle. The line represents the cross section with measurement points of the primitive left ventricle, primitive right ventricle and outflow tract [18].
C/D: B-mode and power Doppler images of the embryonic heart, representing the 3 measurement points.

Statistical Analysis

The data are presented as mean (standard deviation; s.d.). To determine heart rate and temperature variance within embryos during the experimental time span, analysis of variance (One-Way ANOVA) was performed. All other statistics were carried out using the independent-samples t-test. Statistical significance was defined as a p value of less than 0.05. Calculations were performed with SPSS 15.0 (SPSS Inc., Chicago, Illinois, USA).

RESULTS

Standardization of the Measurements

Within both the homocysteine treated and the control group the variance as expressed by the s.d. of the three consecutively measured heart rates per embryo was small, 1.5 bpm and 1.0 bpm respectively. The mean heart rate of homocysteine treated embryos was 134 (22)

bpm, which was significantly lower than the 150 (14) bpm in control embryos (Table 1). The s.d. of the temperature within the embryos was also very small, 0.04ºC within homocysteine and 0.07ºC within control embryos. The mean temperature between the homocysteine and the control group was not significantly different (Table 1).

Table 1 Comparison of general and specific hemodynamic parameters

Location		Variable	Homocysteine treated N=13 Mean (s.d.)		Control N=13 Mean (s.d.)	
General		Heart rate (beats/min)	134	(22)*	150	(14)
		Temperature (ºC)	37.6	(0.3)	37.6	(0.4)
PLV	P wave	VTI (cm)	0.16	(0.08)	0.15	(0.07)
		Peak velocity (cm/s)	1.4	(0.6)	1.7	(0.5)
		P wave/total time (%)	34.3	(10.0)	28.2	(6.9)
	A wave	VTI (cm)	0.15	(0.05)	0.18	(0.05)
		Peak velocity (cm/s)	3.2	(1.2)	4.0	(1.0)
		A wave/total time (%)	17.3	(3.5) *	20.1	(2.0)
	Ejection	VTI (cm)	0.10	(0.04) *	0.13	(0.02)
		Peak velocity (cm/s)	1.3	(0.4)	1.6	(0.3)
		Ejection/total time (%)	23.8	(4.3) *	26.8	(1.5)
	Relaxation	Pre-diastolic/total time (%)	24.5	(6.0)	24.9	(6.1)
PRV	P wave	VTI (cm)	0.08	(0.04)	0.08	(0.04)
		Peak velocity (cm/s)	0.7	(0.2) *	0.9	(0.2)
		P wave/total time (%)	31.1	(9.1)	25.9	(9.8)
	A wave	VTI (cm)	0.09	(0.04) *	0.14	(0.04)
		Peak velocity (cm/s)	2.0	(0.6) *	2.8	(0.9)
		A wave/total time (%)	16.4	(2.5) *	19.4	(2.0)
	Ejection	VTI (cm)	0.18	(0.04) *	0.23	(0.04)
		Peak velocity (cm/s)	2.5	(1.1)	2.9	(0.4)
		Ejection/total time (%)	25.8	(3.2) *	28.7	(1.4)
	Relaxation	Pre-diastolic/total time (%)	26.8	(5.6)	26.0	(9.4)
Outflow tract	Ejection	VTI (cm)	0.47	(0.11)	0.49	(0.10)
		Peak velocity (cm/s)	3.9	(0.8)	4.2	(1.1)
		Ejection/total time (%)	46.8	(4.5) *	52.9	(4.5)
	Diastole	Diastolic/total time (ms)	53.2	(7.5) *	47.1	(4.5)

Comparison of general and specific hemodynamic parameters measured in the primitive left ventricle (PLV), the primitive right ventricle (PRV) and the outflow tract (OFT) in homocysteine treated and control chicken embryos. Includes Velocity-Time-Integral (VTI; cm), peak velocity (cm/s) and time (ms) measurements, as well as wave times in percentage of total cycle time. * means statistically significant ($p<0.05$)

Figure 2

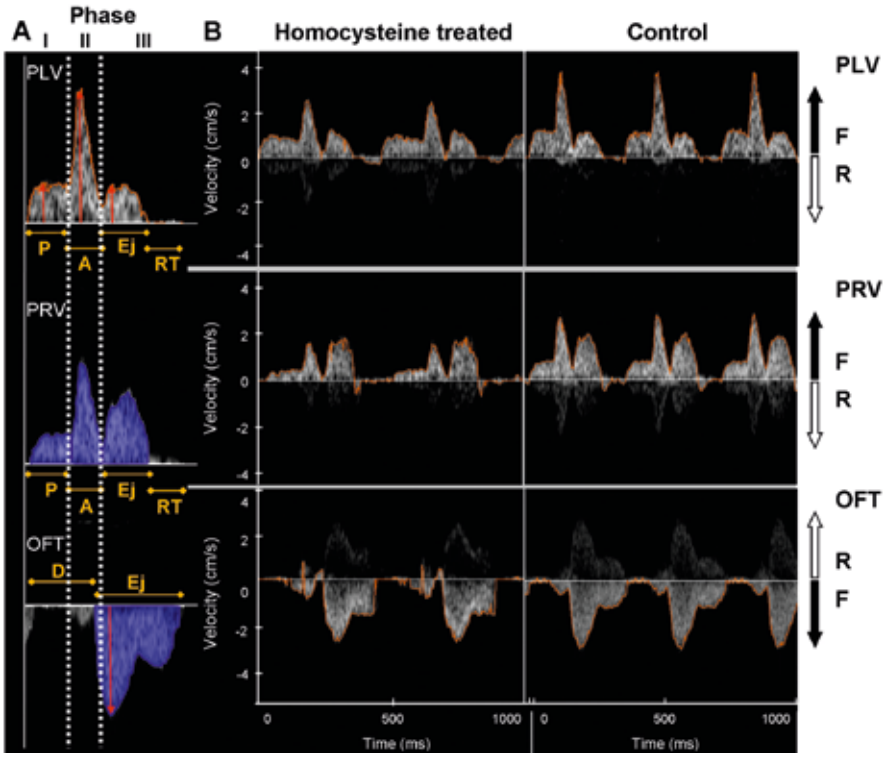

A: Image of the velocity waveforms at the three measurement points. In the primitive left ventricle (PLV) and primitive right ventricle (PRV), ventricular filling consists of a P wave (P) and an A wave (A) followed by the ventricular ejection (Ej) and pre-diastolic relaxation time (RT). Corresponding time intervals are depicted in yellow. In the outflow tract (OFT) signal the time intervals for ejection (Ej) and diastole (D) are depicted in yellow. The red arrows are examples of peak velocity measurements. The blue areas are examples of VTI measurements. Areas I to III, indicated by the dotted line, represent the different phases of the cardiac cycle. Doppler mirror image artifacts are visible on the other side of the baseline due to high gain settings.
B: Representative image of the velocity waveforms of a homocysteine treated and a control embryo. F: Forward flow. R: Reversed flow.

Primitive Left and Primitive Right Ventricle

Figure 2b shows flow velocity waveforms derived from the PLV and the PRV in homocysteine treated and control embryos. The blood flow in both study groups and primitive ventricles was unidirectional during all phases of the cardiac cycle.

The PLV showed a significantly smaller ejection VTI in homocysteine treated embryos compared to control embryos (Table 1). In the PRV both A wave and ejection wave VTI were

significantly decreased in homocysteine treated embryos compared to controls. In the PLV, peak velocities were not significantly different between both study groups. In the PRV, P and A wave peak velocity were significantly lower in homocysteine treated embryos than in control embryos. 'Passive' wave time was significantly prolonged in the PLV of homocysteine treated embryos compared to controls. Although the proportions of 'active' and ejection wave times were significantly decreased in both primitive ventricles in homocysteine treated embryos compared to controls, the increase in 'passive' wave times in percentages of total cycle time were not significantly different.

Outflow Tract

The outflow tract waveform consisted of one dominant forward peak in both homocysteine treated and control embryos (Fig. 2b). The outflow VTI, peak velocity and ejection time were similar in both study groups. Diastolic time, consisting of the wave times of phase I plus phase II, was significantly prolonged in homocysteine treated embryos compared to controls (Table 1). This resulted in a significantly increased proportion of diastolic time and a significantly decreased proportion of ejection time, as shown by the changes in percentages of total cycle time. Backflow in the OFT during ventricular filling was seen in 5 out of 13 homocysteine treated embryos, compared to 1 out of 13 control embryos.

Intraventricular Changes

Within homocysteine treated and control embryos the same differences between the PLV and the PRV waveforms were observed. There was a significant decrease of peak velocities and VTI's of phase I and phase II of the cardiac cycle, from PLV to PRV. The hemodynamic parameters of phase III significantly increased from PLV to PRV.

DISCUSSION

In this chicken embryo study we have shown that application of low dose L-homocysteine thiolactone hydrochloride during cardiogenesis significantly affects hemodynamic parameters of early embryonic chicken heart function. In general, an inhibiting effect of homocysteine on hemodynamic parameters is described. Homocysteine also significantly reduces mean heart rate. These functional changes may precede the development of structural heart defects associated with homocysteine.

We have shown that homocysteine significantly reduces mean heart rate to 134 (22) bpm compared with 150 (14) bpm in controls. The mean heart rate in controls corresponds with the heart rate, 155 bpm, as has previously been described in stage HH 21 chicken

embryos [20] and is lower than the 170 (25) bpm reported in our previous study [18]. This can be explained as an effect of sham treatment, executed in this study. During the experiments temperature was controlled and temperature differences within and between embryos were extremely small, through which temperature can be excluded as a confounder of heart rates. We suggest that the reduction of heart rate in homocysteine embryos reflects a delay in development, as heart rate increases with developmental stage [20]. Homocysteine has been shown to reduce the synthesis of several proteins [21] implicated in growth processes. Reduced somite number, embryonic size [22-23] and mass [24] have been observed after homocysteine treatment in chicken and mouse embryo studies.

The differences in intracardiac blood flow patterns and in proportions of wave times in percentages of total cycle time between homocysteine treated and control embryos demonstrate that there are functional differences between both study groups. The proportions of ventricular ejection as well as outflow ejection time are decreased in homocysteine embryos in contrast with the linear relationship between heart rate and electrical and mechanical systole described in normal mature human subjects [25], implying that ejection time should increase with reduced mean heart rate. These effects exerted by homocysteine do not only reflect the impact of a delay in development. When comparing the hemodynamic parameters of homocysteine embryos in this study to parameters of sham treated embryos of an earlier Hamburger and Hamilton stage, HH 18, the differences reported in this study remain to exist (A.M. Oosterbaan, unpublished data). Therefore we conclude that homocysteine causes direct functional changes of early embryonic chicken heart function that can not only be explained by developmental delay.

So how can homocysteine be linked to altered hemodynamics and eventually to the development of congenital heart defects? Several mechanisms of homocysteine have been described in literature that may potentially inhibit myocardial function and cause disturbed heart development. These mechanisms may occur either in a linked or independent way. For example, the effects homocysteine exerts on endothelial cells, causing endothelial cell damage and dysfunction [26-27]. Also, homocysteine has been shown to derange the synthesis of nitric oxide (NO) [28-29] and induce oxidative stress [30], which may cause disturbed angiogenesis as shown by our research group and by Latacha and Rosenquist [31-32]. Homocysteine exposure increases connexin43 levels in mouse neural crest cells, affecting neural crest cell migration [33]. This increased expression of connexin43 has been shown to result in conotruncal heart defects in mice in vivo [34]. Boot et al have also described a 60% reduction of apoptosis of the myocardial cells at the site of the OFT and a 25% increased volume of the OFT cushion tissue in chicken embryos treated with homocysteine [8]. This may affect myocardial function.

The reported changes in intracardiac blood flow patterns after homocysteine exposure may lead to local changes in shear stress [11]. Changes in shear stress have been previously shown to result in changes in the expression of shear-responsive genes in the endocardial cells of the developing heart [35]. We suggest that the reduction in blood flow brought about by homocysteine in this study may affect genetic cascades, causing a differential regulation of genes implicated in hemodynamics, eventually resulting in altered cardiac morphogenesis.

Since we have approached the embryonic chicken heart in a standardized way, interpretation of the velocity measurements is warranted. Because we were not able to exactly determine the angle of insonation in a 2D image, angle variation was minimized by selecting embryos from the same HH stage, floating on the same side, and by using Power Doppler to obtain the highest velocity signal. The same amount of homocysteine and control embryos floated on the right side, therefore selection bias is limited. This selection, combined with the experimental procedure, may explain the 33% viable embryos in this study, compared to the 64 % survival rate reported by Afman et al. [36] and the >85% survival in the study performed by Rosenquist et al. [9]. Additionally, survival rates may differ because of variations in nutritional factors between the used chicken strains, possibly altering the yolk sac composition [36].

The concentration of 0.05 M L-homocysteine thiolactone hydrochloride applicated to the embryos *in ovo* was half the concentration applicated by Rosenquist et al, causing neural tube defects and congenital heart defects in the chicken embryo [9]. Using this two-fold higher concentration in our study resulted in only 8% viable embryos. Rosenquist et al. determined blood homocysteine levels in the chicken embryo after application of 50 µl 0.1 M homocysteine solution [9]. Blood levels of 15-150 µmol/liter were reported, comparable to the mild to moderate hyperhomocysteinemia in humans associated with neural tube defects and congenital heart defects [6, 37-38]. Although blood homocysteine levels were not measured in this study, we considered the administration of 50 µl 0.05 M L-homocysteine thiolactone hydrochloride adequate, as it is plausible that with this halved concentration homocysteine levels of > 15 µmol per liter are achieved.

In conclusion, homocysteine exposure leads to altered hemodynamic parameters of early embryonic chicken heart function. Several mechanisms have been proposed through which homocysteine may cause these hemodynamic changes. We suggest that the described functional effects may contribute to the development of CHD defects through changes in shear stress and shear stress related genes, as seen before in venous clipping studies [11]. Further research should identify the differential effects of homocysteine on the proteins, genes and pathways involved in the hemodynamics, implicated in heart development.

REFERENCES

1. Botto, L.D. and A. Correa, *Decreasing the burden of congenital heart anomalies: an epidemiologic evaluation of risk factors and survival.* Prog Pediatr Cardiol, 2003. **18**: p. 111-121.
2. Botto, L.D., J. Mulinare, and J.D. Erickson, *Do multivitamin or folic acid supplements reduce the risk for congenital heart defects? Evidence and gaps.* Am J Med Genet A, 2003. **121**(2): p. 95-101.
3. Hoffman, J.I. and S. Kaplan, *The incidence of congenital heart disease.* J Am Coll Cardiol, 2002. **39**(12): p. 1890-900.
4. van Beynum, I.M., et al., *Protective effect of periconceptional folic acid supplements on the risk of congenital heart defects: a registry-based case-control study in the northern Netherlands.* Eur Heart J, 2009.
5. Kang, S.S., P.W. Wong, and M. Norusis, *Homocysteinemia due to folate deficiency.* Metabolism, 1987. **36**(5): p. 458-62.
6. Verkleij-Hagoort, A., et al., *Hyperhomocysteinemia and MTHFR polymorphisms in association with orofacial clefts and congenital heart defects: a meta-analysis.* Am J Med Genet A, 2007. **143A**(9): p. 952-60.
7. van Mil, N.H., A.M. Oosterbaan, and R.P. Steegers-Theunissen, *Teratogenicity and underlying mechanisms of homocysteine in animal models: A review.* Reprod Toxicol, 2010.
8. Boot, M.J., et al., *Cardiac outflow tract malformations in chick embryos exposed to homocysteine.* Cardiovasc Res, 2004. **64**(2): p. 365-73.
9. Rosenquist, T.H., S.A. Ratashak, and J. Selhub, *Homocysteine induces congenital defects of the heart and neural tube: effect of folic acid.* Proc Natl Acad Sci U S A, 1996. **93**(26): p. 15227-32.
10. Hamburger, V. and H.L. Hamilton, *A series of normal stages in the development of the chick embryo.* J Morphol, 1951. **88**: p. 49-92.
11. Hogers, B., et al., *Unilateral vitelline vein ligation alters intracardiac blood flow patterns and morphogenesis in the chick embryo.* Circ Res, 1997. **80**(4): p. 473-481.
12. Stekelenburg-de Vos, S., et al., *Acutely altered hemodynamics following venous obstruction in the early chick embryo.* J Exp Biol, 2003. **206**(Pt 6): p. 1051-1057.
13. Ursem, N.T.C., et al., *Ventricular diastolic characteristics in stage-24 chick embryos after extra-embryonic venous obstruction.* J Exp Biol, 2004. **207**(9): p. 1487-1490.
14. Hogers, B., et al., *Extraembryonic venous obstructions lead to cardiovascular malformations and can be embryolethal.* Cardiovasc Res, 1999. **41**(1): p. 87-99.
15. Phoon, C.K., *Imaging tools for the developmental biologist: ultrasound biomicroscopy of mouse embryonic development.* Pediatr Res, 2006. **60**(1): p. 14-21.
16. McQuinn, T.C., et al., *High-frequency ultrasonographic imaging of avian cardiovascular development.* Dev Dyn, 2007. **236**(12): p. 3503-13.
17. Butcher, J.T., et al., *Transitions in early embryonic atrioventricular valvular function correspond with changes in cushion biomechanics that are predictable by tissue composition.* Circ Res, 2007. **100**(10): p. 1503-11.
18. Oosterbaan, A.M., et al., *Doppler fow velocity waveforms in the embryonic chicken heart at developmental stages corresponding to 5-8 weeks of human gestation.* Ultrasound in Obstetrics and Gynecology, 2009. **33**(6): p. 638-44.
19. Zhou, Y.Q., et al., *Applications for multifrequency ultrasound biomicroscopy in mice from implantation to adulthood.* Physiol Genomics, 2002. **10**(2): p. 113-26.
20. Hu, N. and E.B. Clark, *Hemodynamics of the stage 12 to stage 29 chick embryo.* Circ Res, 1989. **65**: p. 1665-1670.
21. Malanovic, N., et al., *S-adenosyl-L-homocysteine hydrolase, key enzyme of methylation metabolism, regulates phosphatidylcholine synthesis and triacylglycerol homeostasis in yeast: implications for homocysteine as a risk factor of atherosclerosis.* J Biol Chem, 2008. **283**(35): p. 23989-99.

22. Greene, N.D., L.E. Dunlevy, and A.J. Copp, *Homocysteine is embryotoxic but does not cause neural tube defects in mouse embryos.* Anat Embryol (Berl), 2003. **206**(3): p. 185-91.
23. Han, M., et al., *Folate rescues lithium-, homocysteine- and Wnt3A-induced vertebrate cardiac anomalies.* Dis Model Mech, 2009. **2**(9-10): p. 467-78.
24. Miller, R.R., et al., *Homocysteine-induced changes in brain membrane composition correlate with increased brain caspase-3 activities and reduced chick embryo viability.* Comp Biochem Physiol B Biochem Mol Biol, 2003. **136**(3): p. 521-32.
25. Boudoulas, H., et al., *Linear relationship between electrical systole, mechanical systole, and heart rate.* Chest, 1981. **80**(5): p. 613-7.
26. Wall, R.T., et al., *Homocysteine-induced endothelial cell injury in vitro: a model for the study of vascular injury.* Thromb Res, 1980. **18**(1-2): p. 113-21.
27. Lee, S.J., et al., *Nitric oxide inhibition of homocysteine-induced human endothelial cell apoptosis by down-regulation of p53-dependent Noxa expression through the formation of S-nitrosohomocysteine.* J Biol Chem, 2005. **280**(7): p. 5781-8.
28. Upchurch, G.R., Jr., et al., *Homocyst(e)ine decreases bioavailable nitric oxide by a mechanism involving glutathione peroxidase.* J Biol Chem, 1997. **272**(27): p. 17012-7.
29. Welch, G.N., et al., *Homocysteine-induced nitric oxide production in vascular smooth-muscle cells by NF-kappa B-dependent transcriptional activation of Nos2.* Proc Assoc Am Physicians, 1998. **110**(1): p. 22-31.
30. Tyagi, N., et al., *Mechanisms of homocysteine-induced oxidative stress.* Am J Physiol Heart Circ Physiol, 2005. **289**(6): p. H2649-56.
31. Latacha, K.S. and T.H. Rosenquist, *Homocysteine inhibits extra-embryonic vascular development in the avian embryo.* Dev Dyn, 2005. **234**(2): p. 323-31.
32. Oosterbaan, A.M., E.A. Steegers, and N.T. Ursem, *The effects of homocysteine and folic acid on angiogenesis and VEGF expression during chicken vascular development.* Microvasc Res, 2012. **83**(2): p. 98-104.
33. Boot, M.J., et al., *Connexin43 levels are increased in mouse neural crest cells exposed to homocysteine.* Birth Defects Res A Clin Mol Teratol, 2006. **76**(2): p. 133-7.
34. Ewart, J.L., et al., *Heart and neural tube defects in transgenic mice overexpressing the Cx43 gap junction gene.* Development, 1997. **124**(7): p. 1281-92.
35. Groenendijk, B.C., et al., *Changes in shear stress-related gene expression after experimentally altered venous return in the chicken embryo.* Circ Res, 2005. **96**(12): p. 1291-8.
36. Afman, L.A., et al., *Homocysteine interference in neurulation: a chick embryo model.* Birth Defects Res A Clin Mol Teratol, 2003. **67**(6): p. 421-8.
37. Steegers-Theunissen, R.P., et al., *Neural-tube defects and derangement of homocysteine metabolism.* N Engl J Med, 1991. **324**(3): p. 199-200.
38. Steegers-Theunissen, R.P., et al., *Maternal hyperhomocysteinemia: a risk factor for neural-tube defects?* Metabolism, 1994. **43**(12): p. 1475-80.

4.2

Induction of shear stress in the homocysteine exposed chicken embryo

A.M. Oosterbaan, C. Poelma, E. Bon, R.P.M. Steegers-Theunissen, E.A.P. Steegers, P. Vennemann, N.T.C. Ursem

Submitted

ABSTRACT

Introduction The embryonic heart is already beating before cardiac morphogenesis is complete. Therefore, effects of blood flow on cardiogenesis have been subject of many studies. Shear stress, acting on the endocardial cells, has been shown to alter the expression of shear responsive genes, implicated in heart development. The congenital heart defects (CHD) induced in the chicken embryo after altering blood flow and intra-cardiac shear stress are comparable to the type of defects observed after homocysteine exposure. This may suggest a role for altered blood flow and shear stress in the etiology of homocysteine induced CHD.

Methods The aim of this study was to quantitate wall shear stress (WSS) in the outflow tract (OFT) of homocysteine exposed chicken embryos. WSS was derived from the velocity field obtained with microscopic Particle Image Velocimetry (μPIV) in the OFT of the embryonic day 3 homocysteine and sham treated chicken embryos. Homocysteine treatment consisted of L-homocysteine-thiolactone 30 μM solution injected into the neural tube of the embryos.

Results The first results suggest that homocysteine has an inhibiting effect on WSS in the early embryonic chicken heart.

Conclusions These alterations in shear stress may cause altered gene expression and behaviour of endothelial cells, eventually contributing to the development of CHD.

INTRODUCTION

During embryonic development, the heart is already beating before cardiac development is complete. Therefore, the cardiac morphology has often been linked to cardiac function. In recent years the number of studies on the effects of blood flow on cardiac morphogenesis has increased. It has been shown that the formation of the functional heart is regulated by the interaction between blood flow and the vessel wall [1-2] and responds to shear stress [3]. The endocardial cells are endothelial cells that line the inner vessel wall of the heart and are subjected to blood flow. Therefore, they are also the cells that sense shear stress. Shear stress is the frictional force (per unit of area) acting on the endocardial cells, parallel to blood flow. Because of the low Reynolds number embryonic blood flow is laminar flow, despite of irregularities like trabeculations and endocardial cushions. From the definition of the WSS, $\tau = \eta\, du/dn$, where η represents the dynamic viscosity and du/dn is the wall-normal fluid velocity gradient evaluated at the wall, one would expect an increase in WSS with increased blood flow velocity. Shear stress was first shown to influence gene expression *in vitro* [4-5]. Subsequently, increasing *in vivo* evidence has underlined the importance of the effects of shear stress on the expression of genes implicated in heart development [6-7]. Therefore, early cardiac functioning and, specifically, shear stress is considered to play a substantial role in cardiovascular development. Consequently, it is seen as an important epigenetic factor in embryonic cardiogenesis [8-9]. Still, methods to accurately quantitate wall shear stress (WSS) *in vivo*, in a beating heart, are lacking.

To study early cardiovascular development *in vivo*, the chicken embryo model has proven to be a suitable animal experimental model for decades [10-11]. In this model, successful alteration of intracardiac blood flow in order to explore the role of shear stress was achieved by clipping of the right lateral vitelline vein [12-14]. These 'venous clipping studies' have demonstrated that altered hemodynamics in the developing heart can result in cardiovascular malformations, mostly malformations of the outflow tract (OFT) [9, 12].

Maternal hyperhomocysteinemia, an increased level of the methionine derivative homocysteine in maternal blood, has been associated with an approximately three-fold increased risk of congenital cardiovascular malformations [15]. This association has been substantiated in the chicken embryo, as specific cardiac malformations like ventricular septal defects and conotruncal heart defects have been reported after homocysteine treatment [16-18]. These specific defects are comparable to the type of defects observed in the venous clipping model, suggesting that homocysteine may induce its effects, among others, by altering blood flow and shear stress resulting in CHD. To test this hypothesis, our aim was to quantitate WSS in the OFT of the homocysteine exposed chicken embryo. WSS was derived from the velocity field obtained with the use of microscopic Particle Image Velocimetry (μPIV),

since it cannot be measured directly. The OFT of chicken embryos was studied at embryonic day (ED) 3, Hamburger and Hammilton (HH) stage 18 [19]. At this stage, the heart is under constant development, and the OFT of the developing heart has been described to be most sensitive to alterations in blood flow dynamics [12, 20].

MATERIALS AND METHODS

Injection of homocysteine

Fertilized White leghorn chicken eggs (*Gallus Gallus*) (Drost Loosdrecht BV, Loosdrecht, The Netherlands) were incubated horizontally at 37 degrees Celcius. After approximately 30 hours (HH 9-10), the embryos were taken out of the incubator. The egg was placed in a metal holder on a heated plate to maintain temperature at 37 degrees. A small window of approximately 1.5 by 1.5 cm was sawn in the eggshell to allow embryo treatment. Either a homocysteine (n=30) or a sham solution (n=30), with M199 medium (Gibco, Invitrogen corporation) and Indigo Carmine Bleu, was injected into the lumen of the neural tube of the embryos at somite level 4-6, filling the neural tube in the anterior direction until the solution reached the otic placode level. The homocysteine treatment consisted of 30 μM L-homocysteine-thiolactone solution in MilliQ, and was performed according to Boot et al. [21]. This concentration has been demonstrated to result in OFT defects [16]. Sham treatment consisted of the physiological MilliQ solution with M199 medium and Indigo Carmine Blue only. After injection, the eggs were sealed with Scotch tape and placed back into the incubator for further development.

Microscopic Particle Image Velocimetry

At ED 3, the eggs were taken out of the incubator and the window was reopened. Embryos were staged macroscopically with the use of a microscope and HH stage 18 embryos were included for further examination. The egg was placed under an epifluorescent microscope (Leica MZ 16 FA), while partially submerged in a temperature controlled water bath of 37 degrees. To prevent dehydration and allow undistorted imaging, a glass coverslip was placed on top of the window. Visualization of blood flow was achieved by injection of a total injection volume of <1 μl of 1 μm polyethylene glycol (PEG)-coated polystyrene fluorescent tracer particles (Microparticles GmbH, Berlin, Germany) into the right vitelline artery. Due to the small size of the particles, they accurately follow blood flow. The tracer particles were illuminated using a dual-cavity Nd:YLF laser (Pegasus, New Wave, ESI, Fremont CA, USA). Flow velocity was determined by imaging the particles with a CCD camera (Imager Intense QE, LaVision, Goettingen, Germany) that records image pairs at a frame rate of 9.9 Hz. The measurements were taken at the midplane of the OFT (Figure 1a). The delay between the two

images of each of these pairs was set to 500 microseconds, so that the tracer displacement was below 10 pixels. The local displacement was determined by cross-correlating the images and the velocity then follows by dividing by the delay time [22]. Series of 500 image pairs were recorded each measurement, with a duration of approximately 50 s. The cardiac cycle was divided into 10 phase steps and the data were grouped and averaged within a group to improve accuracy. This way a vector field at one phase step is based on typically 50 image pairs. Phase 0 was assigned to systole. Detailed description of the procedure of *in vivo* μPIV was given by Vennemann et al. [22] and Poelma et al [23]. Because of the complexity of the experiments, we achieved to obtain successful μPIV measurements of 3 homocysteine and 4 control embryos. The other embryos did not survive the experimental procedure.

Figure 1

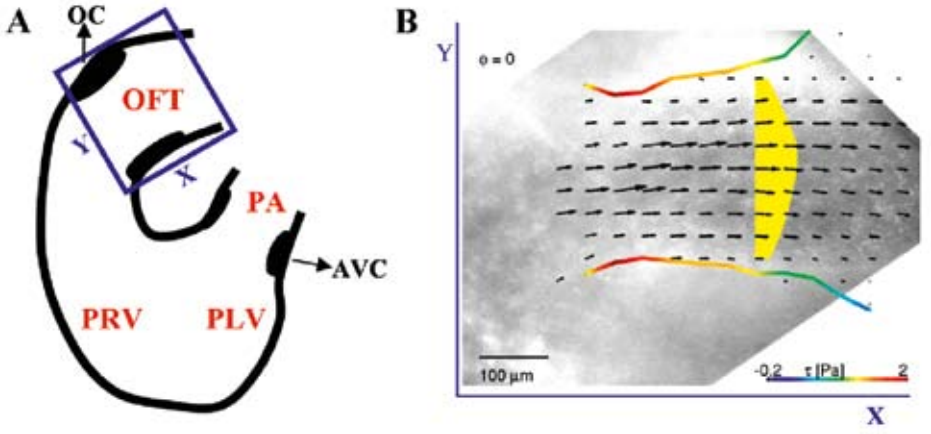

A schematic presentation of the anatomy of a HH18 chicken heart. Blood flows from the primitive atrium (PA) into the primitive left ventricle (PLV). In between, the atrio-ventricular cushions (AVC) are situated. Between the primitive right ventricle (PRV) and the outflow tract (OFT), the outflow cushions (OC) are situated. The blue square containing an X-axis and a Y-axis represent the midplane of the OFT in which μPIV measurements have been recorded. B. An example of the velocity field at the midplane of the OFT. The wall location is reconstructed and color coded with the shear stress level. Shear stress presented in (Pa).

Determination of WSS

The WSS distribution is derived from the velocity fields as determined by μPIV. This is done by making use of the definition of the WSS: $\tau = \eta\, du/dn$, with η the dynamic viscosity of blood and du/dn the gradient of the velocity in the wall-normal direction. This gradient at

the wall (du/dn) is determined by fitting a polynomial function to the velocity profile along a cross-section of the vessel. The location of the wall can be obtained by finding the roots of the polynomial and the WSS follows from the gradient of the polynomial at the wall locations. This process is repeated in the next vessel segment so that the vessel geometry and WSS distribution can be reconstructed. For an extensive explanation of this technique, one is referred to Poelma et al. [23]. This method is applicable to any flow pattern and thus more accurate than conventional approaches that rely on Poiseuille's law, which assumes a parabolic flow profile. For the complex, curved geometry of the embryonic heart and OFT, the latter assumption cannot be relied on.

Statistical Analysis

Statistical analyses for small sample sizes were performed. We applied Student T-tests to compare hemodynamic parameters of sham and homocysteine treated embryos. Data were corrected for heart rate. A Pearson correlation matrix was performed to test correlations between parameters. A p-value of <0.05 was considered statistically significant.

Table 1 Hemodynamic parameters of homocysteine treated and control embryos

		Hcy treated (n=3)	Control (n=4)	Difference Hcy vs Control (%)	Data Hcy corrected for HR	Data Control corrected for HR	Difference Hcy vs control (%) after correction
Heart rate	(1/min)	134.6 (6.9)	117.9 (20.3)	(%)	NA	NA	NA
Maximum velocity	(mm/s)	29.3 (4.6)	34.5 (7.9)	-15	0.22 (0.04)	0.30 (0.08)	-27
OFT diameter	(mm)	0.31 (0.03)	0.32 (0.04)	-3	NA	NA	NA
Mean Wall Shear Stress	(Pascal)	1.12 (0.25)	1.24 (0.22)	-10	0.008 (0.002)	0.011 (0.002)	-27
Shear rate	(1/s)	373,1 (82,0)	414.6 (74.9)	-10	2.78 (0.68)	3.56 (0.67)	-22
Peak flow	(mm3/s)	1,13 (0,18)	1.48 (0.56)	-24	0.008 (0.001)	0.013 (0.006)	-38
Mean flow	(mm3/s)	0,26 (0,06)	0.30 (0.08)	-13	0.002 (0.000)	0.003 (0.001)	-33

Hemodynamic parameters of HH18 homocysteine and sham treated (control) chicken embryos obtained with μPIV measurements presented in mean (SD). The difference between homocysteine and control embryos is presented in percentage. The hemodynamic parameters of homocysteine and control embryos have been adjusted for heart rate by calculating ratios, i.e., maximum velocity/heart rate. After adjustment the differences remained in the same direction and in terms of percentage have increased.

RESULTS

Flow characteristics in the OFT

Hemodynamic parameters obtained with μPIV are presented in Table 1. Although no significance was reached, the mean heart rate was slightly higher in homocysteine treated embryos, with a difference of 14 percent. Others parameters tended to be lower in homocysteine treated embryos compared to control embryos, with a reduction of 10 to 24 percent. After adjustment for heart rate by dividing the presented values by heart rate, the differences between the groups were even more pronounced. For all parameters, also after adjustment, no level of significance was reached when comparing data of homocysteine treated embryos with control embryos. As multiple planes were recorded, the midplane of the OFT was selected for analysis (Figure 1).

Correlation Matrix

Data from all embryos were tested for correlations between the different parameters (Table 2). Maximum velocity was correlated to shear rate, mean WSS and peak flow. Shear rate was correlated to mean WSS. OFT diameter was correlated to peak flow and mean flow. Peak flow was correlated to mean flow.

Table 2 Correlation matrix all embryos

		Heart rate (1/min)	Maximum velocity (mm/s)	OFT diameter (mm)	Mean Wall Shear Stress (Pascal)	Shear rate (1/s)	Peak flow (mm3/s)	Mean flow (mm3/s)
Heart rate	(1/min)	-	-	-	-	-	-	-
Maximum velocity	(mm/s)	-0.40	-	-	-	-	-	-
OFT diameter	(mm)	-0.68	0.39	-	-	-	-	-
Mean Wall Shear Stress	(Pascal)	-0.02	0.83*	-0.19	-	-	-	-
Shear rate	(1/s)	-0.02	0.83*	-0.19	1.00*	-	-	-
Peak flow	(mm3/s)	-0.63	0.87*	0.79*	0.45	0.45	-	-
Mean flow	(mm3/s)	-0.65	0.70	0.88*	0.21	0.21	0.93	-

Correlation matrix of parameters obtained from all embryos (n=7). Values are given for Pearson's correlation. * indicates values that have reached statistical significance ($p<0.05$).

Wall Shear Stress

With the use of flow rate (mm^3/s), obtained by µPIV, wall shear stress was calculated. Additionally, the location of the vessel wall was extracted from the flow data. Figure 2 and 3 present wall shear stress measurements in a homocysteine treated and a control embryo at 5 successive timepoints of one cardiac cycle. These figures show that, in general, wall shear stress was lower in homocysteine treated embryos compared to control embryos, most evidently visible during systole (Φ =0). Mean wall shear stress in homocysteine treated embryos was 1.12 (0.25) Pa, compared to 1.24 (0.22) Pa in control embryos. At different phases of the cardiac cycle the outflow tract cushions (Figure 1a) were closed and no blood flow was detected. Consequently, no vessel wall could be extracted in these plains (Figure 2d/3d). Figures 2f and 3f display the mean blood flow velocity (mm/s) measured in the OFT at 5 successive timepoints of the 2 consecutive cardiac cycles.

Figure 2

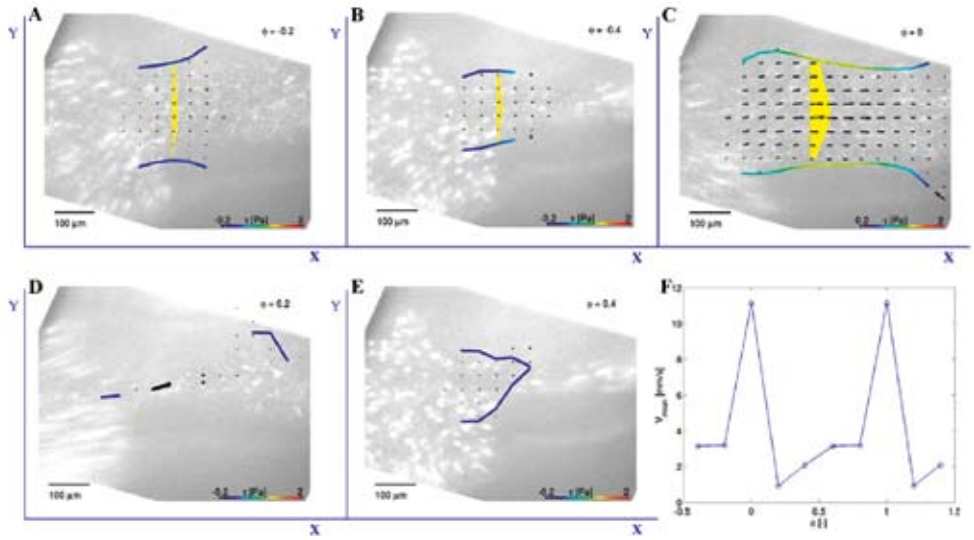

Velocity distribution at the midplane of the OFT in a HH18 homocysteine embryo, at 5 successive time points of one cardiac cycle. Starting from A: phase -0.4 (Φ) until E: Φ= 0.4. Phase 0 represents systole during the cardiac cycle. The wall location is reconstructed and color coded with the shear stress level. Shear stress is presented in (Pa). The arrows indicate flow direction. F: is a schematic representation of mean blood flow velocity (mm/s) present in the OFT at 2 consecutive cardiac cycles. One complete cardiac cycle starts from Φ =-0.4 until Φ =0.6. No wall location is presented in image D because there is no blood flow during this phase of the cardiac cycle.

DISCUSSION

In this study we have shown that homocysteine treatment during early embryonic development tends to reduce wall shear stress in the OFT of the chicken embryonic heart. Additionally, homocysteine treatment causes a reduction of peak flow and peak velocity. This coincides with the results from a previous Doppler study performed by our research group, describing reduced hemodynamic parameters of chicken embryonic heart function like peak velocities and velocity time integrals, after homocysteine treatment [24]. The decrease in shear stress found in this study may follow from a reduction of hemodynamic parameters induced by homocysteine. From the definition of the WSS, $\tau = \eta\, du/dn$, one can expect this decrease: when the flow rate - and thus the associated velocity profile - decreases, the resulting WSS will decrease proportionally. Since the correlation matrix shows no correlation between heart rate and the other parameters, the effect of homocysteine on WSS is independent of heart rate.

Figure 3

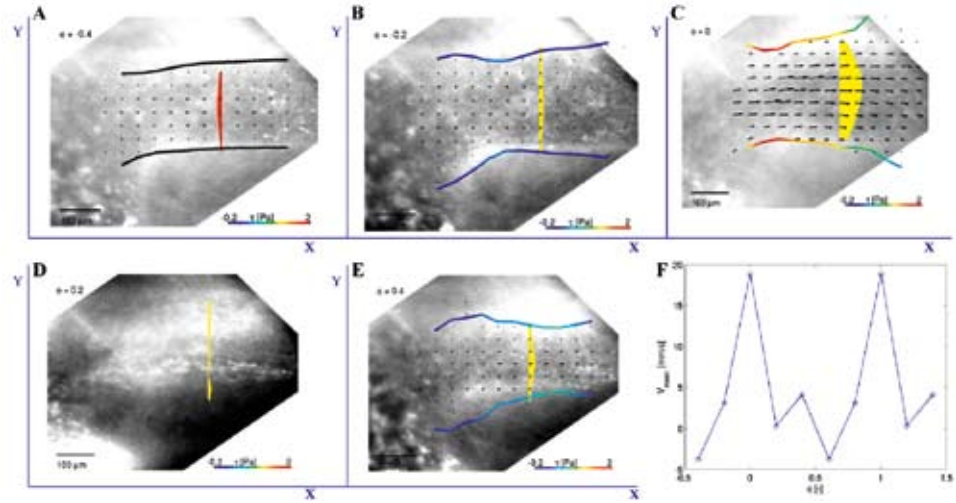

Velocity distribution at the midplane of the OFT in a HH18 control embryo, at 5 successive time points of one cardiac cycle. Starting from A: phase -0.4 (Φ) until E: Φ= 0.4. Phase 0 represents systole during the cardiac cycle. The wall location is reconstructed and color coded with the shear stress level. Shear stress is presented in (Pa). The arrows indicate flow direction. F: is a schematic representation of mean blood flow velocity (mm/s) present in the OFT at 2 consecutive cardiac cycles. One complete cardiac cycle starts from Φ =-0.4 until Φ =0.6. No wall location is presented in image D because there is no blood flow during this phase of the cardiac cycle.

The effects of homocysteine on hemodynamic parameters and shear stress presented in this study may influence cardiogenesis in a similar way as ligation of the right lateral vitelline vein. Homocysteine treatment, as well as venous clipping, results in disturbance of normal intracardiac blood flow patterns. After venous clipping, decreased heart rate and peak velocities have been reported [14]. Shear stress is dependent on volume flow and is therefore affected in a situation of altered flow. Shear stress, exerted on the endothelial cells that line the inner walls of the OFT, drives gene expression [25-26]. Endothelial cells respond to the magnitude, frequency and direction of the shear stress, and alterations from normal shear, either an increase or decrease, will lead to signalling events [25]. Altered expression of the shear stress responsive genes Krüppel-like factor-2 (KLF-2), endothelin-1 (ET-1) and endothelial nitric oxide synthase (NOS-3), have been reported after venous clipping [27]. Altered gene expression in reaction to lowered shear stress may cause changes in cardiac morphology. This is supported by the 'venous clipping studies' that have shown that alterations in blood flow and consequently shear stress levels can lead to the development of specific heart defects [13, 27]. Therefore, we conclude that altered hemodynamics and WSS, exerted by homocysteine treatment, may influence cardiac morphology.

In our experiments, heart rates obtained by µPIV were lower than previously described [28-29]. This may be explained by the fact that Doppler ultrasonography, applied in previous studies describing hemodynamic parameters of the early chicken embryo, requires no manipulation of the embryo preceding the recording of flow velocity profiles. Since the egg was partly placed in a temperature controlled water bath to maintain temperature at 37 degrees, this will not have influenced heart rate or hemodynamic parameters. In this study, heart rates are probably reduced because of the complexity of the performed technique. This is supported by the fact that in only approximately 10 percent of the treated embryos successful µPIV measurements were obtained. Even though the injection of fluorescent tracer particles is needed to be able to perform µPIV measurements and quantitate WSS, it is plausible that this affects the embryo as well as its hemodynamic functioning.

The 30 µmol/L concentration of the homocysteine solution applicated to the embryos in this study has been shown to result in OFT defects in the chicken embryo [16] and is comparable to the mild to moderate hyperhomocysteinemia (15-150 µmol/L) in humans associated with neural tube defects and congenital heart defects [15, 30-31].

The reported shear stress in control embryos, 1.24 Pa, coincides well with levels of 1-3 Pa previously described in HH 18 chicken embryos [23]. It also matches well with the shear stress of 3.1 Pa found by Liu et al.[20], and of 5 Pa described by Vennemann et al. [22] and Hierck et al. [2], since this concerns the maximum shear stress at the inner curvature of the OFT and we have presented mean shear stress levels in the OFT. Also, Liu et al.

has studied older embryos of HH stage 21. During development, as the chicken embryo grows, hemodynamic parameters of chicken embryonic heart function will increase [28], consequently leading to higher shear stress levels.

A limitation of our study is the low sample size. Also, with current techniques like μPIV, it is not possible to directly measure shear stress. However, WSS is in theory much more accurately determined with data obtained by μPIV compared to studies using (Hagen-) Poisseuilles law, requiring less information. Still, shear stress levels are estimated from the velocity profile, which is difficult to measure near the wall of a beating heart.

We conclude that a trend of reduced hemodynamic parameters and wall shear stress is seen after homocysteine treatment in the early embryonic chicken heart. We suggest that the alterations in WSS may cause different behaviour and gene expression of the endothelial cells in the embryonic chicken heart, eventually leading to the development of congenital heart defects. These findings warrant further investigation.

REFERENCES

1. Nerem, R.M., et al., *Hemodynamics and vascular endothelial biology.* J Cardiovasc Pharmacol, 1993. **21**(Suppl 1): p. S6-10.
2. Hierck, B.P., et al., *Fluid shear stress and inner curvature remodeling of the embryonic heart. Choosing the right lane!* ScientificWorldJournal, 2008. **8**: p. 212-22.
3. Takahashi, M., et al., *Mechanotransduction in endothelial cells: temporal signaling events in response to shear stress.* J Vasc Res, 1997. **34**(3): p. 212-9.
4. Malek, A.M. and S. Izumo, *Control of endothelial cell gene expression by flow.* J Biomech, 1995. **28**(12): p. 1515-28.
5. Davies, P.F., *Flow-mediated endothelial mechanotransduction.* Physiol Rev, 1995. **75**(3): p. 519-60.
6. Groenendijk, B.C., et al., *The role of shear stress on ET-1, KLF2, and NOS-3 expression in the developing cardiovascular system of chicken embryos in a venous ligation model.* Physiology (Bethesda), 2007. **22**: p. 380-9.
7. Groenendijk, B.C.W., et al., *Development-related changes in the expression of shear stress responsive genes KLF-2, ET-1, and NOS-3 in the developing cardiovascular system of chicken embryos.* Dev Dyn, 2004. **230**(1): p. 57-68.
8. Hove, J.R., et al., *Intracardiac fluid forces are an essential epigenetic factor for embryonic cardiogenesis.* Nature, 2003. **421**(6919): p. 172-177.
9. Hogers, B., et al., *Extraembryonic venous obstructions lead to cardiovascular malformations and can be embryolethal.* Cardiovasc Res, 1999. **41**(1): p. 87-99.
10. Nakazawa, M., et al., *Hemodynamic effects of environmental hyperthermia in stage 18, 21, and 24 chick embryos.* Pediatr Res, 1986. **20**(12): p. 1213-5.
11. Clark, E.B. and N. Hu, *Developmental hemodynamic changes in the chick embryo from stage 18 to 27.* Circ Res, 1982. **51**: p. 810-815.
12. Hogers, B., et al., *Unilateral vitelline vein ligation alters intracardiac blood flow patterns and morphogenesis in the chick embryo.* Circ Res, 1997. **80**(4): p. 473-481.
13. Broekhuizen, M.L., et al., *Altered hemodynamics in chick embryos after extraembryonic venous obstruction.* Ultrasound Obstet Gynecol, 1999. **13**(6): p. 437-45.
14. Stekelenburg-de Vos, S., et al., *Acutely altered hemodynamics following venous obstruction in the early chick embryo.* J Exp Biol, 2003. **206**(Pt 6): p. 1051-1057.
15. Verkleij-Hagoort, A., et al., *Hyperhomocysteinemia and MTHFR polymorphisms in association with orofacial clefts and congenital heart defects: a meta-analysis.* Am J Med Genet A, 2007. **143A**(9): p. 952-60.
16. Boot, M.J., et al., *Cardiac outflow tract malformations in chick embryos exposed to homocysteine.* Cardiovasc Res, 2004. **64**(2): p. 365-73.
17. Rosenquist, T.H., S.A. Ratashak, and J. Selhub, *Homocysteine induces congenital defects of the heart and neural tube: effect of folic acid.* Proc Natl Acad Sci U S A, 1996. **93**(26): p. 15227-32.
18. van Mil, N.H., A.M. Oosterbaan, and R.P. Steegers-Theunissen, *Teratogenicity and underlying mechanisms of homocysteine in animal models: A review.* Reprod Toxicol, 2010.
19. Hamburger, V. and H.L. Hamilton, *A series of normal stages in the development of the chick embryo.* J Morphol, 1951. **88**: p. 49-92.
20. Liu, A., et al., *Finite element modeling of blood flow-induced mechanical forces in the outflow tract of chick embryonic hearts.* Computers & Structures, 2007. **85**(11-14): p. 727-738.
21. Boot, M.J., et al., *Homocysteine induces endothelial cell detachment and vessel wall thickening during chick embryonic development.* Circ Res, 2004. **94**(4): p. 542-9.
22. Vennemann, P., et al., *In vivo micro particle image velocimetry measurements of blood-plasma in the embryonic avian heart.* J Biomech, 2006. **39**(7): p. 1191-1200.

23. Poelma, C., et al., *Measurements of the wall shear stress distribution in the outflow tract of an embryonic chicken heart.* J R Soc Interface, 2010. **7**(42): p. 91-103.
24. Oosterbaan, A.M., et al., *Homocysteine Affects Early Heart Function In the Chicken Embryo.* Anat Rec, Accepted for Publication 2012 March
25. Fisher, A.B., et al., *Endothelial cellular response to altered shear stress.* Am J Physiol Lung Cell Mol Physiol, 2001. **281**(3): p. L529-533.
26. Malek, A.M., et al., *Fluid shear stress differentially modulates expression of genes encoding basic fibroblast growth factor and platelet-derived growth factor B chain in vascular endothelium.* J Clin Invest, 1993. **92**(4): p. 2013-21.
27. Groenendijk, B.C., et al., *Changes in shear stress-related gene expression after experimentally altered venous return in the chicken embryo.* Circ Res, 2005. **96**(12): p. 1291-8.
28. Oosterbaan, A.M., et al., *Doppler fow velocity waveforms in the embryonic chicken heart at developmental stages corresponding to 5-8 weeks of human gestation.* Ultrasound in Obstetrics and Gynecology, 2009. **33**(6): p. 638-44.
29. Hu, N. and E.B. Clark, *Hemodynamics of the stage 12 to stage 29 chick embryo.* Circ Res, 1989. **65**: p. 1665-1670.
30. Steegers-Theunissen, R.P., et al., *Neural-tube defects and derangement of homocysteine metabolism.* N Engl J Med, 1991. **324**(3): p. 199-200.
31. Steegers-Theunissen, R.P., et al., *Maternal hyperhomocysteinemia: a risk factor for neural-tube defects?* Metabolism, 1994. **43**(12): p. 1475-80.

5

Homocysteine disturbs early heart function in the chicken embryo: effects of folic acid and 5-methyltetrahydrofolate

A.M. Oosterbaan, E.A.P. Steegers, N.T.C. Ursem

Submitted

ABSTRACT

Introduction Maternal hyperhomocysteinemia is associated with a three-fold increased risk of congenital heart defects (CHD) in newborns. This has been substantiated in chicken embryo studies. Furthermore, epidemiological studies have shown that maternal periconceptional folic acid (FA) use reduces the prevalence rate of CHD by approximately 20%. We have previously shown that homocysteine (Hcy) significantly changes hemodynamic parameters of chicken embryonic heart function. The possible protective effects of FA and 5-methyltetrahydrofolate (mefolinate), both serving as substrates in the Hcy pathway, are, however, unknown.

Methods With ultrasound biomicroscopy (Vevo 770), we have studied the effects of homocysteine thiolactone, FA, mefolinate and combined treatment of Hcy and FA on hemodynamic parameters of early embryonic chicken heart function at 3.5 days of incubation.

Results Survival rates of FA and mefolinate treated embryos were similar to control embryos, but significantly increased compared to Hcy and Hcy + FA embryos. Hcy embryos showed reduced survival rates compared to control embryos. Specific hemodynamic parameters of FA and mefolinate embryos were similar to parameters of control embryos, except for FA embryo primitive left ventricle (PLV) passive (P) wave velocity time integral (VTI) and P wave time. Wave times in percentages of total cycle time were significantly different between Hcy and Hcy + FA embryos.

Conclusions We conclude that FA and mefolinate equally stimulate embryo survival. FA in combination with Hcy does not improve survival rates, but FA does show protective features by changing Hcy effects on hemodynamic parameters of embryonic heart function. This could be one of the mechanisms through which human periconceptional FA use prevents CHD in the offspring.

INTRODUCTION

Congenital heart defects (CHD) cause substantial perinatal morbidity and mortality and affect 6 - 19 per 1000 live births worldwide each year [1]. In only about 15% of cases a cause can be identified [2]. Mild to moderate maternal hyperhomocysteinemia has been associated with an approximately three-fold increased risk of CHD in the offspring [3]. Therefore, many studies on underlying mechanisms of CHD have been focussing on the homocysteine (Hcy) pathway.

Maternal periconceptional use of the synthetic folate folic acid (FA) has been shown to protect against CHD [4], reducing CHD prevalence by approximately 20% [5]. FA is converted by the methylene-tetrahydrofolate reductase (MTHFR) into 5-methyl-tetrahydrofolate (5-methyl-THF), the primary circulatory form of FA in the body that serves as a substrate in the remethylation of Hcy into methionine, reducing blood Hcy levels. Mefolinate is the synthetic form of 5-methyl-THF. Besides the indirect effects of FA through the reduction of blood Hcy levels, FA also has direct effects on growth and development. FA serves as a cofactor in nucleic acid synthesis and cell division [6], being involved in purine and thymidine synthesis. Periconceptional FA has been associated with increased fetal growth [7] and has been shown to increase methylation of the insulin-like growth factor 2 gene differentially methylation region (IGF2 DMR), that may influence intrauterine programming of growth and development [8]. Moreover, in the chicken embryo, Hcy has been shown to directly affect neural crest cell differentiation patterns. FA per se also affects these cells [9]. Cardiac neural crest cells are important in heart and pharyngeal arch artery development.

The association between hyperhomocysteinemia and CHD has been substantiated in the chicken embryo, as elevated Hcy exposure has been reported to increase CHD frequencies [10-12]. There is an interesting overlap in the heart defects described in the chicken embryo after Hcy treatment and those observed in studies in which the extra embryonic chicken blood flow has been altered by venous clipping [13-14].

Hcy may cause CHD by affecting endothelial cells [15-18] or neural crest cells during embryo development. Hcy causes endothelial cell damage, as well as disrupted nitric oxide synthesis [19-20] and increased oxidative stress [21] during embryogenesis, that can result in impaired angiogenesis [16, 22]. Impaired angiogenesis may lead to reduced vascularization, embryonic blood flow and altered cardiac function. Above mechanisms offer a potential link between CHD after Hcy exposure and CHD after venous clipping in the chicken embryo.

To test the hypothesis that Hcy induced CHD may be preceded by changes in embryonic heart function, Doppler flow velocity waveforms can be recorded with the use of high frequency ultrasound biomicroscopy [23-24]. With this technique we have shown that Hcy does indeed significantly affect hemodynamic parameters of early chicken embryonic heart function (Oosterbaan et al., 2010, unpublished data). FA may also directly affect embryonic

heart function parameters, or protect from Hcy effects on early heart function, this way reducing CHD prevalence rates. The direct effects of the substrates in Hcy remethylation, i.e. FA and mefolinate, or the possible potency of FA to protect from the effects induced by Hcy on hemodynamic parameters of chicken embryonic heart function have never been investigated. This information will increase our knowledge on the complex aetiology of congenital heart defects in the offspring of mothers with mild to moderate hyperhomocysteinemia and the role of FA and mefolinate.

The purpose of this study was to answer the following questions: (i) Do FA and mefolinate affect chicken embryonic heart function and embryo development? (ii) Do FA and mefolinate have similar effects on hemodynamic parameters of chicken embryonic heart function? (iii) Does FA protect from the effects Hcy exerts on these parameters?

MATERIALS AND METHODS

Embryos

Fertilized White Leghorn chicken eggs (*Gallus Gallus* (L.)) (Drost Loosdrecht BV, Loosdrecht, Netherlands) were incubated blunt-end up at 37.5 ºC. After 24 hours of incubation, a 2 mm hole was made in the shell and the outer shell membrane at the site of the air space to enable treatment of the embryo. At 24, 48 and 72 hours of incubation, a solution was applicated to the embryo via a droplet on the inner shell membrane using a micropipette. This mode of application was based on *in ovo* experiments conducted by Rosenquist et al., resulting in structural cardiac malformations [11].

Group 1, the control group, received 50 µl of a sham solution consisting of Locke's solution only (0.94% NaCl, 0.045% KCl, and 0.033% $CaCl_2$ w/v in Milli-Q). Group 2, the homocysteine group, received 50 µl of 0.05 M L-homocysteine thiolactone hydrochloride (Sigma-Aldrich, Steinheim, Germany) in Locke's solution per day. Group 3, the folic acid group, received 0.1 µg of folic acid (Sigma-Aldrich) in Locke's solution per day. Group 4, the mefolinate group, received 0.12 µg of sodium-L-mefolinate (kindly provided by Merck Eprova AG, Schaffhausen, Switzerland) in Locke's solution per day. We started with 2 combination groups, which either received simultaneous application of 50 µl of 0.05 M Hcy combined with 0.1 µg FA, or received 50 µl of 0.05 M Hcy combined with 0.12 µg mefolinate. Embryo survival was only 5-10 %. After diluting the solutions to 50% of the above concentration, still most embryos were not suitable for further analysis because they were extremely growth retarded and survival was only 15%. Therefore, we proceeded with only one combination group, group 5, put on a treatment schedule according to Kobus et al. [25], which received one single treatment containing 50 µl of 0.1 M Hcy combined with 0.25 µg FA in Locke's solution after 30 hours of incubation.

After each treatment the hole in the shell was covered with a piece of non-toxic magic tape and the egg was placed back in the incubator. Thirty minutes after the last application, the embryos were placed horizontally until they reached 3.5 days of incubation.

Figure 1 Embryo survival rates

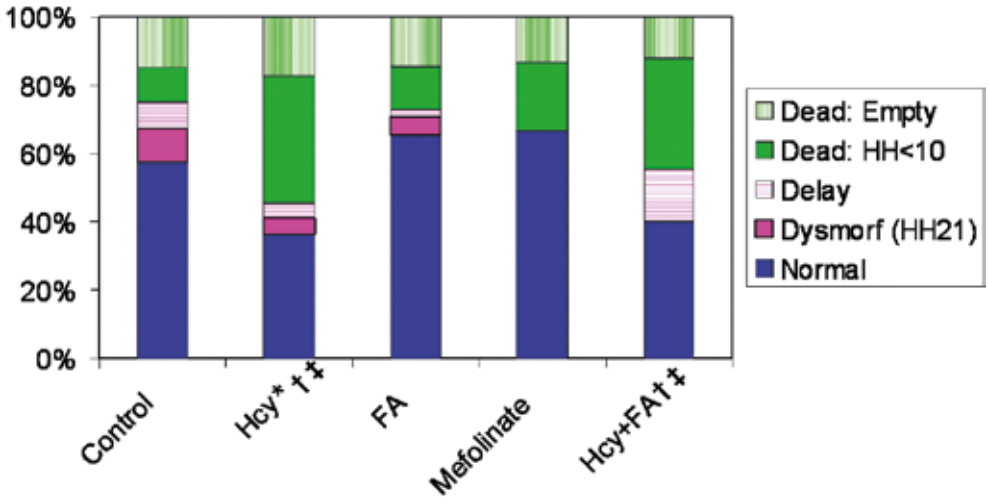

Embryo survival of the 5 research groups; blue: normal HH21 embryos; pink: embryos that had reached HH21 but were dysmorf and not suitable for measurement; pink striped: embryos that were delayed, and had reached stages between HH10 and HH21; green: dead embryos, either HH<10; green striped: empty eggs (partly instigated by the experimental procedure). * means statistically significant survival rate of normal embryos compared to control embryos; † means statistically significant survival rate of normal embryos compared to FA embryos; ‡ means statistically significant survival rate of normal embryos compared to mefolinate embryos

Ultrasound biomicroscopy

After 3.5 days the eggs were taken out of the incubator. Embryos were reached by sawing a window of approximately 1.5 by 1.5 cm in the outer shell. The window was covered by a piece of polyethylene foil on which warmed ultrasonic gel was deposited. Embryo temperature was measured and maintained at 37ºC with the help of a heated plate a heat lamp. The embryo was staged according to Hamburger and Hamilton [26] and HH21 embryos were included. Embryos that showed visible bleeding and embryos that were not positioned on their left side were excluded. The last group was excluded to limit the variation in angle of insonation of the ultrasound probe.

Figure 1 shows embryo survival rates, as a representative of embryo development, and percentages of embryos measured per group. In total 15 embryos per group were studied with the Vevo 770 (VisualSonics Inc., Toronto, Canada), a high frequency ultrasound system with a 55-MHz transducer (RMV 708) and a focal depth of 4.5 mm. Measurements were performed and described in detail previously [23]. From each embryo, Doppler velocity signals were recorded at three cardiac sites; 1. the primitive left ventricle (PLV); 2. the primitive right ventricle (PRV) and 3. the outflow tract (OFT) (Figure 2a). From the obtained velocity waveforms we determined the heart rate (HR; bpm; beats per minute), peak velocities (cm/s), velocities integrated over time (VTI; cm) and wave times (ms) (Figure 2b). M-mode recordings at the site of the outflow cushions were obtained to determine outflow cushions opening and closure times (ms) and the diameter of the outflow tract at the site of the outflow cushions during maximum filling (mm) (Figure 2c). The outer distance between the primitive left ventricle and the outflow tract during maximum filling was determined as a measure of cardiac growth, and referred to as the epicardial diameter (mm) (Figure 2a). The Doppler angle was arbitrarily set to zero as flow direction could not be assessed accurately. Therefore, the Doppler velocities should be interpreted as relative velocities, which more precisely are the vectorial velocities in the direction of the ultrasound beam. From the PLV and PRV velocity waveform, the 'Passive' (P) wave, phase I, and the 'Active' (A) wave, phase II of the cardiac cycle representing ventricular filling, and the ventricular ejection wave, phase III of the cardiac cycle, were determined.

Figure 2 Measurement points and hemodynamic parameters

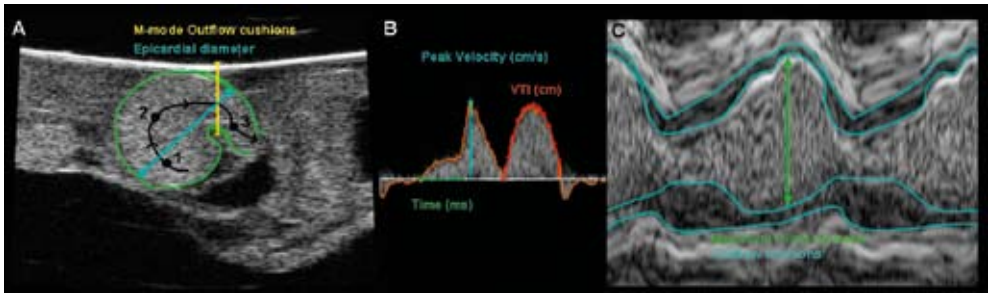

A: B-mode image of measurement points primitive left ventricle (PLV), primitive right ventricle (PLV) and outflow tract (OFT). Blue line indicates the epicardial diameter measurement, yellow line indicates the M-mode measurement point at the site of the outflow tract cushions, black line indicates the direction of blood flow. B: Doppler image of the PRV in a control embryo, with examples of a VTI, a peak velocity and a time measurement. C: M-mode image of the opening and closing of the outflow cushions (blue line). Green line: maximum filling diameter measurement point

Table 1 Comparison of general and specific hemodynamic parameters

Location		Variable	Control (*)	Hcy (†)	FA (‡)	Mefolinate (¤)	Hcy+FA
General		Heart rate (bpm)	155 (8)	146 (12) *	167 (16) * †	162 (8) †	172 (7) * † ¤
		Epicardial diameter (mm)	1.45 (0.09)	1.38 (0.09)	1.43 (0.08)	1.40 (0.10)	1.39 (0.06)
		OFT maximum filling diameter (mm)	0.41 (0.04)	0.38 (0.03) *	0.41 (0.04) †	0.41 (0.03)	0.38 (0.04) * ‡ ¤
PLV		P/A ratio peak velocity	0.31 (0.11)	0.46 (0.29)	0.27 (0.07)	0.38 (0.17)	0.37 (0.25)
		P/A ratio VTI	0.61 (0.37)	1.04 (0.60) *	0.36 (0.19) †	0.62 (0.27) †	0.48 (0.34) †
	P wave	VTI (cm)	0.13 (0.08)	0.17 (0.09)	0.08 (0.04) * †	0.12 (0.06) †	0.09 (0.05) †
		Peak velocity (cm/s)	1.49 (0.66)	1.72 (0.74)	1.35 (0.34)	1.55 (0.64)	1.45 (0.63)
		P wave/total time (%)	25.3 (7.6)	31.2 (9.8) *	19.7 (5.9) †	24.4 (6.9) †	20.9 (7.9) †
	A wave	VTI (cm)	0.21 (0.05)	0.18 (0.05)	0.21 (0.03) †	0.19 (0.03)	0.20 (0.07)
		Peak velocity (cm/s)	4.85 (1.13)	4.09 (1.08)	5.01 (0.78)	4.27 (0.77)	4.49 (1.35)
		A wave/total time (%)	20.2 (2.2)	17.3 (2.9) *	20.4 (3.2) †	21.1 (2.5) †	20.0 (2.5) †
	Ejection	VTI (cm)	0.13 (0.04)	0.10 (0.04)	0.15 (0.04) †	0.14 (0.05) †	0.12 (0.03) ‡
		Peak velocity (cm/s)	1.78 (0.49)	1.49 (0.39)	1.96 (0.45) †	1.92 (0.5) †	1.69 (0.33)
		Ejection/total time (%)	26.9 (5.8)	24.5 (4.8)	30.3 (3.6) †	27.9 (3.9)	29.5 (7.4) †
PRV		P/A ratio peak velocity	0.29 (0.11)	0.39 (0.18)	0.26 (0.06)	0.33 (0.10)	0.31 (0.14)
		P/A ratio VTI	0.54 (0.42)	0.95 (0.58) *	0.36 (0.31) †	0.55 (0.25) †	0.39 (0.29) †
	P wave	VTI (cm)	0.08 (0.04)	0.09 (0.04)	0.05 (0.03) †	0.08 (0.03) ‡	0.05 (0.03) * † ¤
		Peak velocity (cm/s)	1.01 (0.3)	0.90 (0.32)	1.01 (0.23)	1.01 (0.28)	0.87 (0.28)
		P wave/total time (%)	23.7 (8.8)	30.9 (9.0) *	20.4 (7.4) †	25.0 (7.7)	17.4 (8.3) †
	A wave	VTI (cm)	0.16 (0.04)	0.11 (0.04) *	0.18 (0.05) †	0.15 (0.03) †	0.13 (0.04) * ‡
		Peak velocity (cm/s)	3.66 (0.88)	2.48 (0.87) *	4.13 (1.02) †	3.19 (0.65) † ‡	3.05 (0.92) ‡
		A wave/total time (%)	19.3 (2.4)	16.4 (2.8) *	19.9 (3.1) †	20.9 (2.4) †	20.2 (2.1) †
	Ejection	VTI (cm)	0.25 (0.06)	0.20 (0.06) *	0.27 (0.07) †	0.26 (0.06) †	0.22 (0.07) ‡
		Peak velocity (cm/s)	3.12 (0.70)	2.70 (0.90)	3.49 (0.80) †	3.30 (0.65) †	3.04 (0.75)
		Ejection/total time (%)	29.6 (3.2)	26.5 (2.5) *	31.0 (5.0) †	30.5 (3.1) †	29.0 (4.0)
OFT	Outflow	VTI (cm)	0.56 (0.14)	0.48 (0.13)	0.53 (0.09)	0.51 (0.12)	0.48 (0.11)
		Peak velocity (cm/s)	5.07 (1.31)	4.67 (1.47)	5.18 (1.28)	4.47 (1.22)	4.46 (1.04)
		Ejection/total time (%)	50.4 (6.0)	44.1 (9.2) *	49.9 (9.9) †	54.8 (5.3) †	53.5 (8.2) †
		Diastolic/total time(%)	49.7 (5.7)	55.9 (9.1) *	49.9 (9.9) †	44.8 (5.4) †	46.6 (8.3) †
Outflow Cushions	M-mode	Closure/total time (%)	28.2 (5.4)	24.9 (8.6)	28.2 (6.7)	32.0 (8.3)	26.8 (5.7)

Comparison of general and specific hemodynamic parameters measured in the primitive left ventricle (PLV), the primitive right ventricle (PRV) and the outflow tract (OFT), mean (SD) with a significance level of $p<0.05$. VTI: Velocity-Time-Integral; P/A ratio: passive to active filling ratio; * means: Hcy, FA, mefolinate or Hcy + FA embryos are significantly different from control embryos; † means: FA, mefolinate or Hcy + FA embryos are significantly different from Hcy embryos; ‡ means: mefolinate or Hcy + FA embryos are significantly different from FA embryos; ¤ means: mefolinate embryos are significantly different from Hcy + FA embryos

Figure 3 Schematic presentations of the collected flow velocity waveforms

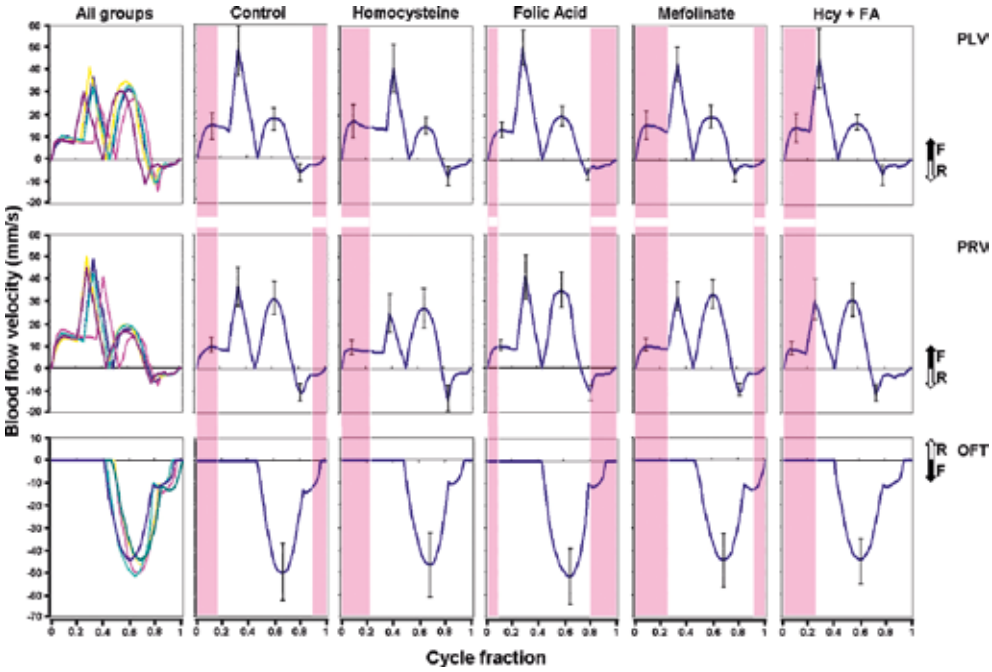

Pink line: control embryos; yellow line: homocysteine embryos; light blue line: folic acid embryos; green line: mefolinate embryos; dark blue line: homocysteine plus folic acid embryos. Pink bars: closure times outflow tract cushions

Data Analysis

Data were checked for normality of the distribution and are presented as mean and standard deviation, mean (SD). To determine group differences analysis of variance (One-Way ANOVA) was performed followed by Post-hoc LSD testing. Statistical significance was defined as a p value of less than 0.05. Calculations were performed with SPSS 15.0 (SPSS Inc., Chicago, USA).

RESULTS

General characteristics

Significant differences in mean heart rate between groups were found (Table 1). Hcy embryos had a significantly lower mean HR of 146 (12) bpm compared to all other group embryos. On the contrary, FA embryos showed a significantly higher mean HR than control embryos and the mean HR of Hcy + FA embryos was significantly higher than that of control and mefolinate embryos. Epicardial diameter measurements were not different between

the study groups. OFT maximum diameter, being the maximum diameter of the OFT during cardiac ejection (Figure 2c), was different between study groups. OFT maximum diameter of Hcy embryos, 0.38 (0.03) mm, was significantly smaller compared to control, 0.41 (0.04) mm, and FA, 0.41 (0.04) mm, embryos. OFT maximum diameter of Hcy + FA embryos, 0.38 (0.04) mm, was smaller than that of control, FA and mefolinate, 0.41 (0.03) mm, embryos. Closure time of the OFT cushions was not different between study groups, and is presented in a schematic representation of the collected Doppler flow velocity waveforms (Figure 3).

Figure 4

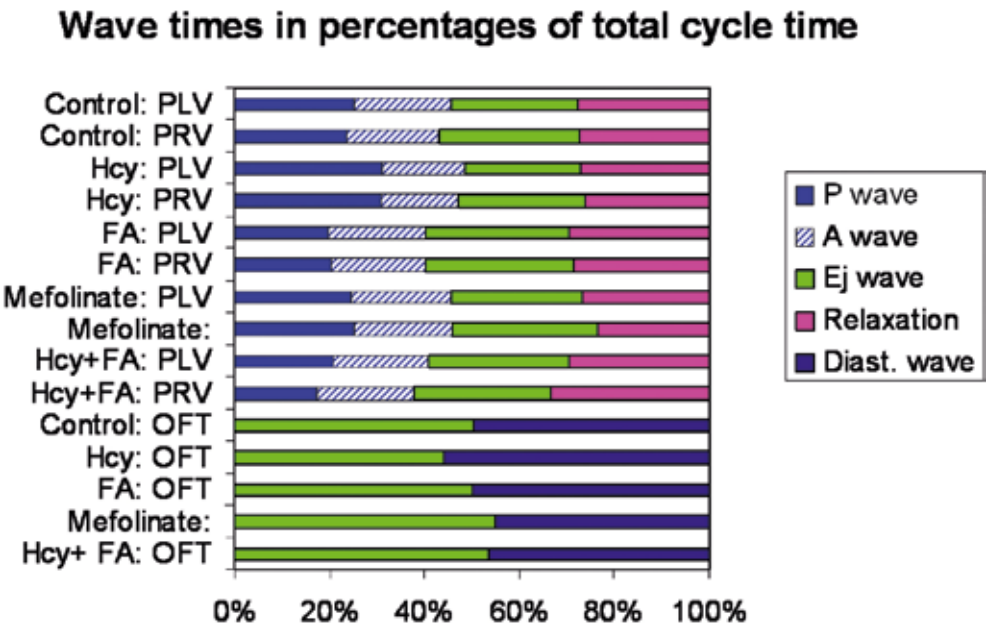

The wave times of each wave of one cardiac cycle are presented in percentage of total cycle time of one cardiac cycle. The bars are coloured and a legend is presented next to the chart. P wave: Passive wave; A wave: Active wave; Ej wave: Ejection wave; Diast. wave: Diastolic wave

Effects of FA and mefolinate

FA and mefolinate survival rates, 65.5% and 66.7% respectively, were comparable to the 57.5% survival rate of control, and significantly increased compared to the 36% of Hcy and the 40% of Hcy + FA embryos (Figure 1). To determine the effects of FA and mefolinate on early embryonic heart function, the hemodynamic parameters of FA and mefolinate embryos were compared to the parameters of control embryos. Additionally, of the

parameters that were significantly different between control and Hcy embryos as displayed in Table 1, the values of FA and mefolinate embryos were also compared to Hcy embryos.

In the PLV, FA embryos showed decreased P wave VTI compared to control embryos. All other parameters of FA and control embryos were similar. No significant differences were found between mefolinate and control embryo hemodynamic parameters. The parameters that were significantly different between control embryos and Hcy embryos, were equally or increasingly different between FA or mefolinate and Hcy embryos, expressed by equal or lower P values. Even more hemodynamic parameters were significantly different between FA or mefolinate embryos and Hcy embryos than between control and Hcy embryos. The additional parameters that were significantly different between FA or mefolinate embryos and Hcy embryos, that were not different between control and Hcy embryos, were PLV P wave VTI, PLV ejection VTI, as well as PLV and PRV ejection velocity.

FA Compared to Mefolinate

FA embryos were compared to mefolinate embryos, and both groups were compared to control embryos to determine whether effects of FA were different from mefolinate effects. Survival rates of both groups were similar. PRV P wave VTI was significantly higher in mefolinate embryos compared to FA embryos, and PRV A wave peak velocity was significantly lower in mefolinate embryos compared to FA embryos.

Preventive Effect of FA in Hcy + FA treated Embryos

Hcy + FA embryos were compared to control embryos. Additionally, we determined the parameters that were significantly different between Hcy and control embryos, and checked the rates of these parameters in Hcy + FA embryos to determine the possible protective effects of FA after combined Hcy + FA treatment. Survival rate of Hcy + FA embryos was 40%, which was not significantly different from the survival rate of control embryos, but significantly decreased compared to the survival of FA and mefolinate embryos.

Significant differences were found between Hcy + FA embryos and control embryos. PRV P and A wave VTI was significantly decreased in Hcy + FA embryos compared to control embryos. P wave time in percentage of total cycle time in both primitive ventricles was increased in Hcy embryos compared to control embryos, but these parameters were similar between Hcy + FA and control embryos (Figure 4). A wave time percentage in both primitive ventricles was decreased in Hcy embryos compared to control embryos. Again, in Hcy + FA embryos, the effect of Hcy was vanished and the rates of these parameters were similar to control embryos. PRV A wave peak velocity as well as A and ejection wave VTI was significantly reduced in Hcy embryos compared to control embryos.

In Hcy + FA embryos, PRV A wave VTI was similar to Hcy embryos and A wave velocity as well as ejection wave VTI were similar to control embryos. P/A ratios of VTI in both primitive ventricles were significantly increased in Hcy embryos compared to controls. In Hcy + FA embryos, these rates were similar to controls. PRV and OFT ejection time percentages were significantly decreased in Hcy embryos compared to control embryos, and Hcy + FA rates of these parameters were similar to controls. OFT diastolic time was significantly increased in Hcy embryos compared to control embryos. Again the rate of this parameter in Hcy + FA embryos was similar to control embryos.

DISCUSSION

Our chicken embryo study demonstrates the direct effects of FA and mefolinate on parameters of early embryonic heart function and embryo survival, as well as FA action in prevention of hemodynamic changes induced by Hcy. Additionally, we have shown that Hcy negatively influences embryo survival rates, even when FA is administered simultaneously wit Hcy.

The combination of increased mean HR with short passive filling wave time and passive filling wave VTI suggests that FA embryos are ahead in development compared to other group embryos. Previous chicken embryo studies have shown that heart rate increases with developmental stage [23, 27]. Additionally, we have shown previously that passive filling becomes less dominant with increasing developmental stage [23]. In the body synthetic FA is first converted to THF, and eventually to 5-methyl-THF. 5-methyl-THF is the cosubstrate that donates the methylgroup in the conversion of Hcy to methionine. Due to this conversion THF is liberated and available for its essential functions like purine and thymidine synthesis, stimulating nucleic acid synthesis and nucleotide excision repair. This may explain the stimulated embryo development after FA administration. However, the reported parameters of embryonic growth, i.e. epicardial diameter and OFT maximum filling diameter, were not significantly increased in FA embryos. We suggest that these parameters are not increased because they are solely measurements of the embryonic heart and not of the entire embryo, and they are not standardized references of embryonic growth like crown rump length (CRL).

Mefolinate embryos also displayed a higher mean HR than control embryos, although not significant, and all hemodynamic parameters were similar to those of control embryos. Therefore we conclude that mefolinate does not influence developmental rate and that overall, the effects on survival rate and hemodynamic parameters observed in mefolinate and FA embryos are largely similar. This coincides with studies in healthy volunteers, reporting mefolinate and FA to be equally effective in reducing plasma total Hcy concentration [28-

29]. Therefore we believe that FA and mefolinate are equally effective in preventing damage induced by elevated Hcy.

The reduced survival rate of Hcy + FA embryos was comparable to that of Hcy embryos. Human maternal hyperhomocysteinemia, an increased level of Hcy in the blood, has been associated with recurrent early miscarriages [30]. Hcy has also been related to inhibited angiogenesis [31]. Angiogenesis is of critical importance for embryo development and survival. We suggest that the inhibiting effect of Hcy on embryo survival is also present in Hcy + FA embryos because it is an early effect of Hcy that occurs even before there is a balance between Hcy and FA in the blood, and Hcy levels are still elevated. In the Hcy + FA embryos that survive this early stage, however, FA is able to protect from Hcy effects on hemodynamic parameters.

We have shown that FA has a preventive effect as, except for OFT maximum diameter and PRV A wave VTI, the significant differences found between Hcy and control embryos were not present in Hcy + FA embryos, illustrated by the comparable rates of these parameters between Hcy + FA and control embryos. Increased mean HR and decreased P wave parameters were present in Hcy + FA embryos, indicating that FA effects dominate Hcy effects on these parameters in Hcy + FA embryos. FA action in prevention of Hcy effects has been described previously in chicken embryo studies [9, 11, 25]. OFT maximum diameter and PRV A wave VTI being similar to Hcy embryos may be due to an imbalance between FA and Hcy levels, as suggested previously by Kobus et al. [25].

The reported effects induced by Hcy on hemodynamic parameters are similar to the results of preceding experiments performed by our research group (Oosterbaan et al., 2010, unpublished data). The effects Hcy exerts on endothelial cells [15, 32-33] and cardiac neural crest cells [10] during embryogenesis may explain the observed hemodynamic changes after Hcy application. Alterations in blood flow have been shown to lead to local changes in shear stress [13] and subsequently to changes in the expression of shear-responsive genes in the endocardial cells of the developing heart [34]. This may eventually result in the development of CHD [13]. Hemodynamics have also been implicated in cushion mechanics and composition, which may provide a link between altered hemodynamics and decreased OFT diameter after Hcy treatment [35], as at the site of the OFT the OFT cushions are situated.

Also the wave times in percentage of total cycle time [23], unpublished data) and the P/A ratio's of peak velocity [23, 35] of control embryos are comparable to previous measurements in ED 3.5 chicken embryos. Therefore, our results can be seen as a representative of the proportions of wave times and hemodynamic parameters belonging to HH21 embryonic chicken heart function.

A limitation of our study was the necessary change of the treatment schedule of embryos receiving a combined treatment. Because of the very low survival rates of the combination groups during our first experiments, and since we were determined to include a group with combined FA and Hcy treatment to be able to answer our research questions, we had to change the treatment schedule of these embryos. Embryos were treated once instead of three times. To ensure effective treatment we implemented the treatment schedule according to Kobus et al. [25].

We conclude that folic acid and mefolinate equally stimulate embryo survival. FA in combination with Hcy has a protective effect, changing Hcy effects on early embryonic heart function. Restoring parameters of early embryonic heart function could be one of the mechanisms through which periconceptional FA use prevents CHD in the offspring. Future research on the effects of Hcy and FA on shear stress and shear stress related genes is desired to further explore their role in the development of congenital heart defects.

REFERENCES

1. Hoffman, J.I. and S. Kaplan, *The incidence of congenital heart disease.* J Am Coll Cardiol, 2002. **39**(12): p. 1890-900.
2. Botto, L.D. and A. Correa, *Decreasing the burden of congenital heart anomalies: an epidemiologic evaluation of risk factors and survival.* Prog Pediatr Cardiol, 2003. **18**: p. 111-121.
3. Verkleij-Hagoort, A., et al., *Hyperhomocysteinemia and MTHFR polymorphisms in association with orofacial clefts and congenital heart defects: a meta-analysis.* Am J Med Genet A, 2007. **143A**(9): p. 952-60.
4. Botto, L.D., J. Mulinare, and J.D. Erickson, *Do multivitamin or folic acid supplements reduce the risk for congenital heart defects? Evidence and gaps.* Am J Med Genet A, 2003. **121A**(2): p. 95-101.
5. van Beynum, I.M., et al., *Protective effect of periconceptional folic acid supplements on the risk of congenital heart defects: a registry-based case-control study in the northern Netherlands.* Eur Heart J, 2009.
6. Smith, A.D., Y.I. Kim, and H. Refsum, *Is folic acid good for everyone?* Am J Clin Nutr, 2008. **87**(3): p. 517-33.
7. Timmermans, S., et al., *Periconception folic acid supplementation, fetal growth and the risks of low birth weight and preterm birth: the Generation R Study.* Br J Nutr, 2009. **102**(5): p. 777-85.
8. Steegers-Theunissen, R.P., et al., *Periconceptional maternal folic acid use of 400 microg per day is related to increased methylation of the IGF2 gene in the very young child.* PLoS One, 2009. **4**(11): p. e7845.
9. Boot, M.J., et al., *Folic acid and homocysteine affect neural crest and neuroepithelial cell outgrowth and differentiation in vitro.* Dev Dyn, 2003. **227**(2): p. 301-8.
10. Boot, M.J., et al., *Cardiac outflow tract malformations in chick embryos exposed to homocysteine.* Cardiovasc Res, 2004. **64**(2): p. 365-73.
11. Rosenquist, T.H., S.A. Ratashak, and J. Selhub, *Homocysteine induces congenital defects of the heart and neural tube: effect of folic acid.* Proc Natl Acad Sci U S A, 1996. **93**(26): p. 15227-32.
12. Han, M., et al., *Folate rescues lithium-, homocysteine- and Wnt3A-induced vertebrate cardiac anomalies.* Dis Model Mech, 2009. **2**(9-10): p. 467-78.
13. Hogers, B., et al., *Extraembryonic venous obstructions lead to cardiovascular malformations and can be embryolethal.* Cardiovasc Res, 1999. **41**(1): p. 87-99.
14. Hogers, B., et al., *Unilateral vitelline vein ligation alters intracardiac blood flow patterns and morphogenesis in the chick embryo.* Circ Res, 1997. **80**(4): p. 473-481.
15. Wall, R.T., et al., *Homocysteine-induced endothelial cell injury in vitro: a model for the study of vascular injury.* Thromb Res, 1980. **18**(1-2): p. 113-21.
16. Nagai, Y., et al., *Homocysteine inhibits angiogenesis in vitro and in vivo.* Biochem Biophys Res Commun, 2001. **281**(3): p. 726-31.
17. Harker, L.A., et al., *Homocystine-induced arteriosclerosis. The role of endothelial cell injury and platelet response in its genesis.* J Clin Invest, 1976. **58**(3): p. 731-41.
18. Woo, K.S., et al., *Hyperhomocyst(e)inemia is a risk factor for arterial endothelial dysfunction in humans.* Circulation, 1997. **96**(8): p. 2542-4.
19. Upchurch, G.R., Jr., et al., *Homocyst(e)ine decreases bioavailable nitric oxide by a mechanism involving glutathione peroxidase.* J Biol Chem, 1997. **272**(27): p. 17012-7.
20. Welch, G.N., et al., *Homocysteine-induced nitric oxide production in vascular smooth-muscle cells by NF-kappa B-dependent transcriptional activation of Nos2.* Proc Assoc Am Physicians, 1998. **110**(1): p. 22-31.
21. Tyagi, N., et al., *Mechanisms of homocysteine-induced oxidative stress.* Am J Physiol Heart Circ Physiol, 2005. **289**(6): p. H2649-56.

22. Oosterbaan, A.M., E.A. Steegers, and N.T. Ursem, *The effects of homocysteine and folic acid on angiogenesis and VEGF expression during chicken vascular development.* Microvasc Res, 2012. **83**(2): p. 98-104.
23. Oosterbaan, A.M., et al., *Doppler fow velocity waveforms in the embryonic chicken heart at developmental stages corresponding to 5-8 weeks of human gestation.* Ultrasound in Obstetrics and Gynecology, 2009. **33**(6): p. 638-44.
24. McQuinn, T.C., et al., *High-frequency ultrasonographic imaging of avian cardiovascular development.* Dev Dyn, 2007. **236**(12): p. 3503-13.
25. Kobus, K., E.M. Nazari, and Y.M. Muller, *Effects of folic acid and homocysteine on spinal cord morphology of the chicken embryo.* Histochem Cell Biol, 2009.
26. Hamburger, V. and H.L. Hamilton, *A series of normal stages in the development of the chick embryo. 1951.* Dev Dyn, 1992. **195**(4): p. 231-72.
27. Hu, N. and E.B. Clark, *Hemodynamics of the stage 12 to stage 29 chick embryo.* Circ Res, 1989. **65**: p. 1665-1670.
28. Lamers, Y., et al., *Supplementation with [6S]-5-methyltetrahydrofolate or folic acid equally reduces plasma total homocysteine concentrations in healthy women.* Am J Clin Nutr, 2004. **79**(3): p. 473-8.
29. Venn, B.J., et al., *Comparison of the effect of low-dose supplementation with L-5-methyltetrahydrofolate or folic acid on plasma homocysteine: a randomized placebo-controlled study.* Am J Clin Nutr, 2003. **77**(3): p. 658-62.
30. Quere, I., et al., *Vitamin supplementation and pregnancy outcome in women with recurrent early pregnancy loss and hyperhomocysteinemia.* Fertil Steril, 2001. **75**(4): p. 823-5.
31. Latacha, K.S. and T.H. Rosenquist, *Homocysteine inhibits extra-embryonic vascular development in the avian embryo.* Dev Dyn, 2005. **234**(2): p. 323-31.
32. Boot, M.J., et al., *Homocysteine induces endothelial cell detachment and vessel wall thickening during chick embryonic development.* Circ Res, 2004. **94**(4): p. 542-9.
33. Lee, S.J., et al., *Nitric oxide inhibition of homocysteine-induced human endothelial cell apoptosis by down-regulation of p53-dependent Noxa expression through the formation of S-nitrosohomocysteine.* J Biol Chem, 2005. **280**(7): p. 5781-8.
34. Groenendijk, B.C., et al., *Changes in shear stress-related gene expression after experimentally altered venous return in the chicken embryo.* Circ Res, 2005. **96**(12): p. 1291-8.
35. Butcher, J.T., et al., *Transitions in early embryonic atrioventricular valvular function correspond with changes in cushion biomechanics that are predictable by tissue composition.* Circ Res, 2007. **100**(10): p. 1503-11.

6

The effects of homocysteine and folic acid on angiogenesis and VEGF expression during chicken vascular development

A.M. Oosterbaan, E.A.P. Steegers, N.T.C Ursem

Microvascular Research 2012 Mar; 83(2):98-104

ABSTRACT

Introduction Homocysteine (Hcy) has been implicated in the development of cardiovascular developmental defects. Additionally, in experimental studies, vasculotoxic properties of Hcy have been described. Although Hcy has been identified as a vascular pathogen, little is known about the direct effects Hcy exerts during early embryonic vascular development. Angiogenesis, highly active during placentation, is a critical process involved in embryo survival and development. There are limited studies on the effects of Hcy on early embryonic vasculogenesis and angiogenesis. Folic Acid (FA) is a B vitamin essential in embryo development, and FA supplementation may lead to reduced Hcy levels. Therefore, the purpose of our study was to explore the effects of Hcy and FA on early embryonic vascular development.

Methods Embryonic day (E) 3.5 chicken embryos were treated with a sham, Hcy or FA solution. We developed a computational program for systematic analysis of microscopic images obtained from the extra-embryonic vascular beds. These results were combined with real time PCR data on the expression of VEGF-A and its receptor in these vascular beds.

Results Our data show that Hcy exposure inhibits early vascular development, displayed by a significant reduction of vessel area and altered composition of the vascular beds. Vascular beds of Hcy embryos for the greater part consisted of vessels of the smallest diameters, compared to middle size vessels in control and FA embryos. Hcy also reduced expression of VEGF-A and VEGFR-2. No significant effects of FA were found.

Conclusions We conclude that Hcy exposure causes impaired early extra-embryonic vascular development, shown by altered composition of the vascular beds as well as reduced expression of VEGF-A and VEGFR-2. These effects of Hcy, and the consecutive cascade of events, may be involved in the development of cardiovascular developmental defects as well as early pregnancy loss.

INTRODUCTION

Maternal hyperhomocysteinemia, an elevated level of the amino acid homocysteine (Hcy) in the blood of the mother, is associated with an increased risk of birth defects, including congenital heart defects [1]. Furthermore, Hcy has been implicated in human adult vascular disease [2]. It is generally hypothesized that Hcy has vasculotoxic properties, causing endothelial cell damage and dysfunction. These effects have been described in experimental studies after Hcy exposure [3-6]. Although maternal hyperhomocysteinemia has been associated with increased risk of cardiovascular developmental defects in the offspring and Hcy has been identified as a vascular pathogen, little is known about the effects of Hcy on embryonic peripheral vascular development.

Maternal periconceptional folic acid (FA) supplementation is known to reduce human birth defect risk. FA is a B vitamin that serves as a cofactor in nucleic acid synthesis and cell division [7]. FA also serves as a substrate in the remethylation of Hcy into methionine. Consequently, FA supplementation leads to a reduction of blood Hcy levels [8-9]. Moreover, FA has been shown to decrease prevalence rates of Hcy-associated birth defects in humans [10]. FA is essential in embryonic development. Moreover, maternal periconceptional FA use has been shown to influence placental development, leading to increased placental weight, birth weight and embryonic growth [11-13]. The exact mechanisms through which FA exerts these stimulating effects on embryonic development remain unknown.

Increased Hcy levels have been implicated in recurrent early pregnancy loss [14-15]. Defective placentation is thought to be the major cause of spontaneous early pregnancy loss [16]. Angiogenesis, highly active during placentation, is a critical process involved in embryo survival and development [17]. There are limited studies describing the direct effects of Hcy on embryonic vasculogenesis and angiogenesis. VEGF signaling is known to be crucial for the regulation and promotion of developmental vasculogenesis [18] as well as angiogenesis [19-20], and is present in the human placental bed throughout pregnancy [21]. Vasculogenesis is the process of de novo formation of new blood vessels, whereas angiogenesis concerns the formation of new blood vessels from pre-existing vessels.

The purpose of our study was to answer the following questions: (i) Does Hcy inhibit the development of the extra-embryonic vasculature? (ii) Does Hcy reduce the expression of VEGF and its receptor in the extra-embryonic vascular bed of the chicken embryo? (iii) Does FA positively affect the development of extra embryonic vasculature, as well as the expression of VEGF and its receptor? To answer these questions we have developed a computational program to systematically quantify the extra-embryonic vascular bed, and have combined these results with real-time PCR data on VEGF-A and VEGF receptor expression in the extra-embryonic vascular beds of embryonic day 3.5 (E 3.5) chicken embryos treated with a sham, Hcy or FA solution.

MATERIALS AND METHODS

Embryo treatment and imaging

Fertilized White Leghorn chicken eggs (*Gallus Gallus* (L.)) (Drost Loosdrecht B.V., Loosdrecht, the Netherlands) were incubated blunt end up at 37.5 degrees. A hole of approximately 2 mm was made in the eggshell and the outer shell membrane at the site of the air space after 24 hours of incubation. The embryos received either sham treatment, homocysteine treatment, or folic acid treatment after 24, 48 and 72 hours of incubation via a droplet on the inner shell membrane, using a micropipette. This mode of application was based on previous *in ovo* experiments conducted by Rosenquist et al. [9] and our study group (Oosterbaan et al., 2010, unpublished data). Sham treatment consisted of 50 µl of the physiological saline Locke's solution (0.94% NaCl, 0.045% KCl, and 0.033% $CaCl_2$ w/v in Milli-Q) per application. These embryos will be called control embryos. Hcy treatment consisted of 50 µl 0.05 M L-homocysteine thiolactone hydrochloride (Sigma-Aldrich, Steinheim, Germany) in Locke's solution per application. FA treatment consisted of 0.1 µg folic acid (Sigma-Aldrich) in Locke's solution per application. After each treatment the hole was covered with non toxic magic tape and incubation was continued. On E 3.5 a window of 20 mm by 20 mm was sawn in the eggshell, which was removed to enable microscopic imaging of the extra-embryonic vasculature (Figure 1a). Imaging of the extra-embryonic vasculature was performed with a Leica KL 1500 LCD light microscope (Leica Microsystems, Germany) (Figure 1b). The microscope was calibrated and images were collected at a magnification of 1.25X.

Figure 1

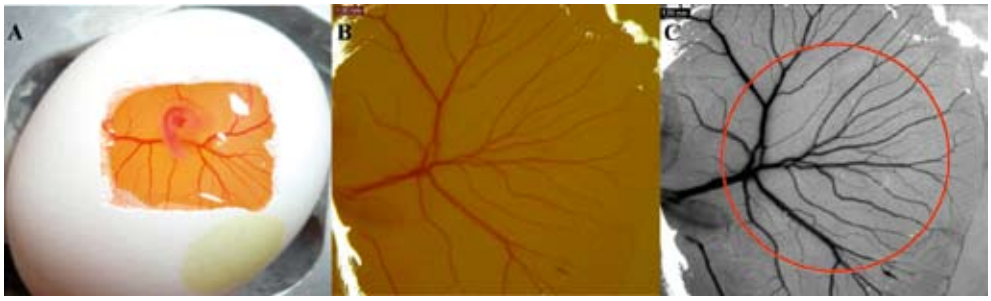

A. E 3.5 chicken embryo, after removing of a window from the eggshell, exposing the embryo floating on its left side on the yolk sac; *B*. Example of a microscopic image of an E 3.5 control embryo, showing one half of the vascular bed, with a part of the embryo visible on the left side of the picture. Scale bar= 1 mm; *C*. Method of area selection. The circle is placed right before the first main branch point of the right lateral vitelline vein, and has an average size of 80.4 mm^2.

Quantification of the extra-embryonic vasculature

A program (Vascalc 1.0) was developed with the use of LabVIEW (National Instruments, Austin, Texas) to enable computational standardized analysis and quantification of vascular development. Microscopic images (TIFF, 8-bit) of the extra-embryonic vascular bed (2088 x 1550 pixels) were loaded in the program LabVIEW (Figure 2a). Each image was transformed to a greenscale image of 256 green levels. For edge detection and to improve contrast for later steps a Sobel filter was applied. Subsequently, a circular region of interest was extracted from the greenscale image. The edge of the circular region was placed on the vascular bed, just before the first main branchpoint of the right lateral vitelline vein (Figure 1c). The area of the circle was uniform, (av. 80.4 $mm^{2)}$, and was determined by identification of the greatest possible circular selection that could be obtained in all images.

Thresholding was done to separate vascular from nonvascular areas, which was difficult because the green levels of the smallest vessels are almost similar to the levels of the background. To optimize this binarization, the method clustering was applied. This method determines the green values present in the image, from 0-255. The values, together with the center of mass, were presented in a histogram. The histogram showed a peak at the value that was present for the greater part in the image. This value, representing the background and thus the nonvascular area, was separated in a binary image from the vascular area. The ratio of vascular/non vascular areas in mm^2 was determined from this binary image (Figure 2b). The Danielsson function was implemented to the binary image (Figure 2c). This distance function assigns a different color value to each pixel, equal to the shortest distance to the border. This border represents the background of the image and displays the edges of the vascular bed. Additionally, the image was skeletonized (Figure 2d).

The program output contained overall vessel area (mm^2), vessel diameter (mm) and vessel length (mm). The vessels were divided in subgroups according to their diameter. The vessel of largest diameter (≥0.22 mm) was extracted from all images and classified as group 1 (G1) (Figure 3). Vessels were classified up to group 9, with the diameter of G2 being 71% of G1 diameter, G3 diameter being 71% of G2 diameter and so on, based on the reasoning that when a blood vessel bifurcates, blood flows most efficiently when the diameter of both branches is 71% of the main branch (square root of 2) [22]. The final and smallest subgroup, G≤9, contained the vessels with a diameter of 0.02 mm and smaller because of limiting resolution for accurate measurement of the smallest diameters.

Figure 2

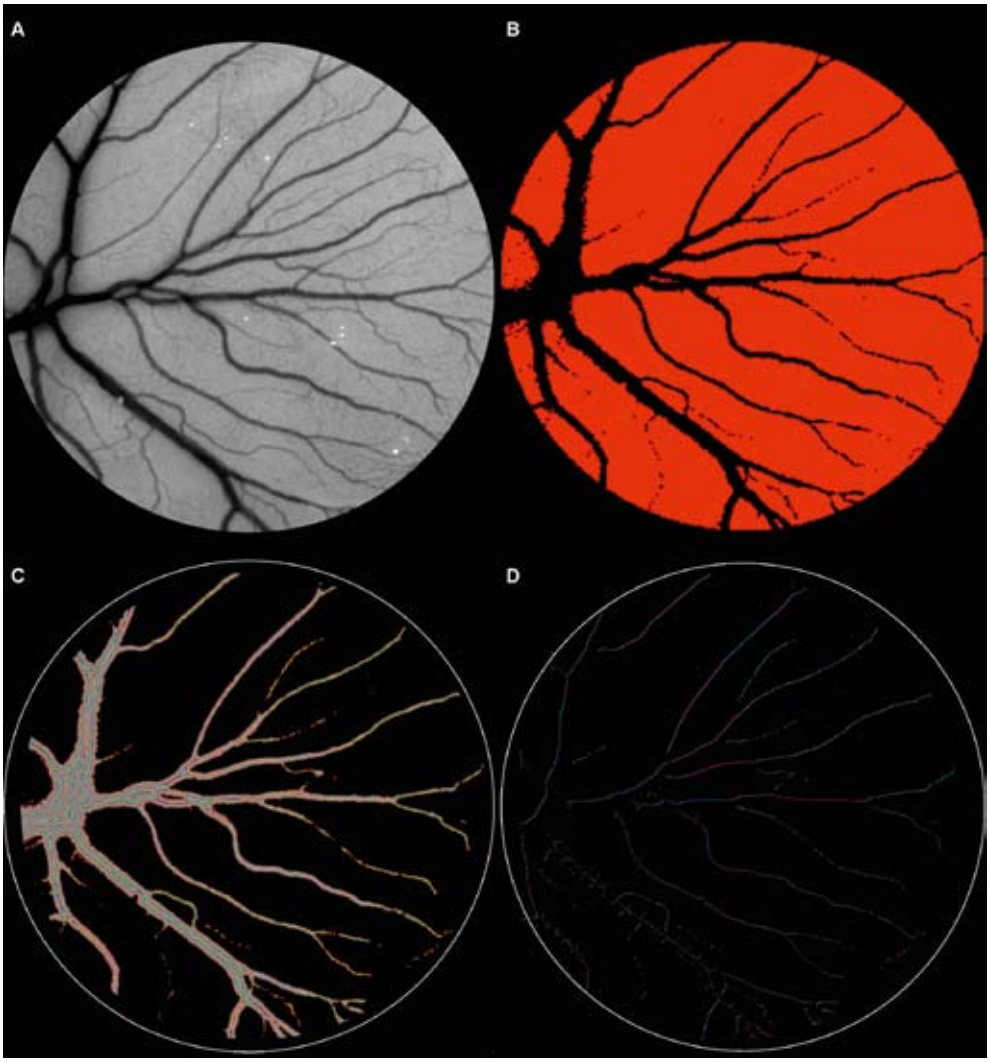

Representative of Vascalc 1.0, 2D analysis of a vascular bed. A. A greenscale image of the vascular bed of an E 3.5 control embryo was uploaded in LabView. A circular region of interest was extracted from this image, selected in a standardized way; B. A binary image was extracted from previous image. First thresholing was done, and then the method clustering was applied. Data concerning vascular/non vascular area was calculated from this image; C. Presentation of the Danielsson function, implemented to the binary image. This distance function assigns a different color value to each pixel, equal to the shortest distance to the border, the edge of the vessels; D. The image has been skeletonized and program output was extracted.

Figure 3

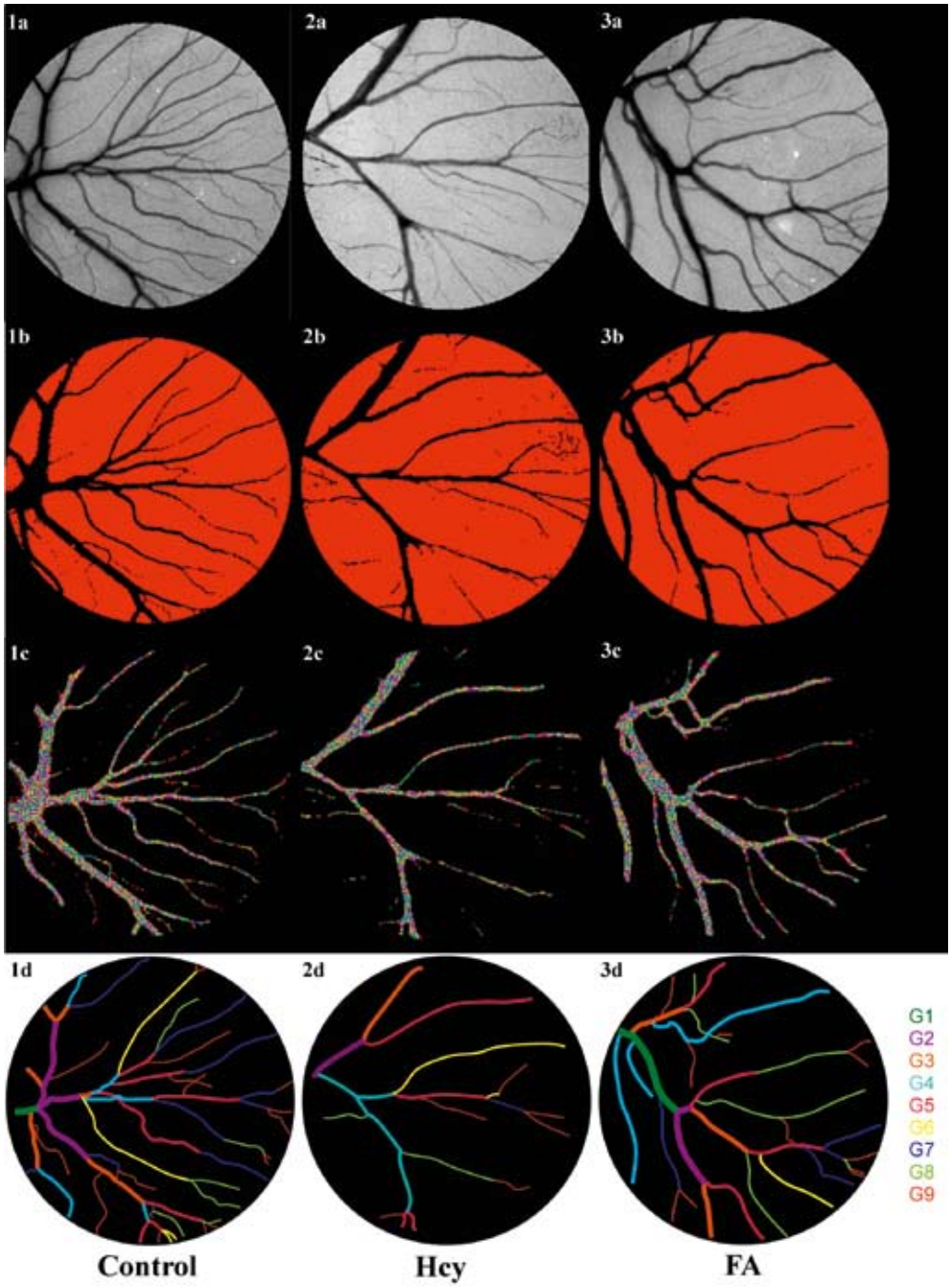

Presentation of the extra-embryonic vascular bed of an average control, Hcy and FA exposed embryo. G1, the vessels of largest diameter, until G9, the vessels of smallest diameter, are presented in specific colors, showing the average distribution of these subgroups in control, Hcy and FA exposed embryos.

RNA isolation and real time PCR

The membrane containing the extra embryonic vasculature was removed from the yolk sac and put in a 1.5 ml microcentrifuge tube. First TRIzol (Invitrogen, United States) was added for tissue lysis and then the tissue was sonified. RNA was isolated with the RNeasy Mini Kit (Qiagen, Germany) according to the supplier's instructions and RNA concentrations were determined with a NanoDrop spectrophotometer (ND-1000, Thermo Scientific, United States). RNA quantification and quality control was performed with the Agilent 2100 Bioanalyzer (Agilent Technologies, United States). Handling of the RNA took place under RNase free conditions. For reverse transcription the First-Strand cDNA synthesis kit was used (Affymetrix, United States). Of each sample 500 ng total RNA was incubated with the components oligo-dT primer, 5x 1st strand reaction mix, DTT and dNTP, and superscript11 to convert samples to cDNA.

Quantification of the protein vascular endothelial growth factor A (VEGF-A), and the vascular endothelial growth factor receptor (VEGF-R) was achieved with real-time PCR. Chicken specific VEGF-A and VEGF-R primers were used. VEGF-A forward primer: gtgaaagctgggtggtttgt; reverse primer: tgagggcctagaatgtgtcc: VEGF-R forward primer: ctgaaggtgcactcctcctc; reverse primer: caagtatggctcaacgcaga. ß-actin was used as the housekeeping gene, forward primer: ttcttttggcgcttgactca; reverse primer: gcgttcgctccaacatgtt. Each primer was dissolved in dH2O to gain a primermix with a concentration of 50 µM. PCR reaction volume contained 12.5 µl Power SYBR Green PCR Mastermix (Applied Biosystems, United States), 9.5 µl RNase-free water, 2 µl primermix and 1 µl 0.005M cDNA sample. Real-time PCR was performed in duplicate.

To determine the gene expression of VEGF-A and VEGFR-2 compared to the ß-actin control, the Bio-Rad CFX manager was used and the comparative C_T method was executed (Bio-Rad Laboratories, United States). The difference between the tested gene and the reference housekeeping gene was determined as ΔC_T. The relative difference was calculated as $RD = 2^{-\Delta CT}$.

Statistical analysis

The data derived from the real-time PCR concerning VEGF-A and VEGFR-2 expression was checked for normality of the distribution. Since data were not normally distributed, the Mann-Whitney U test was performed to compare Hcy and FA embryo protein expression to control embryo expression. Vascalc 1.0 data were normally distributed and analysis of variance (One-Way ANOVA) was performed followed by Post-hoc Bonferroni testing to determine group differences. Statistical significance was defined as a *p* value of less than 0.05. Calculations were performed with SPSS 17.0 (SPSS Inc., Chicago, USA).

Table 1 Data obtained from vascular analysis of control, Hcy and FA exposed embryos

	Control	Homocysteine	Folic Acid
Selection area (mm^2)	80.34 (0.28)	80.42 (0.26)	80.58 (0.42)
Av (mm^2)	**15.33 (4.36)**	**11.52 (3.32)*†**	**16.85 (3.19)**
Av (%)	**19.07 (5.48)**	**14.33 (4.11)*†**	**20.32 (3.76)**
Total Lv (mm)	351.20 (172.94)	424.08 (297.03)	534.94 (351.83)
Av G1 (%)	11.90 (9.35)	8.90 (3.39)	10.55 (5.15)
Av G2 (%)	17.37 (4.27)	13.98 (4.11)	16.28 (3.18)
Av G3 (%)	15.35 (2.80)	15.70 (4.40)	17.32 (7.54)
Av G4 (%)	**19.23 (3.43)**	**14.73 (3.35)*†**	**18.39 (1.58)**
Av G5 (%)	18.96 (5.27)	19.69 (2.07)	18.68 (1.08)
Av G6 (%)	9.87 (4.13)	12.32 (1.94)	11.07 (1.73)
Av G7 (%)	**3.10 (0.78)**	**4.82 (1.10)*†**	**3.47 (0.61)**
Av G8 (%)	**2.38 (0.48)**	**5.96 (2.14)*†**	**2.31 (0.53)**
Av G9 (%)	**1.85 (0.90)**	**3.90 (1.77)*†**	**1.93 (0.42)**
Lv G1 (%)	2.89 (2.64)	1.55 (0.96)	2.29 (1.13)
Lv G2 (%)	**5.44 (1.77)**	**3.34 (1.74)***	**4.92 (1.24)**
Lv G3 (%)	6.80 (1.98)	5.16 (2.82)	7.54 (3.38)
Lv G4 (%)	**12.95 (4.56)**	**6.88 (2.57)*†**	**11.41 (0.75)**
Lv G5 (%)	**17.71 (2.67)**	**13.49 (2.74)*†**	**17.26 (1.18)**
Lv G6 (%)	14.13 (4.54)	13.24 (2.00)	16.28 (1.11)
Lv G7 (%)	7.55 (1.47)	8.25 (0.56)	8.28 (1.01)
Lv G8 (%)	**11.74 (6.61)**	**16.48 (3.11)*†**	**9.11 (1.20)**
Lv G9 (%)	**20.79 (9.84)**	**31.62 (8.22)*†**	**22.89 (2.72)**

Results generated by Vascalc 1.0 software include vessel area (Av) and vessel length (Lv). The vessels were divided in subgroups according to their diameter. G1, the vessels of largest diameter, until G9, the vessels of smallest diameter. Composition of the vascular beds of Hcy, Folic acid exposed and embryos were compared. Av G1-G9 (%) means vessel area of group 1-group 9 in percentage of total vessel area; Lv G1-G9 (%) means vessel length of group 1-group 9 in percentage of total vessel length; * means Hcy exposed embryos are significantly different from control embryos; † means Hcy exposed embryos are significantly different from FA embryos (P value < 0.05).

RESULTS

Quantification of extra embryonic vasculature

Data obtained from analysis of the extra embryonic vascular beds are presented in Table 1. The total size of the selection area was comparable between study groups, 80.42 (0.26) mm^2 in Hcy treated, 80.58 (0.42) mm^2 in FA treated and 80.34 (0.28) mm^2 in control embryos. Total vessel area and total background area were presented in mm^2 and in percentages of total selection area. Hcy treated embryos displayed reduced vessel development compared to FA

treated and control embryos (Figure 3). Total vessel area, in mm^2 and in percentage of the total selection area, was significantly smaller in Hcy treated embryos compared to FA treated and control embryos (Table 1).

Composition of the vascular beds after Hcy treatment

Not only vessel area was altered in Hcy treated embryos. The distribution of the different subgroups, based on vascular diameter, was also significantly different in Hcy treated embryos, compared to FA treated and control embryos (Figure 4). The distribution of the subgroups, displayed by length in percentage of total vessel length, showed that the vascular beds of Hcy treated embryos for the greater part consisted of vessels of the smallest diameters. The vessels of smallest diameters, group 7-9, were most dominantly present in the vascular beds of Hcy treated embryos, indicated by the significantly higher percentages of the area of group 7-9 in percentage of total vessel area, and the higher percentage of the length of group 7-9 in percentage of total vessel length compared to FA treated and control embryos (Figure 4).

Vascular development FA treated embryos

No differences were found between parameters of FA treated and control embryos. The distribution of the subgroups was comparable between both study groups, demonstrated by the similar percentages of subgroups presented in Table 1. The distribution of the vessel subgroups in FA treated and control embryos showed that the vascular beds of these embryos for the greater part consisted of middle group, group 4-6, vessels. This was presented by the area in percentage of total vessel area of 48.1 (0.8) % and 48.1 (7.9) %, as well as the length in percentage of total vessel length of 45.0 (0.9) % and 44.8 (4.0) % of group 4-6 in FA treated and control embryos respectively (Figure 4).

VEGF-A en VEGFR-2 expression

The expression of VEGF-A as well as the VEGF receptor was significantly lower in the extra-embryonic vascular beds of Hcy treated embryos compared to control embryos (Table 2). The expression of VEGF-A in FA treated embryos was similar to that of control embryos (Table 2). However, the expression of the VEGF receptor in the extra-embryonic vascular beds of FA treated embryos was significantly reduced compared to controls.

Table 2 Comparison of VEGF-A and VEGF receptor expression

	Control		Homocysteine		Folic acid	
	Mean	(SD)	Mean	(SD)	Mean	(SD)
VEGF-A	**0.00446**	0.00259	**0.00244 ***	0.00186	**0.00476**	0.01150
VEGFR-2	**0.00273**	0.00095	**0.00183***	0.00140	**0.00119***	0.00065

Comparison of VEGF-A and VEGFR-2 expression in extra-embryonic vascular beds of Hcy exposed, FA exposed and control embryos. Data obtained with real time PCR. Protein expression was normalized for the expression of ß-actin. * means Hcy or FA exposed embryo expression was significantly different from control embryo expression (P value <0.05). Differences between groups were analyzed by the Mann-Whitney U test.

Figure 4

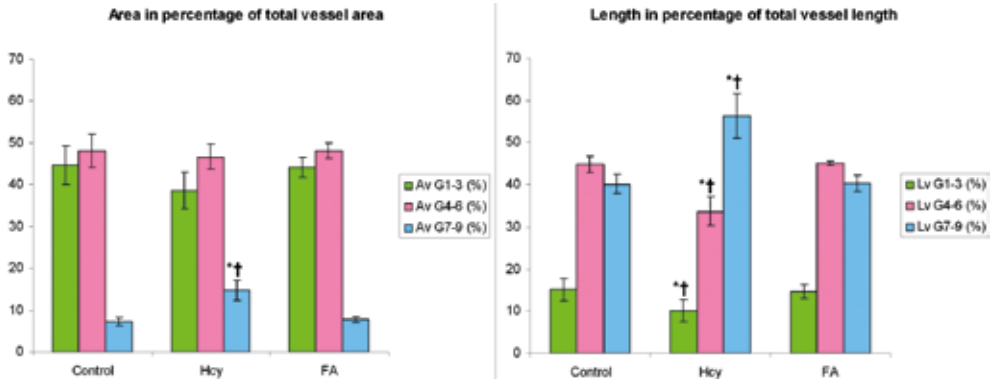

Presentation of the distribution of area in percentage of total vessel area and length in percentage of total vessel length of the different subgroups of control, Hcy and FA exposed embryos, divided in groups of 3; G1-G3 the vessels of largest diameter, G4-G6 the vessels of medium diameter, and G7-G9 the vessels of smallest diameter. Av means vessel area; Lv means vessel length; * means Hcy exposed embryos are significantly different from control embryos (P value < 0.05); † means Hcy exposed embryos are significantly different from FA exposed embryos (P value < 0.05).

DISCUSSION

In this chicken embryo study we have demonstrated that Hcy exposure inhibits early vascular development and causes a reduction in the expression of VEGF-A and its receptor. This impaired vascular development may provide a link between Hcy and cardiovascular developmental defects. No significant positive effects of FA on vascular development or VEGF-A and VEGF-R2 expression was found.

Because of the demonstrated decrease in total vessel area, total vessel length, and the shift of vessel subgroup distribution to dominance of the smallest vessels in Hcy treated embryos, we conclude that Hcy negatively affects vascular development. Different direct effects of Hcy have been described in literature, among which many experimental animal studies [23]. Hcy has been reported to cause endothelial cell damage [4, 24] as well as endothelial cell apoptosis [5, 25-26]. Hcy has been described to promote oxidative damage in endothelial cells, causing increased production of free oxygen radicals, resulting in oxidative stress [27-29]. Also, Hcy can cause disrupted nitric oxide (NO) synthesis [30-31]. These effects of Hcy may be involved in vasculogenesis and angiogenesis, explaining the reduced vascular development in Hcy treated embryos in this study.

We have shown that Hcy exposure affects the expression of VEGF, a regulator of key endothelial activities like cell proliferation, migration, maturation and permeability, crucial for the angiogenic formation of new vessels [20]. To explain the reduced expression of VEGF-A and VEGFR-2, we suggest the following cascade of events. The endothelial cell damage and reduced availability of NO, with subsequent inhibition of vasculogenesis and angiogenesis induced by Hcy, may cause impaired flow of blood through these smaller vessels. This decreased blood flow coincides with our previous finding that Hcy causes a reduction of heart rate and hemodynamic parameters like peak velocities and velocity time integrals (VTI's) in the early embryonic chicken heart (Oosterbaan et al. 2010, unpublished data). Alterations in blood flow may be followed by a decrease in shear stress, sensed by the endothelial cells [32]. Normally, as wall shear stress increases, factors like VEGF-A, VEGFR-2 and endothelial nitric oxide synthase (eNOS) that act pro-angiogenic, are upregulated [33]. Thus, a suggested decrease in shear stress after Hcy exposure may cause reduced VEGF-A and VEGFR-2 expression. This reduction in VEGF-A and VEGFR-2, as well as in available NO, will result in decreased neovascularisation, including vasculogenesis and angiogenesis [19]. The reduction in the expression of vascular endothelial growth factor (VEGF) and its receptor coincides well with the results reported by Latacha and Rosenquist [34]. The reduction in VEGF-A, that has been shown to be critical for placental angiogenesis [35], may result in defective placentation and consequently loss of pregnancy as described in women with hyperhomocysteinemia [14].

No significant differences between control and FA treated embryos were found after analysis of the data obtained from these vascular beds. Therefore we conclude that FA does not positively affect extra-embryonic vascular development or VEGF-A and VEGFR-2 expression. The concentration of FA used in this study was comparable to the dose that has been previously shown to protect the chicken embryo from Hcy induced defects [9]. There does seem to be the tendency towards a stimulating effect of FA on vascular development, as total vessel area and total vessel length are increased in FA treated embryos, but this was

not significant. Zahibi et al. have shown enhanced VEGF-A expression induced by FA in the yolk sacs of diabetic rats [36]. VEGF-A expression was comparable between FA and control embryos in our study. Probably, a level of significance will be reached with an increased number of embryos studied. Another explanation may be that FA affects other isoforms of the growth factors and receptors of the VEGF family [18], not investigated in this study. The different VEGF growth factors have different functions on vascular growth [37]. This may also provided an explanation for the decreased expression of the VEGF receptor in the vascular beds of FA treated embryos.

This is the first study to perform quantification of chicken extra embryonic vascular beds after Hcy and FA exposure with the help of a computational program, providing elaborate data on the vascular development and composition of the vascular beds, instead of solely calculating the number of branches per mm^2. Our findings coincide well with previously reported changes in vascular development after Hcy exposure [34]. Additionally, our data show that Hcy not only limits the number of vessels and branches, but also the total vessel area and the composition of the vascular beds, resulting in dominance of the vessels of smallest diameter.

A limitation of our study is the accuracy of the computational program, Vascalc 1.0. For example, in the situation of occasionally overlapping vessels, the program may have approximated them as joined vessels. Using 3D-images and analysis would overcome this limitation. Additionally, limiting resolution for accurate measurement of the smallest vessels caused the vessels of a diameter of ≤0.020 mm and smaller to be lumped into group 9.

We conclude that Hcy exposure causes impaired vascular development, indicated by decreased vasculogenesis and angiogenesis as well as reduced expression of VEGF-A and VEGFR-2. These Hcy induced effects, and the consecutive cascade of events, may be involved in the development of cardiovascular developmental defects as well as early pregnancy loss. In future research we will explore possible alterations of wall shear stress after Hcy exposure.

ACKNOWLEDGEMENTS

We want to greatly thank Liesbeth Kuhne for assistance in the real-time PCR experiments and are grateful to Chantal van der Kaa for the development of the computational program Vascalc 1.0, designed for the quantification of extra embryonic vascular beds.

REFERENCES

1. Verkleij-Hagoort, A., et al., *Hyperhomocysteinemia and MTHFR polymorphisms in association with orofacial clefts and congenital heart defects: a meta-analysis.* Am J Med Genet A, 2007. **143A**(9): p. 952-60.
2. McCully, K.S., *Homocysteine, vitamins, and vascular disease prevention.* Am J Clin Nutr, 2007. **86**(5): p. 1563S-8S.
3. Harker, L.A., et al., *Homocystine-induced arteriosclerosis. The role of endothelial cell injury and platelet response in its genesis.* J Clin Invest, 1976. **58**(3): p. 731-41.
4. Wall, R.T., et al., *Homocysteine-induced endothelial cell injury in vitro: a model for the study of vascular injury.* Thromb Res, 1980. **18**(1-2): p. 113-21.
5. Lee, S.J., et al., *Nitric oxide inhibition of homocysteine-induced human endothelial cell apoptosis by down-regulation of p53-dependent Noxa expression through the formation of S-nitrosohomocysteine.* J Biol Chem, 2005. **280**(7): p. 5781-8.
6. Boot, M.J., et al., *Homocysteine induces endothelial cell detachment and vessel wall thickening during chick embryonic development.* Circ Res, 2004. **94**(4): p. 542-9.
7. Smith, A.D., Y.I. Kim, and H. Refsum, *Is folic acid good for everyone?* Am J Clin Nutr, 2008. **87**(3): p. 517-33.
8. Hansen, D.K., et al., *Lack of embryotoxicity of homocysteine thiolactone in mouse embryos in vitro.* Reprod Toxicol, 2001. **15**(3): p. 239-44.
9. Rosenquist, T.H., S.A. Ratashak, and J. Selhub, *Homocysteine induces congenital defects of the heart and neural tube: effect of folic acid.* Proc Natl Acad Sci U S A, 1996. **93**(26): p. 15227-32.
10. Goh, Y.I., et al., *Prenatal multivitamin supplementation and rates of congenital anomalies: a meta-analysis.* J Obstet Gynaecol Can, 2006. **28**(8): p. 680-9.
11. Rolschau, J., et al., *The influence of folic acid supplement on the outcome of pregnancies in the county of Funen in Denmark. Part I.* Eur J Obstet Gynecol Reprod Biol, 1999. **87**(2): p. 105-10; discussion 103-4.
12. Timmermans, S., et al., *Periconception folic acid supplementation, fetal growth and the risks of low birth weight and preterm birth: the Generation R Study.* Br J Nutr, 2009. **102**(5): p. 777-85.
13. Rolschau, J., J. Date, and K. Kristoffersen, *Folic acid supplement and intrauterine growth.* Acta Obstet Gynecol Scand, 1979. **58**(4): p. 343-6.
14. Steegers-Theunissen, R.P., et al., *Hyperhomocysteinaemia and recurrent spontaneous abortion or abruptio placentae.* Lancet, 1992. **339**: p. 1122-3.
15. Quere, I., et al., *Vitamin supplementation and pregnancy outcome in women with recurrent early pregnancy loss and hyperhomocysteinemia.* Fertil Steril, 2001. **75**(4): p. 823-5.
16. Jauniaux, E. and G.J. Burton, *Pathophysiology of histological changes in early pregnancy loss.* Placenta, 2005. **26**(2-3): p. 114-23.
17. Breier, G., et al., *Angiogenesis in embryos and ischemic diseases.* Thromb Haemost, 1997. **78**(1): p. 678-83.
18. Neufeld, G., et al., *Vascular endothelial growth factor (VEGF) and its receptors.* FASEB J, 1999. **13**(1): p. 9-22.
19. Ferrara, N. and T. Davis-Smyth, *The biology of vascular endothelial growth factor.* Endocr Rev, 1997. **18**(1): p. 4-25.
20. Ferrara, N., H.P. Gerber, and J. LeCouter, *The biology of VEGF and its receptors.* Nat Med, 2003. **9**(6): p. 669-76.
21. Schiessl, B., et al., *Localization of angiogenic growth factors and their receptors in the human placental bed throughout normal human pregnancy.* Placenta, 2009. **30**(1): p. 79-87.

22. Vickerman, M.B., et al., *VESGEN 2D: automated, user-interactive software for quantification and mapping of angiogenic and lymphangiogenic trees and networks.* Anat Rec (Hoboken), 2009. **292**(3): p. 320-32.
23. van Mil, N.H., A.M. Oosterbaan, and R.P. Steegers-Theunissen, *Teratogenicity and underlying mechanisms of homocysteine in animal models: A review.* Reprod Toxicol, 2010.
24. Nagai, Y., et al., *Homocysteine inhibits angiogenesis in vitro and in vivo.* Biochem Biophys Res Commun, 2001. **281**(3): p. 726-31.
25. Zhang, C., et al., *Homocysteine induces programmed cell death in human vascular endothelial cells through activation of the unfolded protein response.* J Biol Chem, 2001. **276**(38): p. 35867-74.
26. Hossain, G.S., et al., *TDAG51 is induced by homocysteine, promotes detachment-mediated programmed cell death, and contributes to the cevelopment of atherosclerosis in hyperhomocysteinemia.* J Biol Chem, 2003. **278**(32): p. 30317-27.
27. Loscalzo, J., *The oxidant stress of hyperhomocyst(e)inemia.* J Clin Invest, 1996. **98**(1): p. 5-7.
28. Au-Yeung, K.K., et al., *Hyperhomocysteinemia activates nuclear factor-kappaB in endothelial cells via oxidative stress.* Circ Res, 2004. **94**(1): p. 28-36.
29. Chambers, J.C. and J.S. Kooner, *Homocysteine--an innocent bystander in vascular disease?* Eur Heart J, 2001. **22**(9): p. 717-9.
30. Upchurch, G.R., Jr., et al., *Homocyst(e)ine decreases bioavailable nitric oxide by a mechanism involving glutathione peroxidase.* J Biol Chem, 1997. **272**(27): p. 17012-7.
31. Welch, G.N., et al., *Homocysteine-induced nitric oxide production in vascular smooth-muscle cells by NF-kappa B-dependent transcriptional activation of Nos2.* Proc Assoc Am Physicians, 1998. **110**(1): p. 22-31.
32. Groenendijk, B.C., et al., *Changes in shear stress-related gene expression after experimentally altered venous return in the chicken embryo.* Circ Res, 2005. **96**(12): p. 1291-8.
33. Resnick, N., et al., *Hemodynamic forces as a stimulus for arteriogenesis.* Endothelium, 2003. **10**(4-5): p. 197-206.
34. Latacha, K.S. and T.H. Rosenquist, *Homocysteine inhibits extra-embryonic vascular development in the avian embryo.* Dev Dyn, 2005. **234**(2): p. 323-31.
35. Charnock-Jones, D.S., P. Kaufmann, and T.M. Mayhew, *Aspects of human fetoplacental vasculogenesis and angiogenesis. I. Molecular regulation.* Placenta, 2004. **25**(2-3): p. 103-13.
36. Zabihi, S., U.J. Eriksson, and P. Wentzel, *Folic acid supplementation affects ROS scavenging enzymes, enhances Vegf-A, and diminishes apoptotic state in yolk sacs of embryos of diabetic rats.* Reprod Toxicol, 2007. **23**(4): p. 486-98.
37. Yue, X. and R.J. Tomanek, *Effects of VEGF(165) and VEGF(121) on vasculogenesis and angiogenesis in cultured embryonic quail hearts.* Am J Physiol Heart Circ Physiol, 2001. **280**(5): p. H2240-7.

7

General Discussion

The aim of this thesis was to study early embryonic heart function and cardiovascular development in the chicken embryo. Our hypothesis regarding the influence of hemodynamics on cardiac morphology was explored. Homocysteine exposure was related to changes in hemodynamic parameters and shear stress levels. The effects of homocysteine on peripheral vascular development were studied. Also, the possible protective effects of folic acid and mefolinate on homocysteine induced effects during cardiogenesis were studied. Several techniques were used to obtain the data on early chicken embryonic cardiovascular development presented in this thesis. High frequency ultrasound biomicroscopy was applied to collect Doppler flow velocity waveforms. Micro particle image velocimetry (μPIV) was used to gain information on shear stress levels in the outflow tract of the chicken embryonic heart. Real time imaging of the extra-embryonic vascular bed by microscope allowed computational quantification of vascular development by the software program Vascalc 1.0. This program was designed for this thesis by our research group. With the use of real time polymerase chain reaction (PCR), information on vascular endothelial growth factor (VEGF) expression of the vascular bed was achieved.

7.1 EARLY HEMODYNAMICS AND CARDIAC MORPHOLOGY

The early embryonic heart already functions well before cardiac morphogenesis has been completed. It starts functioning even before there is any oxygen demand [1]. The question arises why this is happening. The hypothesis that early functioning of the heart is needed to affect and regulate structural development offers a possible explanation. The actual way the early embryonic heart functions remains a subject of discussion. It has been proposed that the early embryonic heart functions like a suction pump changing into a piston-like pumping mechanism [2-4]. The changes in Doppler flow velocity waveforms over time, presented in this thesis (**Chapter 2**), support these studies suggesting that different pumping mechanisms are present during successive early stages of heart development.

We suggest that another reason for the embryonic heart to start functioning at this early stage could be to stimulate angiogenesis, as previously mentioned by Burggren et al [1]. The pumping of blood creates a pressure pulse that, among others, causes the release of VEGF and therefore stimulates angiogenesis. In **chapter 4.1** it is demonstrated that alterations in early heart function arise after homocysteine exposure and **chapter 6** provides evidence on the inhibiting effect of homocysteine on VEGF expression and angiogenesis during extra embryonic vascular development. This thesis therefore supports the theory that normal early functioning of the heart is needed for adequate angiogenesis.

7.2 LINKING HOMOCYSTEINE, ALTERED HEMODYNAMICS AND CONGENITAL HEART DEFECTS (CHD)

Maternal hyperhomocysteinemia has been associated with an increased risk of CHD [5]. This association has been substantiated in the chicken embryo, showing CHD after low dose homocysteine exposure [6-7]. Homocysteine exposure induces the same type of CHD as observed in chicken embryo studies in which embryonic blood flow has been altered by clipping of the right lateral vitelline vein [8]. Therefore, further investigation of the potential relation between homocysteine and altered embryonic blood flow was warranted.

In figure 1 our findings on the effects of homocysteine during cardiovascular development are combined with results from previous studies. This figures represents our theory on how to link homocysteine to altered hemodynamics and CHD. Homocysteine exerts multiple direct toxic effects during embryogenesis (**Chapter 3**). Homocysteine can cause disrupted nitric oxide (NO) synthesis [9-10], increase oxidative stress [11] and affect and damage endothelial cells [12-14]. These processes lead to a reduced vasculogenesis and angiogenesis, resulting in inhibited vascular development [15]. Additional evidence on the adverse effects of homocysteine on vascularization is provided in this thesis (**Chapter 6**). Homocysteine exposure can affect neural crest cells, as described by Boot et al [6]. This results in neural crest cells failing to undergo apoptosis and in reduced myocardialization of the outflow tract in chicken embryos. Above mentioned mechanisms can lead to altered hemodynamics, specifically impaired blood flow. This is substantiated by the findings presented in **chapter 4.1**, showing reduced hemodynamic parameters of early embryonic chicken heart function after homocysteine exposure. In contrast to the findings presented in **chapter 4.1** and **chapter 5**, embryonic heart rate in **chapter 4.3**, although not significant, was lower in control embryos compared to homocysteine treated embryos. This can be explained by the differences in experimental set up, e.g. different methods of homocysteine treatment, different developmental stages studied, and different locations of measurements. Also, the control embryos used in **chapter 4.3** may coincidently have suffered more from the experimental procedure than the homocysteine embryos studied in **chapter 4.1** and **chapter 5**. This is supported by a previous μPIV study reporting a mean heart rate for HH17 control embryos that coincides well with the mean heart rate of control embryos presented in **chapter 4.1** and **chapter 5** [16]. Despite the higher heart rate of homocysteine embryos in **chapter 4.3**, hemodynamic parameters like peak flow and maximum velocity seemed decreased after homocysteine exposure. Therefore, we conclude that homocysteine exposure causes a reduction of hemodynamic parameters of early embryonic chicken heart function.

The Frank-Starling mechanism is a compensatory mechanism that has been shown to function in the early chicken embryo [17]. According to the length-tension relationship

of the cardiac muscle a decrease in heart rate would result in an increase in dorsal aortic blood flow and blood flow velocity, as well as an increase in cardiac output offered by a more contractile ventricular myocardium. We have shown decreased blood flow velocities after homocysteine exposure, independent of an increase or decrease in heart rate (**Chapter 4**). We suggest that the intrinsic compensatory mechanism that controls early cardiac function in normal conditions may be malfunctioning after homocysteine exposure.

The altered hemodynamic parameters and consequent altered functioning of the embryonic heart after homocysteine exposure may contribute to the development of congenital heart defects.

Figure 1

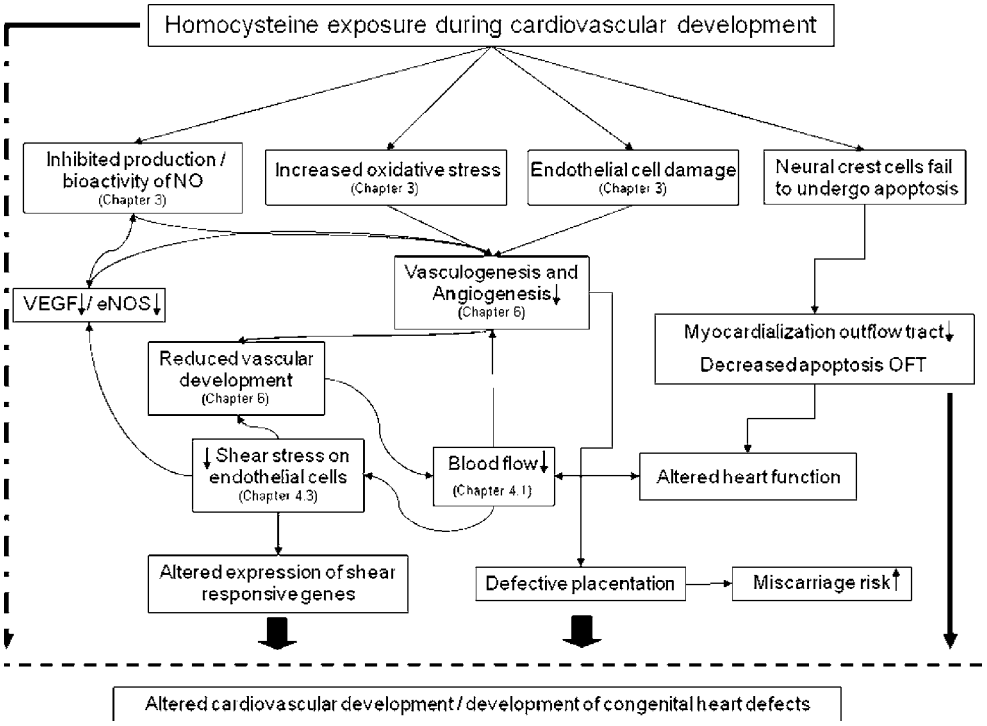

7.3 ALTERATIONS OF BLOOD FLOW PATTERNS AND CARDIAC MALFORMATIONS

As presented in this thesis, stage and location dependent intra-cardiac blood flow patterns are present during early heart development (**Chapter 2**). Normal blood flow is considered to play an important role in heart development [8, 18]. Alterations in blood flow, leading to changes in shear stress, have been shown to result in altered expression of shear responsive genes [19-20] and the development of cardiovascular malformations [8]. **Chapter 4.3** provides evidence on reduced shear stress levels after homocysteine exposure. These changes in shear stress may cause altered behaviour and gene expression of shear responsive genes, eventually leading to the development of congenital heart defects.

7.4 HOMOCYSTEINE AND EARLY VASCULAR DEVELOPMENT

Homocysteine causes reduced extra embryonic vascular development and expression of VEGF-A and its receptor (**Chapter 6**). VEGF-A is an endothelial specific growth factor that acts pro-angiogenic *in vivo* [21]. NO is also directly involved in angiogenesis [22]. NO production by endothelial cells requires endothelial nitric oxide synthase (eNOS) [23]. NO significantly contributes to the growth promoting effect of VEGF [22]. As previously mentioned, homocysteine inhibits the production of NO, that will consequently lead to a reduced effect of VEGF (Figure 1). This will result in reduced vasculogenesis and angiogenesis.

Indirectly, homocysteine may inhibit vascular development by reducing shear stress acted on endothelial cells (**Chapter 4.3**). Normally, as shear stress increases, pro-angiogenic factors like VEGF and eNOS are upregulated [24]. Lower shear stress levels may cause a reduction of available NO and VEGF, resulting in decreased vascular development [21-22]. In addition, this reduced shear stress may cause altered gene expression, inhibiting extra-embryonic vascular development. An altered composition of the extra-embryonic vascular bed can lead to shifted blood flow patterns through the heart.

Increased homocysteine levels have been implicated in recurrent early pregnancy loss [25-27], of which defective placentation is thought to be the major cause. Angiogenesis is highly active during placentation. We suggest that homocysteine might play a role in early pregnancy loss, increasing miscarriage risk by inhibiting early angiogenesis, followed by inadequate vascularization and defective placentation (Figure 1). This suggestion is substantiated by the findings presented in **chapter 6** of this thesis, showing reduced development of the extra-embryonic vascular bed in the chicken embryo after homocysteine exposure.

7.5 FOLIC ACID, MEFOLINATE AND EMBRYO DEVELOPMENT

In animal experimental models, folic acid has been shown to prevent adverse, homocysteine-induced, effects [7, 28-29]. Stimulating effects on embryo development have been ascribed to folic acid. For example in humans periconceptional folic acid use by the mother has been associated with increased fetal growth and development [30-33]. We have shown that folic acid positively influences embryo survival (**Chapter 5**). Similar effects were seen after mefolinate treatment. The exact mechanisms through which folic acid exerts its stimulating effects on embryo development remain unknown. The direct effects of folic acid on nucleic acid synthesis and cell division [34] may be involved. For example, biosynthesis of thymidine, needed for the incorporation of uracil into DNA, is a folate-requiring step and is therefore related to the blood folate concentration. An indirect effect may be that folic acid, converted to tetrahydrofolate and consequently to 5-methyl-tetrahydrofolate (5-methyl-THF), serves as a substrate in the remethylation of homocysteine into methionine, reducing blood homocysteine levels. Mefolinate is the synthetic form of 5-methyl-THF. As folic acid can reduce elevated homocysteine levels, its protective effects on complex, homocysteine-associated, congenital malformations can be explained by a restoration of oxidative stress, protein- and lipid synthesis and methylation, DNA synthesis and chromatin methylation (**Chapter 3**).

7.6 EPIGENETICS AND GENE IMPRINTING

Gene imprinting is controlled epigenetically by differential DNA methylation, which in turn can be influenced by environmental factors including nutrition. Folic acid is an important methyl donor involved in DNA methylation, and therefore influences gene imprinting. Therefore, we want to emphasize the importance of an optimal maternal periconception balance of folate and homocysteine for health, reproduction and disease in early and later life.

7.7 FUTURE RESEARCH

Different effects of homocysteine during cardiovascular development were presented in this thesis. These effects were linked to the development of CHD, as presented in figure 1. Homocysteine has been shown to cause altered hemodynamics in the chicken embryonic heart, and also to cause altered shear stress rates. In future research it would be interesting to study the expression of genes, implicated in the development of CHD, in the chicken embryonic heart after homocysteine exposure. This could confirm and strengthen our ideas on the role of homocysteine in cardiovascular development.

In the future, provided that we are able to develop safe clinical tools to study early heart

function in the human embryo, the knowledge gained from animal experimental studies like presented in this thesis might help to detect abnormal cardiac functioning. With recent developments in fetal therapy, this will hopefully even lead to the development of prenatal intra-uterine therapeutic tools to prevent or arrest progressing damage to the developing heart.

REFERENCES

1. Burggren, W.W., S.J. Warburton, and M.D. Slivkoff, *Interruption of cardiac output does not affect short-term growth and metabolic rate in day 3 and 4 chick embryos.* J Exp Biol, 2000. **203**(Pt 24): p. 3831-8.
2. Butcher, J.T., et al., *Transitions in early embryonic atrioventricular valvular function correspond with changes in cushion biomechanics that are predictable by tissue composition.* Circ Res, 2007. **100**(10): p. 1503-11.
3. Forouhar, A.S., et al., *The embryonic vertebrate heart tube is a dynamic suction pump.* Science, 2006. **312**(5774): p. 751-3.
4. Liebling, M., et al., *Rapid three-dimensional imaging and analysis of the beating embryonic heart reveals functional changes during development.* Dev Dyn, 2006. **235**(11): p. 2940-8.
5. Verkleij-Hagoort, A., et al., *Hyperhomocysteinemia and MTHFR polymorphisms in association with orofacial clefts and congenital heart defects: a meta-analysis.* Am J Med Genet A, 2007. **143A**(9): p. 952-60.
6. Boot, M.J., et al., *Cardiac outflow tract malformations in chick embryos exposed to homocysteine.* Cardiovasc Res, 2004. **64**(2): p. 365-73.
7. Rosenquist, T.H., S.A. Ratashak, and J. Selhub, *Homocysteine induces congenital defects of the heart and neural tube: effect of folic acid.* Proc Natl Acad Sci U S A, 1996. **93**(26): p. 15227-32.
8. Hogers, B., et al., *Unilateral vitelline vein ligation alters intracardiac blood flow patterns and morphogenesis in the chick embryo.* Circ Res, 1997. **80**(4): p. 473-481.
9. Upchurch, G.R., Jr., et al., *Homocyst(e)ine decreases bioavailable nitric oxide by a mechanism involving glutathione peroxidase.* J Biol Chem, 1997. **272**(27): p. 17012-7.
10. Welch, G.N., et al., *Homocysteine-induced nitric oxide production in vascular smooth-muscle cells by NF-kappa B-dependent transcriptional activation of Nos2.* Proc Assoc Am Physicians, 1998. **110**(1): p. 22-31.
11. Tyagi, N., et al., *Mechanisms of homocysteine-induced oxidative stress.* Am J Physiol Heart Circ Physiol, 2005. **289**(6): p. H2649-56.
12. Boot, M.J., et al., *Homocysteine induces endothelial cell detachment and vessel wall thickening during chick embryonic development.* Circ Res, 2004. **94**(4): p. 542-9.
13. Lee, S.J., et al., *Nitric oxide inhibition of homocysteine-induced human endothelial cell apoptosis by down-regulation of p53-dependent Noxa expression through the formation of S-nitrosohomocysteine.* J Biol Chem, 2005. **280**(7): p. 5781-8.
14. Wall, R.T., et al., *Homocysteine-induced endothelial cell injury in vitro: a model for the study of vascular injury.* Thromb Res, 1980. **18**(1-2): p. 113-21.
15. Latacha, K.S. and T.H. Rosenquist, *Homocysteine inhibits extra-embryonic vascular development in the avian embryo.* Dev Dyn, 2005. **234**(2): p. 323-31.
16. Poelma, C., et al., *Measurements of the wall shear stress distribution in the outflow tract of an embryonic chicken heart.* J R Soc Interface, 2010. **7**(42): p. 91-103.
17. Wagman, A.J., N. Hu, and E.B. Clark, *Effect of changes in circulating blood volume on cardiac output and arterial and ventricular blood pressure in the stage 18, 24 and 29 chick embryo.* Circ Res, 1990. **67**: p. 187-192.
18. Hogers, B., et al., *Intracardiac blood flow patterns related to the yolk sac circulation of the chick embryo.* Circ Res, 1995. **76**(5): p. 871-7.
19. Poelmann, R.E., A.C. Gittenberger-de Groot, and B.P. Hierck, *The development of the heart and microcirculation: role of shear stress.* Med Biol Eng Comput, 2008. **46**(5): p. 479-84.
20. Groenendijk, B.C., et al., *Changes in shear stress-related gene expression after experimentally altered venous return in the chicken embryo.* Circ Res, 2005. **96**(12): p. 1291-8.
21. Ferrara, N. and T. Davis-Smyth, *The biology of vascular endothelial growth factor.* Endocr Rev, 1997. **18**(1): p. 4-25.

22. Ziche, M. and L. Morbidelli, *Nitric oxide and angiogenesis.* J Neurooncol, 2000. **50**(1-2): p. 139-48.
23. Knowles, R.G. and S. Moncada, *Nitric oxide synthases in mammals.* Biochem J, 1994. **298 (Pt 2)**: p. 249-58.
24. Resnick, N., et al., *Hemodynamic forces as a stimulus for arteriogenesis.* Endothelium, 2003. **10**(4-5): p. 197-206.
25. Steegers-Theunissen, R.P., et al., *Hyperhomocysteinaemia and recurrent spontaneous abortion or abruptio placentae.* Lancet, 1992. **339**: p. 1122-3.
26. Quere, I., et al., *Vitamin supplementation and pregnancy outcome in women with recurrent early pregnancy loss and hyperhomocysteinemia.* Fertil Steril, 2001. **75**(4): p. 823-5.
27. Wouters, M.G., et al., *Hyperhomocysteinemia: a risk factor in women with unexplained recurrent early pregnancy loss.* Fertil Steril, 1993. **60**(5): p. 820-5.
28. Boot, M.J., et al., *Folic acid and homocysteine affect neural crest and neuroepithelial cell outgrowth and differentiation in vitro.* Dev Dyn, 2003. **227**(2): p. 301-8.
29. Kobus, K., E.M. Nazari, and Y.M. Muller, *Effects of folic acid and homocysteine on spinal cord morphology of the chicken embryo.* Histochem Cell Biol, 2009.
30. Rolschau, J., et al., *The influence of folic acid supplement on the outcome of pregnancies in the county of Funen in Denmark. Part I.* Eur J Obstet Gynecol Reprod Biol, 1999. **87**(2): p. 105-10; discussion 103-4.
31. Timmermans, S., et al., *Periconception folic acid supplementation, fetal growth and the risks of low birth weight and preterm birth: the Generation R Study.* Br J Nutr, 2009. **102**(5): p. 777-85.
32. Steegers-Theunissen, R.P., et al., *Periconceptional maternal folic acid use of 400 microg per day is related to increased methylation of the IGF2 gene in the very young child.* PLoS One, 2009. **4**(11): p. e7845.
33. Rolschau, J., J. Date, and K. Kristoffersen, *Folic acid supplement and intrauterine growth.* Acta Obstet Gynecol Scand, 1979. **58**(4): p. 343-6.
34. Smith, A.D., Y.I. Kim, and H. Refsum, *Is folic acid good for everyone?* Am J Clin Nutr, 2008. **87**(3): p. 517-33.

&

SUMMARY

With a prevalence rate of 7-8 per 1000 live births per year in the Netherlands, congenital heart defects (CHD) are the most common birth defects in newborns. Unfortunately, in only about 15 percent of cases a cause can be identified. Studies on the etiology of CHD are needed to increase our knowledge and reveal possible underlying mechanisms and pathways.

To be able to understand and detect what is abnormal, first normal heart development and function need to be understood. Correct early heart functioning is vital, as alterations in heart function may precede the onset of structural heart defects. Still there is no consensus on the exact functioning of the heart during the early stages of development, as the heart undergoes constant morphological changes. Therefore, **Chapter 2** of this thesis presents a study on early cardiac hemodynamics, to increase our insight into the way the embryonic heart functions and to be able to achieve earlier and improved detection of abnormalities. Doppler flow velocity waveforms of the chicken embryonic heart at developmental stages that coincide with 5-8 weeks of human pregnancy are presented, obtained with high frequency ultrasound biomicroscopy. These Doppler profiles provide significant information on normal early embryonic hemodynamics. We have shown that location as well as stage specific flow velocity waveforms are present. Our data are suggestive that different pumping mechanisms are active in this period of time.

In **Chapter 3,** studies on the teratogenicity of homocysteine in animal experimental models are reviewed and we elaborated on the possible underlying mechanisms. Homocysteine was shown to induce a wide range of congenital malformations, CHD among others, especially in the chicken embryo. The congenital malformations observed in the chicken embryo share the mutual involvement of homocysteine sensitive neural crest cells. The wide range of effects induced by homocysteine follows from the interaction between homocysteine and pathways that are involved in vascularization, growth, metabolism, signaling, DNA synthesis and methylation, affecting growth and differentiation processes as well as implantation, embryogenesis and placentation. We concluded that the derangement of different pathways by homocysteine has adverse effects on both reproduction and long term health.

Hyperhomocysteinemia, an elevated level of homocysteine in maternal blood, has been associated with an increased risk of offspring with CHD. Additionally, homocysteine exposure in the chicken embryo resulted in CHD. Since early heart function may influence cardiac morphology, we hypothesized that homocysteine may affect early embryonic heart function. Therefore, hemodynamic parameters of embryonic chicken heart function in the homocysteine exposed chicken embryo were collected in **chapter 4**. We have shown that

homocysteine in general exerts inhibiting effects on early heart function, like, among others, a reduction of heart rate. This chapter also shows the effects of homocysteine on shear stress rates at the site of the OFT. The results support our hypothesis that homocysteine exposure causes early functional changes that may precede the development of CHD.

Epidemiological studies have shown that maternal periconceptional folic acid (FA) use reduces the prevalence rate of CHD by approximately 20%. In **chapter 5** the possible effects of FA and 5-methyltetrahydrofolate (mefolinate), that serve as substrates in the homocysteine pathway, on early embryonic heart function and embryo survival are discovered. Also, combined treatment of folic acid and homocysteine was applicated. We have shown that folic acid and mefolinate equally stimulate embryo survival and that folic acid in combination with homocysteine does not improve survival rates. This combined treatment is suggestive for a protective effect of folic acid since the specific effects previously subscribed to homocysteine were not present in these embryos. This could be one of the mechanisms through which human periconceptional FA use prevents CHD in the offspring.

Homocysteine has not only been implicated in the development of CHD, also vasculotoxic properties have been ascribed to homocysteine, making homocysteine a vascular pathogen. Still, little is known about the direct effects homocysteine exerts during early embryonic vascular development. Therefore, **chapter 6** is a study on the effects of homocysteine, as well as folic acid, on early embryonic vascular development. To quantitate vascular development, we developed a computational program for systematic analysis of microscopic images obtained from the extra-embryonic vascular beds of chicken embryos. Also, real time PCR data on the expression of VEGF-A and its receptor were obtained. We have shown that homocysteine exposure inhibits early vascular development, causing a significant reduction of vessel area and altered composition of the vascular beds. Homocysteine also reduced the expression of VEGF-A and VEGFR-2. No significant effects of folic acid were found. These effects of homocysteine, and the consecutive cascade of events, may be involved in the development of CHD, as well as early placentation problems.

In the General Discussion, **chapter 7**, the findings and implications of this thesis are discussed. We provide a figure that combines the effects ascribed to homocysteine during cardiovascular development in previous literature and have added the results presented in this thesis. We link homocysteine to altered early heart function and eventually to the development of congenital heart defects. Also ideas for future research are provided.

SAMENVATTING

Met een prevalentie van 7-8 per 1000 levendgeborenen per jaar in Nederland behoren aangeboren hartafwijkingen tot de meest voorkomende aangeboren afwijkingen bij de mens. Helaas kan maar in 15 procent van de gevallen een onderliggende oorzaak aangewezen worden. Studies naar de etiologie van aangeboren hartafwijkingen zijn daarom hard nodig om onze kennis te vergroten en mogelijke onderliggende mechanismen en cascades te ontdekken.

Om te kunnen begrijpen en opsporen wat abnormaal is, moeten eerst normale hartontwikkeling en hartfunctie begrepen worden. Dat het vroege embryonale hart correct functioneert is van vitaal belang gezien functionele veranderingen vooraf zouden kunnen gaan aan het ontstaan van structurele aangeboren hartafwijkingen. Er is nog steeds geen consensus over hoe het hart tijdens de vroege stadia van ontwikkeling, een periode waarin het hart aan constante mophologische verandering onderhevig is, exact functioneert. Daarom presenteert **hoofdstuk 2** van dit proefschrift een studie naar hemodynamiek van het vroege hart, om ons inzicht te vergroten in hoe het embryonale hart functioneert en met het doel om in de toekomst vroegere en verbeterde detectie van abnormaliteiten te kunnen bereiken. Doppler bloedstroomsnelheid patronen in het embryonale kippenhart, tijdens fasen van de ontwikkeling die overeen komen met 5-8 weken amenorrhoeduur bij een humane zwangerschap, worden gepresenteerd, verkregen met hoogfrequent ultrageluid biomicroscopie. Deze Doppler profielen leveren significante informatie op wat betreft normale vroege embryonale hemodynamiek. We hebben laten zien dat zowel stadium als locatie specifieke bloedstroomprofielen aanwezig zijn. Onze data suggereren dat er verschillende pompmechanismen actief zijn tijdens deze periode van de embryonale ontwikkeling.

In **hoofdstuk 3** zijn studies naar de teratogeniciteit van homocysteïne in dierexperimentele modellen beschreven en wordt uitvoerig ingegaan op de mogelijke onderliggende mechanismen. Er wordt laten zien dat homocysteïne een breed spectrum aan aangeboren afwijkingen kan induceren, onder andere hartafwijkingen, met name in het kippenembryo. De aangeboren afwijkingen die werden gezien in het kippenembryo delen de gemeenschappelijke betrokkenheid van neurale lijst cellen die gevoelig zijn voor homocysteïne. De grote verscheidenheid aan effecten die homocysteïne teweegbrengt komen voort uit de interactie tussen homocysteïne en routes die zijn betrokken in vascularisatie, groei, metabolisme, signaaltransductie, DNA synthese en methylering, en zo groei en differentiatie processen alsmede ook implantatie, embryogenese en placentatie beinvloeden. We concluderen dat de verstoring van de verschillende cascades door homocysteïne ongunstige effecten heeft op zowel reproductie als de gezondheid op lange termijn.

Hyperhomocysteïnemie, een verhoogd homocysteïne gehalte in het bloed van de moeder, is geassocieerd met een verhoogd risico op nageslacht met een aangeboren hartafwijking. Daarbij resulteerde blootstelling aan homocysteïne in het kippenembryo in aangeboren hartafwijkingen. Gezien vroege hartfunctie de uiteindelijke morphologie van het hart kan beïnvloeden was onze hypothese dat blootstelling aan homocysteïne effect heeft op vroege embryonale hartfunctie. Daarom hebben wij in **hoofdstuk 4** hemodynamische parameters van vroege hartfunctie in het kippenembryo verzameld. We hebben laten zien dat homocysteïne in het algemeen een inhiberend effect heeft op de vroege hartfunctie, waaronder een verlaging van hartslag. Dit hoofdstuk beschrijft ook de invloed van homocysteïne op de wandschuifspanning ter plaatse van het uitstroomtraject. De resultaten ondersteunen onze hypothese dat blootstelling aan homocysteïne vroege functionele veranderingen veroorzaakt die mogelijk voorafgaan aan het ontstaan van aangeboren hartafwijkingen.

Epidemiologische studies hebben laten zien dat periconceptionele inname van foliumzuur door de moeder de prevalentie van aangeboren hartafwijkingen met ongeveer 20% doet afnemen. In **hoofdstuk 5** hebben we de mogelijke effecten van foliumzuur en 5-methyltetrahydrofolaat (mefolinaat), beiden substraten in de homocysteïne metabolisme, op vroege embryonale hartfunctie en embryo overleving onderzocht. Ook hebben we gekeken wat een combinatie behandeling van foliumzuur en homocysteïne voor gevolgen heeft. We hebben laten zien dat foliumzuur en mefolinaat de embryo overleving beiden evenredig stimuleren, en dat foliumzuur gecombineerd met homocysteïne de embryo overleving niet verbetert. Deze gecombineerde behandeling is suggestief voor een beschermend effect van foliumzuur gezien de specifieke effecten die eerder werden toegekend aan homocysteïne niet aanwezig zijn in deze embryos. Dit zou een van de mechanismen kunnen zijn waardoor bij de mens inname van periconceptioneel foliumzuur beschermt tegen aangeboren hartafwijkingen.

Homocysteïne is niet alleen betrokken bij het ontstaan van aangeboren hartafwijkingen, ook vasculotoxische eigenschappen zijn toegekend aan homocysteïne die maken dat dit een vasculair pathogeen is. Er is echter nog weinig bekend van de directe effecten die homocysteïne uitoefent tijdens de vroege embryonale vaatontwikkeling. Daarom presenteren wij in **hoofdstuk 6** een studie naar de effecten van homocysteïne, alsook foliumzuur, op vroege embryonale vaatontwikkeling. Om vaatontwikkeling te kunnen kwantificeren hebben we een computer programma ontwikkeld voor systematische analyse van microscopische plaatjes van het extra-embryonale vaatbed van het kippenembryo. Ook hebben we real time PCR data verzameld wat betreft de expressie van VEGF-A en diens receptor. We hebben laten zien dat blootstelling aan homocysteïne de vroege vaatontwikkeling

verhinderd, zichtbaar door een significante vermindering van vaat oppervlakte en een veranderde opbouw van het vaatbed. Homocysteïne verlaagt ook de expressie van VEGF-A en VEGFR-2. Er werd geen significant effect van foliumzuur gevonden. De effecten van homocysteïne, en de daaropvolgende cascade van gebeurtenissen, zouden betrokken kunnen zijn bij de ontwikkeling van aangeboren hartafwijkingen, alsook in het veroorzaken van problemen in de vroege placentatie.

In de algemene discussie, **hoofdstuk 7**, worden de bevindingen en implicaties van dit proefschrift bediscussieerd. We verschaffen een figuur dat de verschillende effecten van homocysteïne tijdens de cardiovasculaire ontwikkeling, zoals beschreven in eerdere literatuur, combineert met de resultaten gepresenteerd in dit proefschrift. We koppelen homocysteïne aan veranderde vroege hartfunctie en uiteindelijk het ontstaan van aangeboren hartafwijkingen. Ook worden suggesties voor toekomstig onderzoek gedaan.

ABOUT THE AUTHOR

Annelien Maria Oosterbaan was born on the 30th of March 1983 in 's-Hertogenbosch, the Netherlands. From 1995 she attended Gymnasium Bernrode in Heeswijk-Dinther. In 2001 she graduated (Gymnasium β) and moved to Rotterdam. She studied medicine from 2002 and started her research on the department of Obstetrics and Gynecology of the Erasmus University Medical Center in 2007, first for a period of 5 months. Thereafter she followed a 2 year internship program at different hospitals in and near Rotterdam. In 2009 she graduated as a medical doctor. She returned to the department of Obstetrics and Gynecology as a PhD student and continued her research under the supervision of Prof. Dr. Eric Steegers and Dr. Nicolette Ursem. After 1 year as a fulltime researcher she started as a resident ObGyn at the Maasstad Hospital in Rotterdam from October 2010. August 2011 she gave birth to her first daughter, Philine. From the beginning of 2012 she started her in-training residency in Obstetrics and Gynecology at the Albert Schweitzer Hospital in Dordrecht

PHD PORTFOLIO
SUMMARY OF PHD TRAINING AND TEACHING

Name PhD student: Annelien M. Oosterbaan	PhD period: September 2009 – June 2012
Erasmus MC Department: Obstetrics & Gynecology	Promotor: Prof. dr. Eric A.P. Steegers
Research School: Erasmus University Medical Center	Supervisor: Dr. Nicolette T.C. Ursem

	Year
General courses	
- Biomedical English Writing and Communication	Jan 2010
Presentations	
- Oral poster presentation ISUOG, Florence, Italy	2007
- Poster presentation SGI, San Diego, USA	2008
- Poster presentation Gynaecongres, Papendal, Netherlands	2009
- Several presentations, research meeting Division of Obstetrics and Prenatal Medicine, Erasmus MC, Rotterdam, The Netherlands	2009-2010
- Oral presentation, Schellekens Symposium, The Hague, Netherlands	2012
(Inter)national conferences	
- ISUOG, Florence, Italy	2007
- SGI, San Diego, USA	2008
- Gynaecongres, Papendal, the Netherlands	2009
- SGI, Orlando, USA	2010
- Weekly research meetings: Department of Obstetrics and Gynecology, division of Obstetrics and Prenatal medicine	2009-2010
- 9e Wim Schellekenssymposium, The Hague, The Netherlands	2012
- Gynaecongres, World Forum, The Hague, The Netherlands	2012
Supervising practicals and excursions, Tutoring	
- Supervising trainee Chantal van der Kaa, 2nd year student technical natural sciences, The Hague	2010

LIST OF PUBLICATIONS

Chapter 2

A.M. Oosterbaan, N.T.C. Ursem, P.C. Struijk, J.G. Bosch, A.F.W. van der Steen, E.A.P. Steegers. Doppler flow velocity waveforms in the embryonic chicken heart at developmental stages corresponding to 5–8 weeks of human gestation. *Ultrasound in Obstetrics and Gynecology* 2009; 33: 638–644

Chapter 3

N.H. van Mil, **A.M. Oosterbaan**, R.P.M. Steegers-Theunissen. Teratogenicity and mechanisms of homocysteine in animal models: a review. *Reproductive Toxicology* 2010 Dec;30(4):520-31

Chapter 4.1

A.M. Oosterbaan, E. Bon, R.P.M. Steegers-Theunissen, A.F.W. van der Steen, N.T.C. Ursem. Homocysteine affects hemodynamic parameters of early embryonic chicken heart function. *Accepted The Anatomical Record Advances in Integrative Anatomy and Evolutionary Biology 2012*

Chapter 4.3

A.M. Oosterbaan, C. Poelma, E. Bon, R.P.M. Steegers-Theunissen, E.A.P. Steegers, P. Vennemann, N.T.C. Ursem. Induction of shear stress in the homocysteine exposed chicken embryo. *Submitted*

Chapter 5

A.M. Oosterbaan, E.A.P. Steegers, N.T.C. Ursem. Homocysteine disturbs early heart function in the chicken embryo. Effects of folic acid and mefolinate. *Submitted*

Chapter 6

A.M. Oosterbaan, E.A.P. Steegers, N.T.C. Ursem. Influence of homocysteine and folic acid on angiogenesis and VEGF expression in chicken extra-embryonic vascular development. *Microvascular Research* 2012 Mar; 83(2):98-104

DANKWOORD

Graag wil ik eenieder bedanken die op welke manier dan ook heeft bijgedragen aan de totstandkoming van dit proefschrift. Hoewel ik niet kan zeggen dat het een langdurig traject is geweest was het hierdoor zeker niet minder pittig. Zeer verheugd ben ik dan ook dat het is afgerond en u nu dit boekje voor u heeft liggen. Speciale dank aan de leden van de kleine commissie voor uw bereidheid hierin plaats te nemen, alsook de leden van de grote commissie voor uw aanwezigheid bij de plechtigheid. Onderstaande personen wil ik in het bijzonder noemen.

Om te beginnen mijn promotor, **Prof. dr. Eric Steegers**. Als 1e jaars geneeskunde student heb ik u voor het eerst ontmoet. Ik kwam nog maar net kijken toen ik u vroeg of ik in het kader van de studie een dagje met u mee mocht lopen. Vanaf deze eerste ontmoeting heeft u mij geboeid, vandaar dat ik u een aantal jaren later weer wist te vinden, ditmaal voor een onderwerp voor mijn keuze-onderzoek. Ik wist dat ik bij u aan het goede adres was voor leuk en uitdagend onderzoek, en zo geschiedde, ik kon aan de slag. Met veel vrijheid en vertrouwen heeft u mij mijn promotietraject laten doorlopen, daar heb ik veel van geleerd en ben ik u dankbaar voor. U bent een inspirerend professor, die in veel dingen een nieuwe onderzoeksvraag weet te ontdekken. Buiten dank voor de begeleiding ook veel dank voor de gezelligheid op de vele congressen en borrels die ik heb mogen bezoeken, waar u ook meermaals aanwezig danwel aanstichter van was.

Beste Dr. Ursem, lieve **Nicolette**, jij bent een prachtig rolmodel. Een harde werker naast het hebben van een gezin, altijd gezellig en nooit zeuren. Je was mijn dagelijkse begeleidster en ik had me geen betere kunnen voorstellen. Ruimte geven waar het kan, en de teugels aantrekken als het nodig is. Je gaf me de nodige complimentjes om mij enthousiast te houden, positief ingesteld. Jammer dat we elkaar het laatste stuk van mijn promotietraject door onze nieuwe banen zo weinig hebben gezien. Gelukkig liep de samenwerking en afronding desondanks gesmeerd. Ik wens je heel veel succes met je carriere en hoop dat we elkaar in de toekomst nooit helemaal uit het oog zullen verliezen.

Beste Prof. dr. Steegers-Theunissen, beste **Regine**, dank voor de tijd die je nam voor het doornemen van mijn manuscripten. Goede discussies en bruikbaar commentaar brachten mijn onderzoek naar een hoger niveau. Een talentvolle wetenschapster waar ik veel respect voor heb, zeer terecht gekroond tot professor.

Lieve **Karin**, mijn paranimf en mede RVSV-studiemaat vanaf het aller begin. We begonnen de studie geneeskunde niet al te best maar eindigden allebei als een goede nerd. Dank voor je hulp bij het inzetten van mijn eitjes en de gezellige koffietjes op de uni en nog veel meer. Onze vriendschap is van grote waarde en ik hoop dat die nog lang mag bestaan. Ik vind het super om je vandaag naast me te hebben staan. In de toekomst hoop ik dat de eer andersom is en dat we nog maar vele mijlpalen samen mogen beleven.

Lieve **Evelyne**, mijn andere paranimf, we begonnen in hetzelfde cogroepje maar waren niet meteen de beste vrienden. Bij ons gaat de uitspraak "you never get a second chance to make a first impression" niet op. Toen we door ons promotie-onderzoek op dezelfde kamer belandden bleken we een goede match en zijn we meer dan collega's geworden. Dit natuurlijk mede dankzij onze gedeelde liefde voor pils en kaasstengels. Dank voor alle steun en de leuke tijd, je bent een topwijf en ik weet zeker dat we nog heel veel drankjes zullen doen!

Beste collega's van het onderzoek, **Dineke, Annelous, Lindy, Sam, Sharon, Sarah, Melek, Robbert, Jinke, Fatima, John, Sylvia, Marijana, Babs, Jashvant, Wendy, Yvon, Kim, Annelinde, Marielle, Marieke, Nina**, en in het bijzonder **Babette en Nienke**. Bedankt voor alle borrels, etentjes, kamers delen en keten op congressen, het luisteren naar mijn getetter, lelijke gezang en soms frustraties, en zeker ook dank voor de hulp met SPSS ;-) Ik ben blij dat de meeste van jullie hetzelfde vak ambieren, dan hebben we nog vele jaren voor ons om lol met elkaar te hebben.

Beste collega's en bazen uit het **Maasstad Ziekenhuis**, de helft van mijn onderzoekstijd heb ik bij jullie gewerkt, dus jullie horen ook zeker voor te komen in mijn dankwoord. Het was soms best zwaar het hebben van 2 banen, maar doordat ik het zo naar mijn zin had bij jullie heb ik nooit moeite gehad de kliniek met het onderzoek te combineren, zelfs niet met een zwangere buik. Dank voor de fijne, vruchtbare en zeer leerzame tijd, voor de ruime compensatiedagen die mij de kans gaven mijn onderzoek af te maken, en zeker ook voor de leuke dingen die we samen hebben meegemaakt.

Beste collega's en bazen uit het **Albert Schweitzer Ziekenhuis**, dank voor het warme welkom. Bij jullie zet ik mijn eerste stapjes in mijn carrière als AIOS. Ik weet nu al dat ik goed terecht ben gekomen. Op een leerzame en leuke samenwerking!

JC Dizzy, supermooi. Ookal heb ik jullie de afgelopen maanden onvrijwillig verwaarloosd door het harde werken en het verse moederschap, ik weet zeker dat we vrienden voor het leven zijn.

Lieve **schoonfamilie**, dank voor jullie steun, jullie begrip en enthousiasme wat betreft mijn werk en onderzoek, voor de heerlijke etentjes en de warme band die we hebben. Barry en Lucille, dit proefschrift betekent veel voor mij, maar mijn grootste wens is dat de wetenschap nog eens wonderen voor jullie gaat doen, wie weet.

Lieve **zusjes**, jullie zijn heel belangrijk voor mij. Ik ben trots op wat jullie tot nu toe bereikt hebben en wat ik vandaag voor elkaar heb gekregen heb ik ook aan jullie steun te danken. Niet alleen de laatste maanden door soms op Philine te passen want het is heel bijzonder te merken hoeveel jullie om je kleine nichtje geven, maar ook door er altijd voor me te zijn. We zijn een hechte familie en ik hoop dat we dat altijd blijven.

Pap en mam, jullie zijn mijn grote voorbeeld, allebei gedreven, hard werkend, enthousiast, ambiteus en liefdevol. Jullie hebben mij geleerd om iets te willen bereiken, doelen te stellen en ook te halen, nuchter te zijn en eerlijk. Daarnaast ook het belang van het hebben van een hecht en warm gezin, en zeker ook van een goede relatie. Ik hou van jullie en ben jullie heel dankbaar voor alles wat ik tot nu toe bereikt heb, daar zijn jullie grotendeels verantwoordelijk voor. **Mam**, dank voor al je oppasdagen en alles wat je voor ons doet. Ik heb woorden tekort om je te bedanken, je bent mijn held. Dank ook voor je hulp met de manuscripten, met name wat betreft de engelse taal. Ik hoop net zo'n supermoeder te worden als jij bent. **Pap**, dank dat je af en toe stukjes voor me wilde doorlezen. Dank voor onze vele telefoongesprekken, voor je adviezen en je steun. Het is super om een vader te hebben die precies weet hoe het is om te promoveren en om deze carriere tot gynaecoloog te doorlopen. En wat heb ik aan jou een prachtig voorbeeld. Ik zal de titel Dr. Oosterbaan met trots dragen en ik hoop en weet zeker in de toekomst nog veel aan je steun te hebben en met je te kunnen delen.

Philine, je bent nog zo klein maar de grote hoeveelheid liefde die ik voor je voel blaast me dagelijks omver. De knuffeltjes met jou bezorgen me altijd een grote glimlach en een ongelofelijk warm gevoel van binnen. Je hebt me, zonder dat je dit nog beseft, door vele emotionele momenten gesleept.

Lieve Patrick, ofwel lieve **Patty**. Jij klaagt nauwelijks over het vele werken wat ik doe en wat dit voor jou betekent. Door mijn vak, en zeker de afgelopen periode van afronding van dit proefschrift, moet jij veel voor ons en zeker ook voor Philine zorgen. Dit doe je altijd vrijwillig en met liefde. Daarnaast ben je zelf ook succesvol en daar ben ik heel trots op. Ook zorg je ervoor dat onze sociale agenda volle toeren blijft draaien en dat het leven een groot feest is. Ik kan niet in woorden uitdrukken hoeveel je voor me betekent, zonder jou kon ik nooit bereiken wat ik zou willen zonder me schuldig te voelen. Jij en Philine zijn alles voor mij, we zijn een super team. Ik hou van je, dank dat je bestaat.